

Design of a Cruising Sailing Yacht with an Experimental Fluid Dynamics Investigation into Hydrofoils

Juliette DEWAVRIN

Master Thesis

Presented in partial fulfilment
of the requirements for the double degree:
“Advanced Master in Naval Architecture” conferred by University of Liege
“Master of Sciences in Applied Mechanics, specialization in Hydrodynamics, Energetics and Propulsion” conferred by Ecole Centrale de Nantes

Developed at West Pomeranian University of Technology, Szczecin
in the framework of the

“EMSHIP”
Erasmus Mundus Master Course
in “Integrated Advanced Ship Design”
EMJMD 159652 – Grant Agreement 2015-1687

ZUT **Dr. Inż. Monika Bortnowska,**
Supervisor: West Pomeranian University of Technology, Szczecin, Poland
Internship **Senior Lecturer Jean-Baptiste R. G. Souppiez,**
Supervisor: Southampton Solent University, Southampton, UK
Reviewer: **Prof. Pierre Ferrant**
Ecole Centrale de Nantes, Nantes, France

Szczecin, February 2018

ABSTRACT

Despite the early discovery of hydrofoils, first conceived in 1906 [1], there has been renewed interest in recent years, particularly for racing yachts, most likely thanks to the progress in material properties. As a consequence, the concept is beginning to filter through to the cruising yacht sector despite the limited technical literature.

The main benefits of including hydrofoils on a sailing yacht are: performance, velocity along with stability, and seakeeping. There does however remain challenges to the designs and hydrodynamics when adopting foils.

The aim of this master thesis is to implement three existing concepts of hydrofoil into a standard design of cruising yacht, and to establish and resolve the design integration problems and tackle the hydrodynamic advantages. Firstly, the design is going to be explored in order to find the best way to include the hydrofoils into the boat. Subsequently, the selected designs will be tested by experimental fluid dynamic approach in a towing tank testing and their hydrodynamic results outlined.

Keywords: design, sailing yacht, cruising, hydrofoils, experimental fluid dynamics, towing tank testing, hydrodynamic results

ACKNOWLEDGEMENTS

First of all, I would like to thank my parents for all their moral and financial support during this one year and a half master.

Then, I would like to thank my supervisor in Southampton Solent University, Jean-Baptiste Soupeze, who guided me throughout my internship at Southampton Solent University from the beginning to the very end of the research. I really appreciate his time and patience, he was constantly available for technical support during this master thesis and his recommendations have been a great guidance.

I would like to thank Prof. Giles Barkley from Southampton Solent University for his shared theoretical and practical knowledge. I have got very useful and significant viewpoints about the behaviours of the foiling sailboats in the sea as well as in the towing tank thanks to his valuable advice.

I would like to thank Jack Cunningham Burley from Southampton Solent University for his shared knowledge in composites and for his assistance in the workshop when building the yacht and foils model.

I would like to thank Southampton Solent University for allowing me to use the university facilities: the workshop, the 3D printers and the towing tank. I could not achieve my work during the internship without it.

I would like to thank Gordon J.W. Kay, director of Infiniti Performance Yachts, for sharing his time with me, for trusting me and sharing technical information about Infiniti 56 foiling yacht. I have got very useful viewpoint about the yacht and the DSS hydrofoil design.

I would also like to thank Quentin Stewart, owner of the Infiniti 46R racing yacht, and all the crew members of the Maverick team, who invited me to sail during the Channel Race 2017 between Cowes and Cherbourg. I have had an incredible and unforgettable offshore sailing experience and a practical understanding and sensation of the DSS foils.

I would like to thank my supervisor from West Pomeranian University of Technology in Szczecin, Dr. Inż. Monika Bortnowska, who assisted me on the writing of the master thesis with her general recommendations and support.

Finally, I would like to thank James Starkey, for reading and reviewing the grammar language of this master thesis as a final correction.

CONTENTS

ABSTRACT	3
ACKNOWLEDGEMENTS	5
TABLE OF FIGURES	10
TABLE OF TABLES	14
DECLARATION OF AUTHORSHIP	17
NOMENCLATURE - Symbols Explanations	19
1. INTRODUCTION	21
2. STATE OF THE ART - FOIL ASSISTED SAILING YACHTS	22
2.1. The Aim of Hydrofoils - Introduction to Foil Theory	22
2.2. History: The First Boats Equipped With Hydrofoils.....	26
2.3. The Different Types of Hydrofoils on Monohull Sailing Yacht Nowadays	27
2.3.1. "Dali Moustache" Foils on IMOCA 60 Racing Yachts.....	29
2.3.2. "Chistera" foils on the New Figaro 3 Bénéteau RacingYacht.....	31
2.3.3. DSS foils on Infiniti 56C cruising yachts.....	32
3. METHODOLOGY AND PLANNING.....	34
3.1. Content, Resources and Objectives	34
3.1.1. Design of a Foiling Cruising Yacht.....	34
3.1.2. Hydrodynamic Analysis - Experimental Approach	35
3.2. GANTT Diagram	38
4. PART 1: DESIGN OF A SAILING CRUISING YACHT WITH HYDROFOILS	39
4.1. Preliminary Design.....	39
4.2. Detailed Design	40
4.2.1. Hull Geometry, Hydrostatics and Lines Plan	41
4.2.2. Sailing Equilibrium: Sails and Appendages Design.....	42
4.2.3. Hydrofoil Design	52
4.2.4. General Arrangement and Deck Plan	56
4.2.5. Resistance and Engine Selection	57
4.2.6. Hull and Deck Scantling - Structural Design	60
4.2.7. Mast and Rigging Dimensions	63
4.2.8. Weight Estimation	64
4.2.9. Stability Analysis	66
4.2.10. Velocity Prediction Programme (VPP)	69
5. PART 2: HYDRODYNAMIC ANALYSIS BY AN EXPERIMENTAL TANK	

TESTING APPROACH.....	72
5.1. Experimental Tank Testing Approach.....	73
5.1.1. Model Dimensions	73
5.1.2. Manufacturing Process and Towing Tank Preparation	75
5.1.3. Towing Tank Testing Theory	82
5.2. Hydrodynamic Analysis	94
5.2.1. Upright Hull Resistance Comparison.....	94
5.2.2. Resistance, Lift, Heave and Trim Comparisons	95
5.2.3. Influence of Angle of Attack	99
5.2.4. Effective Draft Results	102
6. CONCLUSIONS.....	106
6.1. Conclusions on the Design	106
6.2. Conclusions on the Hydrodynamic Analysis	107
6.2.1. Tank Testing General Observations	107
6.2.2. Tank Testing Hydrodynamic Results	107
6.2.3. Future Works	109
6.3. Hydrofoils Advantages and Drawbacks	110
7. REFERENCES.....	111
8. APPENDICES	114
APPENDIX A1: GANTT DIAGRAM	115
APPENDIX A2: KEY DESIGN RATIO FROM PARAMETRIC STUDY	116
APPENDIX A3: HULL LINES GEOMETRY - BARE HULL.....	118
APPENDIX A4: SAIL SIDE FORCE AND KEEL SIDE FORCE CALCULATION	119
APPENDIX A5: GENERAL ARRANGEMENT AND DECK PLAN DRAWINGS	122
APPENDIX A6: MAXSURF HULL RESISTANCE RESULTS	124
APPENDIX A7: ENGINE VOLVO PENTA CHARACTERISTICS.....	125
APPENDIX A8: HULL AND DECK SCANTLING RESULTS WITH HULLSCANT	127
APPENDIX A9: HULL AND DECK STRUCTURAL ARRANGEMENT.....	131
APPENDIX A10: MAST AND RIG CALCULATION SPREADSHEET (NBS)	133
APPENDIX A11: TANK LOADING	134
APPENDIX A12: WEIGHT ESTIMATION IN LIGHTSHIP CONDITION	135
APPENDIX A13: VPP TABLES FOR BEST SPEED, HEEL ANGLE, LEEWAY ANGLE AND SAILSET.....	137
APPENDIX A14: PROHASKA PLOT BARE HULL.....	140

APPENDIX A15: DRAG, SIDE FORCE, HEAVE AND TRIM GRAPHS.....	141
APPENDIX A16: RESISTANCE COMPARISON BETWEEN LOW AND HIGH HEEL ANGLE FOR EACH FOIL AT DIFFERENT LEeway ANGLE	145
APPENDIX A17: EFFECTIVE DRAFT GRAPHS (DRAG VS SIDE FORCE SQUARED) 146	
APPENDIX A18: EFFECTIVE DRAFT GRAPHS (T_{EFF} VS FROUDE NUMBER).....	149
APPENDIX A19: MINIMUM DRAG CONFIGURATION BASED ON THE EFFECTIVE DRAFT METHOD	150

TABLE OF FIGURES

Figure 1: Velocity difference around a foil structure in a free stream [3].....	22
Figure 2: Pressure profile around foil [3].....	22
Figure 3: Lift and Drag forces. 2D foil theory [4].	23
Figure 4: 3D foil theory - Vortexes around a 3D foil [3].....	23
Figure 5: 3D foil theory. Induce drag and downwash generation [3].	24
Figure 6: Hydrodynamic resistance with and without foils [5].....	24
Figure 7: V-shape foil [6].....	25
Figure 8: T-shape foil [7].	25
Figure 9: Hydrofoil boat 1910 Forlanini: Lake Maggiore [1].....	26
Figure 10: Icarus catamaran, 1969 (left) and Eric Tabarly trimaran, 1976 (right) [8].....	26
Figure 11: The fully foiling 75-foot concept for the AC75 (Virtual Eye) [9].....	27
Figure 12: Safran II (2015, VPLP and Guillaume Verdier design) equipped with "Dali Moustache" foils [10].....	28
Figure 13: Bénéteau Figaro 3 (2017, VPLP design and Bénéteau) equipped with foils [11]..	28
Figure 14: Infiniti 56C (2017, Farr Yacht design and Infiniti Performance Yachts) equipped with DSS foils (Virtual View) [12].....	28
Figure 15: Dali moustache foils - Section view [13].	29
Figure 16: Movable foiling daggerboard [10].....	30
Figure 17: Articulating keel [10].....	30
Figure 18: Figaro 3 Chistera foils - Cross section view [16].	31
Figure 19: Technical drawing of Figaro Bénéteau 3 (2016, VPLP design) [17].	32
Figure 20: DSS foil - Flat shape - Section view [18].	33
Figure 21: DSS foil on Infiniti 36 racing yacht [19].....	33
Figure 22: From model testing to full scale extrapolation. Own elaboration.	36
Figure 23: Activities done for the master thesis. Own elaboration.	38
Figure 24: Design spiral. Own elaboration.	40
Figure 25: Sail and rig dimensions - Notation. Own elaboration.....	43
Figure 26: NACA 0012 Lift and Drag coefficient curves ($Re_{\text{rudder}} = 1.40E+06$) [40].....	45
Figure 27: NACA 64-012 Lift and Drag coefficient curves ($Re_{\text{keelfin}} = 2.60E+06$) [40].	46
Figure 28: NACA 65-015 Lift and Drag coefficient curves ($Re_{\text{bulb}} = 1.91E+07$) [40].....	47
Figure 29: Aerodynamic and hydrodynamic forces acting on a sailing yacht [20].	48
Figure 30: Standard planform chosen for the keel and rudders [20].....	49

Figure 31: 3D Rhinoceros representation of the hull with bulbous keel and twin rudder. Own elaboration.	50
Figure 32: Balance and geometric centres representation. Own elaboration.	52
Figure 33: NACA 63-412 section geometry [42].....	53
Figure 34: NACA 63-412 Lift and Drag coefficient curves for $Re=5.0E+06$ [42].....	54
Figure 35: Figaro 3 general shape. AutoCAD design. Own elaboration.	55
Figure 36: Dali moustache general shape. AutoCAD design. Own elaboration.	55
Figure 37: DSS general shape. AutoCAD design. Own elaboration.	55
Figure 38: Longitudinal position of the foils and integration in the GA. AutoCAD design. Own elaboration.	56
Figure 39: Transversal sections with hydrofoils. AutoCAD design. Own elaboration.....	57
Figure 40: Resistance curves comparison from Maxsurf Resistance.....	58
Figure 41: Sail power versus Froude number. Maxsurf resistance.	58
Figure 42: Power required for the engine [45].....	59
Figure 43: "Squat" top-hat stiffeners dimensions*. Available from [32].....	61
Figure 44: Panel size** [32].....	62
Figure 45: Panel curvature** [32].....	62
Figure 46: Sloop rig design and dimensions (meters). AutoCAD drawings. Own elaboration.	64
Figure 47: Centre of gravity Lightship for configuration 1, 2, 3 and 4. AutoCAD drawings. Own elaboration.	65
Figure 48: Required minimum downflooding angle. Available from [34].....	67
Figure 49: Model for Stability analysis - Hull with keel up, roof and cockpit. Maxsurf Modeler.	67
Figure 50: Centre of gravity, tank position and zero point for loadcase N°3 (Figaro 3 Lightship) - Maxsurf Stability display.	68
Figure 51: GZ curves for loadcases N°1, 2, 3 and 4 (defined in Table 23) - Maxsurf Stability results.	68
Figure 52: VPP Rig and Sail plan - WinDesign VPP representation.....	70
Figure 53: Speed Polar Plot (knots) for Upwind (red curves) and Downwind (black curves) conditions- WinDesign VPP results.	71
Figure 54: Hand lay-up process in the workshop. Own picture.....	76
Figure 55: Resin and micro balloons paste covering. Own picture.	76
Figure 56: Longitudinal position of appendages and post. Rhinoceros. Own elaboration.	76

Figure 57: Appendages and post installation on the hull model. Own picture.	77
Figure 58: 3D representation of the model with appendages and foils. Rhinoceros. Own elaboration.	77
Figure 59: Dali foil attachment on the hull (Starboard). Own picture.	78
Figure 60: Figaro 3 foil attachment on the hull (Port). Own picture.	78
Figure 61: DSS foil attachment on the hull (Starboard). Own picture.	78
Figure 62: Keel fin plywood laminates. Half of the sanding process. Own picture.	79
Figure 63: 3D printers in Southampton Solent University. Own picture.	79
Figure 64: Plywood keel fin, bulb and hydrofoils after 3D printing. Own picture.	79
Figure 65: Keel fin and keel bulb. Own picture.	80
Figure 66: Vacuum bagging process (DSS foil). Own picture.	80
Figure 67: Hydrofoils with threaded rod, after vacuum bagging and finish coating. Own picture.	80
Figure 68: Model in Southampton Solent university's towing tank and towing tank dimensions. Own picture.	82
Figure 69: Schematic diagram of the towing mechanisms [48].	83
Figure 70: Modern sailboat hull particularity [50].	87
Figure 71: Prohaska plot from the towing tank test matrix. Upright (no leeway angle, no heel angle).	88
Figure 72: Effective draft against Froude number comparison for 20 degree of heel.	91
Figure 73: Effective draft graph from the tank test matrix. Comparison between the model without foil, with DSS foil, and with Figaro foil at Froude number 0.35 and 10 degree of heel.	92
Figure 74: Upright resistance comparison between software prediction and towing tank tests.	94
Figure 75: Model with foils heeled at 10 degree.	95
Figure 76: Influence of the parameters on the Resistance Prediction. Own elaboration.	95
Figure 77: Drag force at leeway 4° and heel angle 20°	96
Figure 78: Side force at leeway 4° and heel angle 20°	96
Figure 79: Heave at leeway 4° and heel angle 20°	96
Figure 80: Trim at leeway 4° and heel angle 20°	96
Figure 81: Vortex generation from the bow and interference with Figaro foil at high speeds in the tank. Own picture.	97
Figure 82: Lift and Drag coefficient against angle of attack for NACA 63 412 at $Re=5.0 \text{ E}+06$ [42].	99

Figure 83: Drag, Side Force, Heave and Trim comparison for different angle of attack with Dali foil	100
Figure 84: Drag, Side Force, Heave and Trim comparison for different angle of attack with Figaro foil.....	100
Figure 85: Drag, Side Force, Heave and Trim comparison for different angle of attack with DSS foil. Available from Charles Kitting test results [49].	101
Figure 86: Drag against Side force squared graph for upwind condition (Heel angle 20 degree and Froude number 0.35, 0.40 and 0.45)	103
Figure 87: Effective draft graph against Froude number for upwind condition - Heel 20 degree	104
Figure 88: Drag against Side force squared graph for downwind condition (Heel angle 10 degree and Froude number 0.45, 0.50, 0.60 and 0.70). Zoomed for easier comprehension. .	104
Figure 89: Effective draft against Froude number for downwind condition - Heel 10 degree	105
Figure 90: Water length to length overall ratio from parametric study	116
Figure 91: Length to beam ratio from parametric study	116
Figure 92: Beam to draft ratio from parametric study	116
Figure 93: Slenderness ratio from parametric study	117
Figure 94: Sail area to displacement ratio from parametric study	117
Figure 95: Ballast to displacement ratio from parametric study	117
Figure 96: True and Apparent wind representation.	119
Figure 97: Lift and drag coefficients versus AWA for sails. Available from [4]	120
Figure 98: Sailing equilibrium on the horizontal plane. Available from [4].....	120
Figure 99: Prohaska plot upright position. Form factor $(1+k) = 1.0878$	140
Figure 100: Prohaska plot 10deg heel position. Form factor $(1+k) = 1.0925$	140
Figure 101: Prohaska plot 20deg heel position. Form factor $(1+k) = 1.1274$	140
Figure 102: Drag, SF, Heave and Trim comparison for 0deg of leeway and 10deg of heel..	141
Figure 103: Drag, SF, Heave and Trim comparison for 0deg of leeway and 20deg of heel..	141
Figure 104: Drag, SF, Heave and Trim comparison for 2deg of leeway and 10deg of heel..	142
Figure 105: Drag, SF, Heave and Trim comparison for 2deg of leeway and 20deg of heel..	142
Figure 106: Drag, SF, Heave and Trim comparison for 4deg of leeway and 10deg of heel..	143
Figure 107: Drag, SF, Heave and Trim comparison for 4deg of leeway and 20deg of heel..	143
Figure 108: Drag, SF, Heave and Trim comparison for 6deg of leeway and 10deg of heel..	144
Figure 109: Drag, SF, Heave and Trim comparison for 6deg of leeway and 20deg of heel..	144

TABLE OF TABLES

Table 1: Design brief.....	34
Table 2: Experimental approach brief.....	36
Table 3: Key design ratios.....	40
Table 4: First approximation for the dimensions of the sailing yacht.....	40
Table 5: Main dimensions and hydrostatics of the hull	41
Table 6: DSYHS check	42
Table 7: Parametric study SA/D ratio with and without foils	42
Table 8: Sails and rigs parameters.....	43
Table 9: Sail side force and Keel side force results. From APPENDIX A4	48
Table 10: Keel and Rudder area.....	49
Table 11: Twin rudder geometry.....	49
Table 12: Keel fin geometry.....	50
Table 13: Keel bulb geometry	50
Table 14: Reynolds number appendages.....	51
Table 15: Balance and geometric centres.....	51
Table 16: Hydrofoils characteristics from parametric study	53
Table 17: Advantages and drawbacks of NACA 63-412 section.....	53
Table 18: Hydrofoil Reynolds number.....	54
Table 19: Fuel Consumption Estimation (Fuel tanks)	59
Table 20: Composite material input in Hullscant.....	60
Table 21:Rig loads and dimensions	63
Table 22: Weight estimation for different configurations.....	65
Table 23: Loadcase configurations - input parameters in Maxsurf Stability	67
Table 24: Tank location - input parameters in Maxsurf Stability	67
Table 25: Downflooding point - input in Maxsurf Stability	67
Table 26: Sail inventory	69
Table 27: Sail sets	69
Table 28:Operation sets.....	69
Table 29: Towing tank dimensions and restrictions for the model	74
Table 30: Hull ship and model dimensions	74
Table 31: Appendages dimensions model size	75
Table 32: Location of the roughness strip calculation for the hull model.....	81
Table 33: Model size ballast and weightage estimation.....	82

Table 34: Best speed, heel angle and leeway angle from VPP analyse	84
Table 35: Number of runs estimation and real	84
Table 36: Wetted surface area of each foil at 20 degree of heel in calm water at full scale	96
Table 37: Drag and Side Force contribution of each foil compared to the results without foils. Heel 20 degree and leeway 4 degree.	98
Table 38: Angle of attack chosen for each foil	102
Table 39: Advantages and drawbacks of the three foils based on the design and hydrodynamic analysis	110
Table 40: Sailing conditions.....	119
Table 41: Keel and rudder forces calculation.....	121
Table 42: Total lightweight with the keel DOWN and Figaro 3 foil	135
Table 43: Total lightweight with the keel UP and Figaro 3 foil	135
Table 44: Total lightweight with the keel DOWN and DSS foil	136
Table 45: Total lightweight with the keel UP and DSS foil.....	136
Table 46: Best boatspeeds (knots).....	137
Table 47: Best Boatspeeds (Fr)	137
Table 48: Best heel angle (degree).....	138
Table 49: Best Leeway angle (degree)	138
Table 50: Best point of sail (Upwind or Downwind).....	139
Table 51: Best configuration upwind and downwind based on R_T vs SF^2 graphs	150
Table 52: Best configuration upwind and downwind based on T_E vs Fr graphs	150

DECLARATION OF AUTHORSHIP

Declaration of Authorship

I, Juliette DEWAVRIN, declare that this thesis and the work presented in it are my own and have been generated by me as the result of my own original research.

"Design of a Cruising Sailing Yacht with an Experimental Fluid Dynamics Investigation into Hydrofoils"

Where I have consulted the published work of others, this is always clearly attributed.

Where I have quoted from the work of others, the source is always given. With the exception of such quotations, this thesis is entirely my own work.

I have acknowledged all main sources of help.

Where the thesis is based on work done by myself jointly with others, I have made clear exactly what was done by others and what I have contributed myself.

This thesis contains no material that has been submitted previously, in whole or in part, for the award of any other academic degree or diploma.

I cede copyright of the thesis in favour of the University of

Date:

Signature

NOMENCLATURE - Symbols Explanations

A_N	Nominal Total Sail [m ²]	$H_{\text{mast}}/\text{ISP}$	Mast height [m]
$A_{N \text{ fore}}$	Nominal Fore Sail area [m ²]	HA	Heeling Arm [m]
$A_{N \text{ jib}}$	Nominal Jib Sail area [m ²]	HBI	Height of base I [m]
$A_{N \text{ main}}$	Nominal Main Sail area [m ²]	Ht	Freebord to base of I [m]
ABS	Acrylonitrile Butadiene Styrene	I	Jib leech [m]
AR_e	Effective Aspect Ratio [-]	ITTC	International Towing Tank Conference
AR_g	Geometric Aspect Ratio [-]	IMOCA	International Monohull Open Class Association
AWA	Apparent Wind Angle [deg]		
AWS	Apparent Wind Speed [knots]	J	Jib foot [m]
b	Span [m]	(k+1)	Form Factor [-]
BAD	Boom above deck [m]	KSF	Keel Side Force [N]
B_{OA}	Beam Over all [m]	L	Lift force [N]
B_{WL}	Beam at Waterline [m]	L_α	Leeway angle [deg]
c	Chord [m]	L_{OA}	Length OverAll [m]
C_D	Drag Coefficient [-]	L_{WL}	Waterline Length [m]
C_F	Frictional Resistance Coefficient [-]	LCB	Longitudinal Centre of Buoyancy
C_L	Lift Coefficient [-]	LCF	Longitudinal Center of Floatation
C_R	Residual Resistance Coefficient [-]	LP	Jib luff perpendicular [m]
CE	Center of Effort	LPP	Length Between Perpendicular [m]
CFD	Computational Fluid Dynamics	NACA	National Advisory Committee for Aeronautics
CLR	Centre of Lateral Resistance		
CNC	Computer Numerical Control	P	Pressure [Pa]
D	Drag force [N]	P	Main luff [m]
DSS	Dynamic Stability System	Re	Reynolds Number [-]
DSYHS	Delft Systematic Yacht Hull Series	R_h	Heel Resistance [N]
		R_i	Induced Drag [N]
E	Main foot [m]	R_t	Total Resistance [N]
Fr	Froude Number [-]	R_u	Upright Resistance [N]

R_v	Viscous Resistance [N]	TWA	True Wind Angle [deg]
R_w	Wave Resistance [N]	TWS	True Wind Speed [knots]
RM	Righting Moment [N.m]	V	Volume [m ³]
S	Planform area [m ²]	V_B	Boat speed [knots]
SA	Sail Area [m ²]	V_M	Model Velocity [m/s]
SF	Side Force [N]	V_S	Ship Velocity [m/s]
SLA	Stereolithography	VMG	Velocity Made Good [m/s]
SSF	Sail Side Force [N]	WSA	Wetted Surface Area [m ²]
STIX	Stability Index	α	Angle of Attack [deg]
t	thickness [mm]	θ	Heel angle [deg]
t/c	thickness to chord ratio	λ	Scale Factor [-]
Tc	Canoe body draft [m]	μ	Dynamic Viscosity [kg.s ⁻¹ .m ⁻¹]
Te	Effective Draft [-]	ν	Kinematic Viscosity [m ² .s ⁻¹]
Tk	Keel Draft [m]	ρ	Density [kg.m ⁻³]
Tr	Draft rudder [m]	Δ	Displacement [kg]
TR	Taper Ratio [-]		

1. INTRODUCTION

The main objective of this master thesis is to study the effect and advantages of hydrofoils on a cruising sailing monohull yacht. To do so, the work during the internship was to combine the design of a standard monohull cruising yacht with different foils and the hydrodynamic analysis by an experimental approach in Southampton Solent University's towing tank facilities.

Today is the “*age of foil assisted sailing*” [2] in racing as well as in cruising yachts. Usually, the foils have most interest on the racing yachts since there is a high demand for races such as Vendée Globe, or the American's Cup. Indeed, the big advantage with the integration of hydrofoils on racing yachts is the gain in performance and velocity for particular points of sailing and the improvement of stability and seakeeping behaviour. The cruising yacht domain was chosen for the following reasons: lack of cruising yachts with foils, design challenge and performance and comfort criteria. First of all, very few cruising yachts are equipped with foils, so the research area in this field is still to be explored further. Then, one particular design issue will be to draw the interior design, taking into account the integration of foils. Finally, the performance and comfort criteria are a main concern for cruising yachts owners. The hydrodynamics and stability improvements provided by hydrofoils on a cruising yacht is therefore of huge interest.

In this master thesis, the design of the sailing yacht and hydrofoils is first developed. The design of the yacht is based on a generic boat type configuration such as a 50 feet monohull cruising yacht. Three very different types of foils are designed, and modelled: Dynamic Stability System (DSS) foils illustrated in Figure 14, Dali-moustache foils illustrated in Figure 12 and the Chistera foils of the new *Figaro 3 Bénéteau* racing yacht illustrated in Figure 13.

Then, the hydrodynamic analysis performed by an experimental approach is described. In order to perform the tests, the hull model, keel and three different types of hydrofoil had to be built, based on the drawings, in Southampton Solent's workshop facility. Then, the model could be tested in Southampton Solent University's towing tank, following ITTC (International Towing Tank Committee) recommended procedures [2]. The resistance, side force, heave and trim were measured in the tank, and the lift, resistance, and effective draft were quantified in a pure hydrodynamic analysis, allowing to highlight the impact of foils on hydrodynamic performance. Because of time constraint, the stability and seakeeping impact could not be analysed, but are suggested as further work.

2. STATE OF THE ART - FOIL ASSISTED SAILING YACHTS

2.1. The Aim of Hydrofoils - Introduction to Foil Theory

The hydrofoil usually consists of a wing-like structure immersed in the water and mounted on the hull, or across the keels for catamaran. They are similar in appearance and purpose to aerofoil used by airplanes. The foil, which is placed in an oncoming fluid at a specified angle of attack (Figure 1), produce forces that can be shown to be dependent on the foil planform area 'S', the dynamic pressure in the flow according to the Bernoulli's equation (Eq. 1). There is an equilibrium depending on the pressure P and velocity values. These parameters have opposite relation in the Bernoulli's equation to keep it constant.

$$P \text{ (Static)} + 1/2 \rho V^2 \text{ (Dynamic)} + \rho g z \text{ (Hydrostatic)} = P_0 \quad \text{Eq. 1}$$

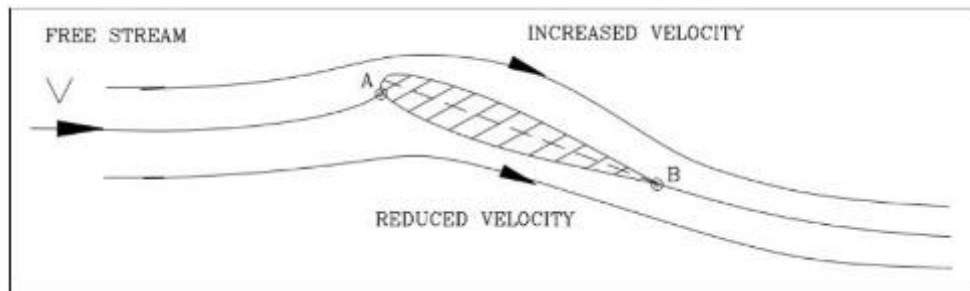


Figure 1: Velocity difference around a foil structure in a free stream [3]

Deflection effect of the foil on the free stream and pressure difference (Figure 2) generates the two forces which are the lift L and drag D (Figure 3).

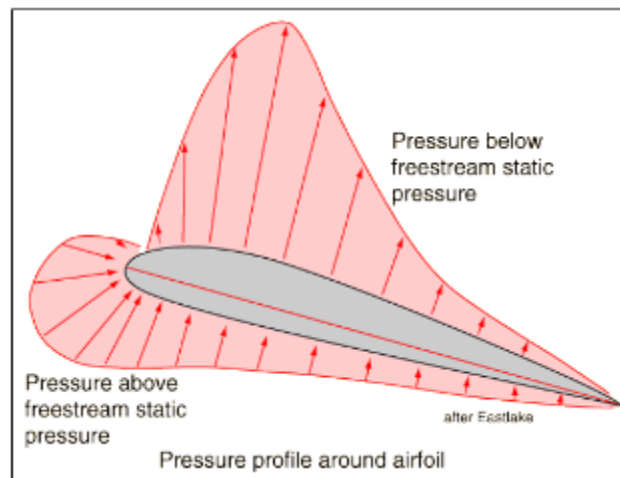


Figure 2: Pressure profile around foil [3]

The lift force is generated because of the foil's angle of attack and shape, and is perpendicular to the free stream. Due to the solid structure of it, there is also a drag force, which is parallel to the free flow.

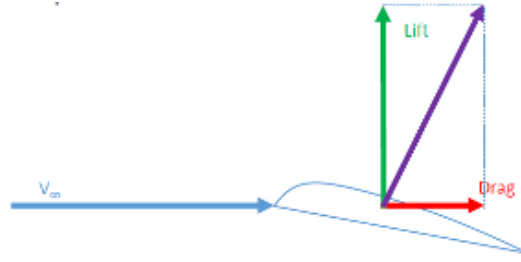


Figure 3: Lift and Drag forces. 2D foil theory [4].

A 2D foil produces the lift and drag forces as shown in Eq. 2 and Eq. 3:

$$L = 1/2 \rho V^2 S C_L \quad \text{Eq. 2}$$

$$D = 1/2 \rho V^2 S C_D \quad \text{Eq. 3}$$

with its non-dimensional lift and drag coefficients C_L and C_D

A 2D hydrofoil represents a 3D wing of infinite span, however real foils are not of infinite aspect ratio and therefore the effect of flow near the tips of the foil is considered.

For that reason, the flow around tips of the foil is induced because of the pressure differences between the bottom and top surfaces of the foil. Therefore, tip vortex will occur across the chord length of the foil, and the tip vortex streaming will have increase with the flow interaction between the tip and the chord length of the foil at the trailing edge tip (Figure 4).

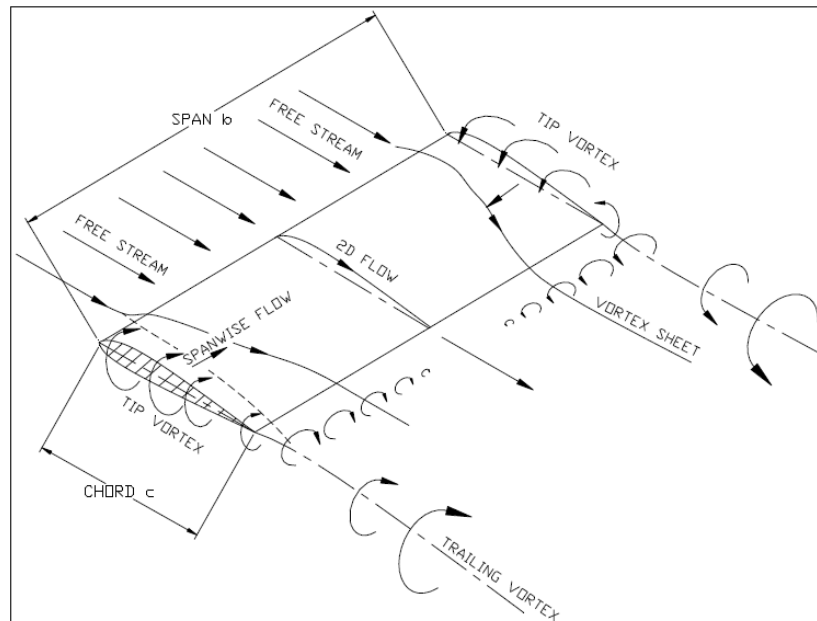


Figure 4: 3D foil theory - Vortexes around a 3D foil [3].

The effects of wingtip vortices are known to decrease foil lift (downwash) and increase drag (induced drag), see on Figure 5. The induced drag D_I is induced by the trailing vortices which are produced when a 3D foil generates lift and is proportional to the lift squared (Eq. 4).

$$C_{DI} = C_L^2 / (\pi \cdot AR_G) \quad \text{Eq. 4}$$

with $AR_G = b^2/S$, geometric aspect ratio.

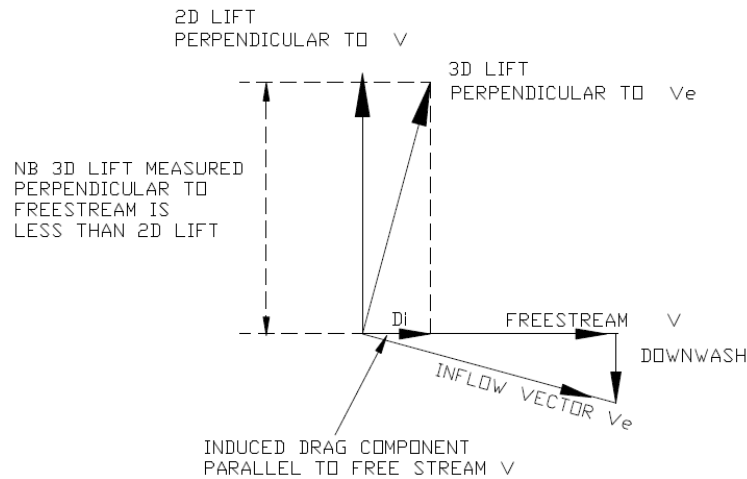


Figure 5: 3D foil theory. Induce drag and downwash generation [3].

As a hydrofoil-equipped watercraft increases in speed, the hydrofoil elements below the hull(s) develop enough lift to raise the hull, which reduces hull drag or hydrodynamic resistance as shown in Figure 6. This provides a corresponding increase in speed and fuel efficiency. But as shown in Figure 6, there is also a penalty in the resistance at low speeds because of the added wetted surface area (WSA) of the foil in the water.

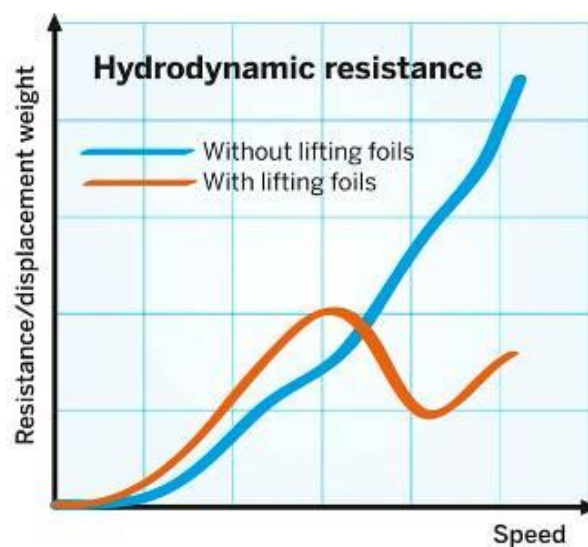


Figure 6: Hydrodynamic resistance with and without foils [5].

Hydrofoils can be split in two categories:

- Surface piercing foils: or V-shape foils whose tips pierce through the water surface and are therefore self adjusted thanks to a dynamic reduction in wetted surface area (Figure 7).

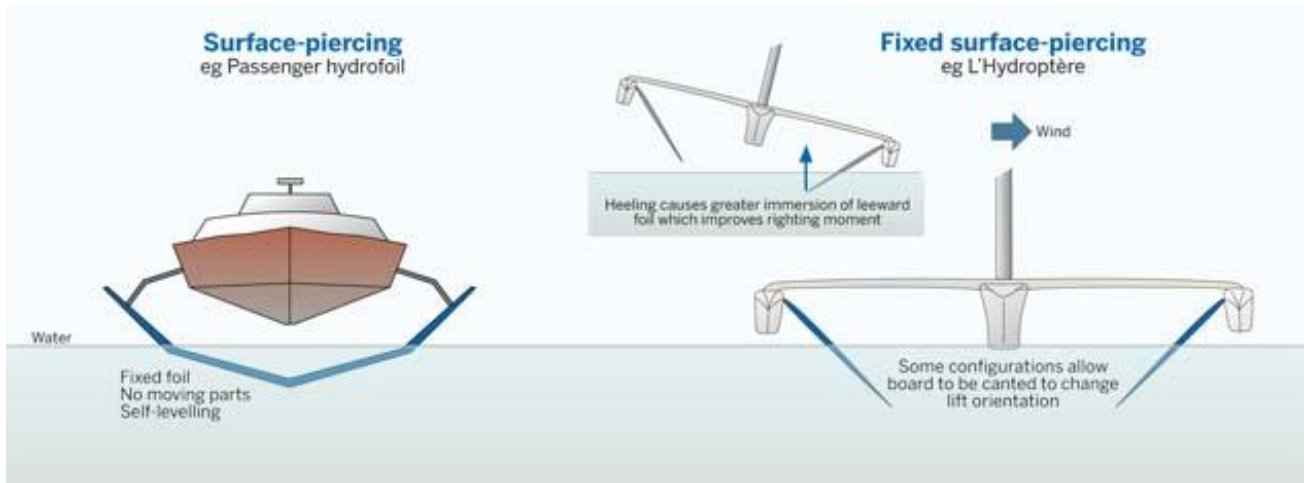


Figure 7: V-shape foil [6].

- Submerged foils: or T-shape foils whose is completely submerged in the water. Those type of foil have initiated the Y, L, U or O-shape foils. The ride high is kept constant by varying the lift coefficient, and thus requires a mechanical system to control the elevator tab (Figure 8).

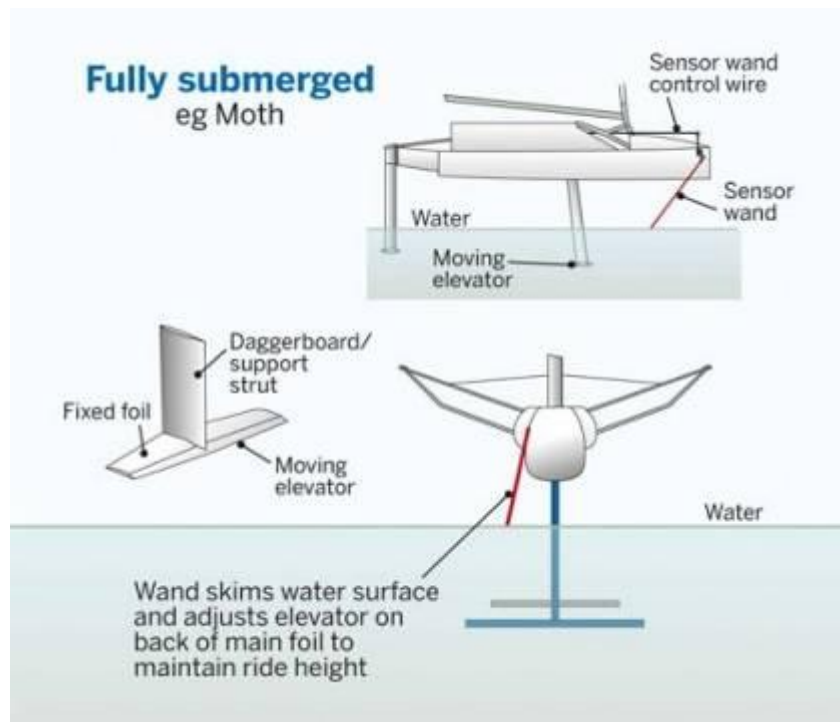


Figure 8: T-shape foil [7].

2.2.History: The First Boats Equipped With Hydrofoils

Nowadays, foils are very fashionable in yacht design, but hydrofoils have been used on different watercraft for 100 years.

The first hydrofoil boat was designed and built in 1906 by Enrico Forlanini (Figure 9). It had a classic Ladder type construction with multiple struts coming down with multiple wings between each of them.



Figure 9: Hydrofoil boat 1910 Forlanini: Lake Maggiore [1].

In sailing yacht design, the first hydrofoils appeared in the 70's on multihull yachts with Icarus catamaran and Eric Tabarly trimaran (Figure 10).



Figure 10: Icarus catamaran, 1969 (left) and Eric Tabarly trimaran, 1976 (right) [8].

More recently, the Hydroptère, an experimental sailing hydrofoil trimaran was designed by French yachtsman Alain Thébault and VPLP design. On 4 September 2009, the Hydroptère broke the outright world record, sustaining a speed of 52.86 knots for 500 m in 30 knots of wind.

2.3. The Different Types of Hydrofoils on Monohull Sailing Yacht Nowadays

Until today, very few monohull could fly over the water (except from the flying Moth). An exciting new era in America's Cup racing has been unveiled, as the concept for the AC75 (Figure 11), to be sailed in the 36th America's Cup is released. This incredible new flying monohull could be faster than the AC50 catamarans.



Figure 11: The fully foiling 75-foot concept for the AC75 (Virtual Eye) [9].

In this master thesis, three types of hydrofoils already present on existing monohulls will be tackled:

- "Dali-moustache" foils from *Safran II* racing yacht (Figure 12),
- "Chistera" foils from the new *Bénéteau Figaro 3* racing yacht (Figure 13),
- Dynamic Stability System (DSS) foils from *Infiniti 56C* cruising/racing yacht (Figure 14).

Those foils only make the hull rise slightly and not completely out of the water. The thinking is that instead of lifting the boats fully out of the water, foils are used to increase power by generating more righting moment. It is also reducing the weight on the hull, hence the drag and the heel, and increase the speed of the boat.

Below is shown a general representation of the three systems mentioned above. Further description is done later in the report in sections 2.3.1, 2.3.2, and 2.3.3.



Figure 12: Safran II (2015, VPLP and Guillaume Verdier design) equipped with "Dali Moustache" foils [10].



Figure 13: Bénéteau Figaro 3 (2017, VPLP design and Bénéteau) equipped with foils [11].

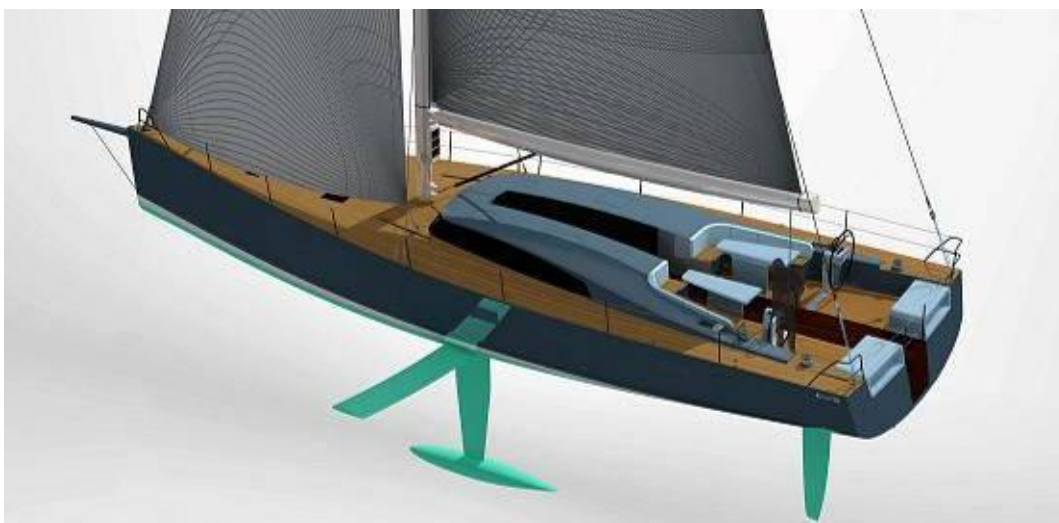


Figure 14: Infiniti 56C (2017, Farr Yacht design and Infiniti Performance Yachts) equipped with DSS foils (Virtual View) [12].

2.3.1. "Dali Moustache" Foils on IMOCA 60 Racing Yachts

The Vendée Globe race always brings innovations in order to gain in speed to win the race. For this purpose, foiling daggerboards innovation were developed and applied to a new generation of IMOCA 60. The first monohull to test the hydrofoils was *Safran II*. This boat equipped with V-shape foiling daggerboards (Figure 15), which looked somewhat like Salvador Dali's moustache, hence the name, has led the way. Other five VPLP-Verdier designed boats were launched and are also equipped with the same daggerboard: *Banque Populaire*, *Edmond de Rothschild*, *Hugo Boss*, *Vento di Sardegna* and *St Michel-Virbac*.

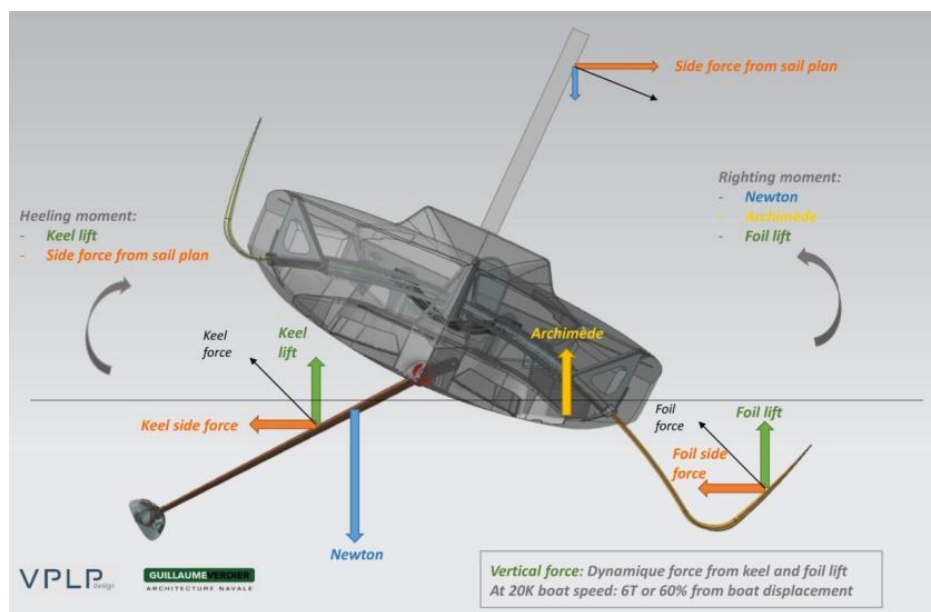


Figure 15: Dali moustache foils - Section view [13].

The *Safran II* racing yacht is equipped with five appendages as imposed by the IMOCA class rules: two movable foiling daggerboards, an articulating canting keel, and two rudders.

The V-shape foiling daggerboard is composed of a shaft and a tip (Figure 16). The foil is immersed on the same side as the sail to limit the amount of heel with the tip offering lift to the boat which sails higher in the air, reducing the wetted surface area, hence the effective displacement of the yacht, and therefore the drag.

The curved foil configuration have a bound section which joins the straight shaft (vertical lift force part) and curved tip (horizontal side force part) parts of the daggerboard and it prevents the tip vortices, therefore, it has less induced drag due to the joint section.



Figure 16: Movable foiling daggerboard [10].

The foil supplements the effect of the canting keel, which already takes the weight of the hull by providing lift (Figure 17).

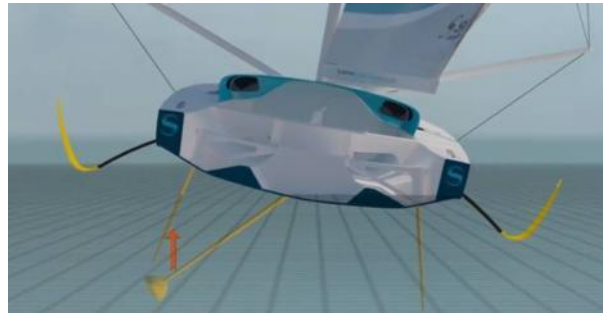


Figure 17: Articulating keel [10].

This force in the opposite direction increases with the speed, and gradually the boat raises out of the water. The result: an incredible gain in speed. These foils are believed to add as much as 1-2 knots in power reaching conditions, but due to the limitations of the class to five appendages (so swapping daggerboards for foils) the new boats are said to be at their weakest upwind.

The other advantage of this foils is that it reduces significantly the pitch angle of the boat, which enables a great stability under autopilot and improves safety.

The only disadvantage of this kind of foils is that usually, they are not as efficient in upwind conditions and in light winds. However during the Vendée Globe race, these situations rarely happens.

This is explained by the fact that the foil, adding wetted surface area, has an impact on the drag. Moreover, the low heel angle does not allow much side force generation from the foils and a high leeway results from this.

Last year, Teksen Aygor, an EMSHIP student, also studied the hydrodynamic efficiency of this curved V-shape foil on an IMOCA hull model in Southampton Solent University towing tank [14]. He compared the results with those of a straight daggerboard.

Based on the results of the tests, he could analyse that the efficiency of the curved foil configurations are not good enough in the upwind condition as compared to the straight daggerboard configuration based on the effective draft values (ratio between drag force and side force squared). However, the curved foil configurations generate considerably more lift

force than the straight vertical foil or daggerboard configuration in same sailing conditions based on the model heave analysis. Therefore, the lifting advantage of the curved foil is important to get less displacement (less wetted surface area and total resistance) so it provides more boat speed. Therefore a lighter boat with less hydrodynamicly efficient foils is actually better than a heavy boat with more efficient daggerboard.

Also, it was found that the angle of attack, which was kept same for both curved and straight configurations, was not great enough to generate side force for the curved daggerboards so it required more leeway angle for producing the side force. It was recommended for future work that the optimum angle of attack of the curved configuration could be higher than for a straight shape foil in order to generate more side force value without increasing the leeway angle. In this master thesis, these recommendations have been taken into account.

2.3.2. "Chistera" foils on the New Figaro 3 Bénéteau RacingYacht

Bénéteau has launched the new Figaro 3, a 35 feet racing sailing yacht designed by VPLP design firm. The first trials took place in summer 2017. In contrast to the foils on the IMOCA 60, the latter has an inward-facing (Figure 18) as Vincent Lauriot-Prévost, naval architect in VPLP explains: «*The versatile foil we've created provides more than just the dynamic power and vertical lift that is sought after in IMOCA. We've designed it in such a way that it creates as little resistance as possible in the light airs and reduces leeway at full speed.*» [15]

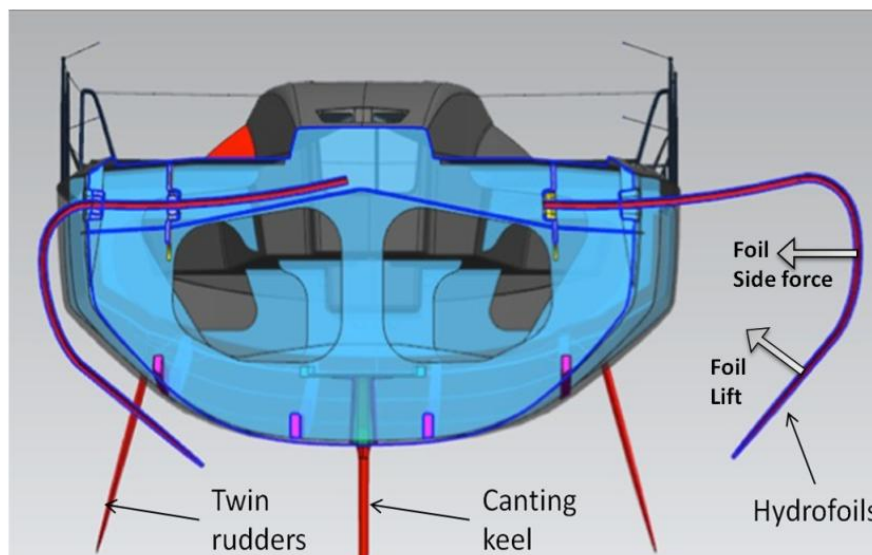


Figure 18: Figaro 3 Chistera foils - Cross section view [16].

These new foils are designed to replace the traditional weighty ballast tanks used on past Figaro models. Described as ‘asymmetric tip foils’ they work by creating side force to supplement the skinny keel and reduce leeway while causing minimal drag. An important factor is that they are able to retract within the boat’s maximum beam. In this master thesis, the same idea will be followed on the design of the cruising yacht because of the marine mooring implication and the also because of the impact on drag. The Figure 19 shows the lines plan of this new racing yacht.

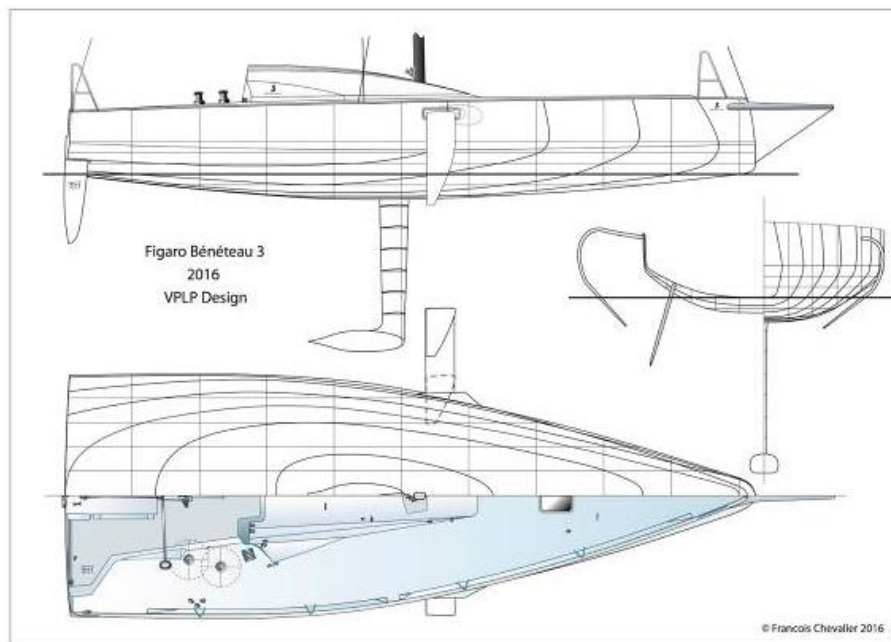


Figure 19: Technical drawing of Figaro Bénéteau 3 (2016, VPLP design) [17].

According to designers and naval architects, the *Figaro 3* with foils is expected to be up to 15 percent faster than its predecessor *Figaro 1* and *Figaro 2*.

2.3.3. DSS foils on *Infiniti 56C* cruising yachts

The *Infiniti 56C* is a new cruising yacht designed by Farr Yacht Design. This is the first performance blue water cruiser in the market which will be equipped with Dynamic Stability Systems (DSS), a single transverse foil (Figure 20). Based on the *Infiniti 36R* (Figure 21) or *Infiniti 46R* racing foiling yachts, it is now available for performance cruising.

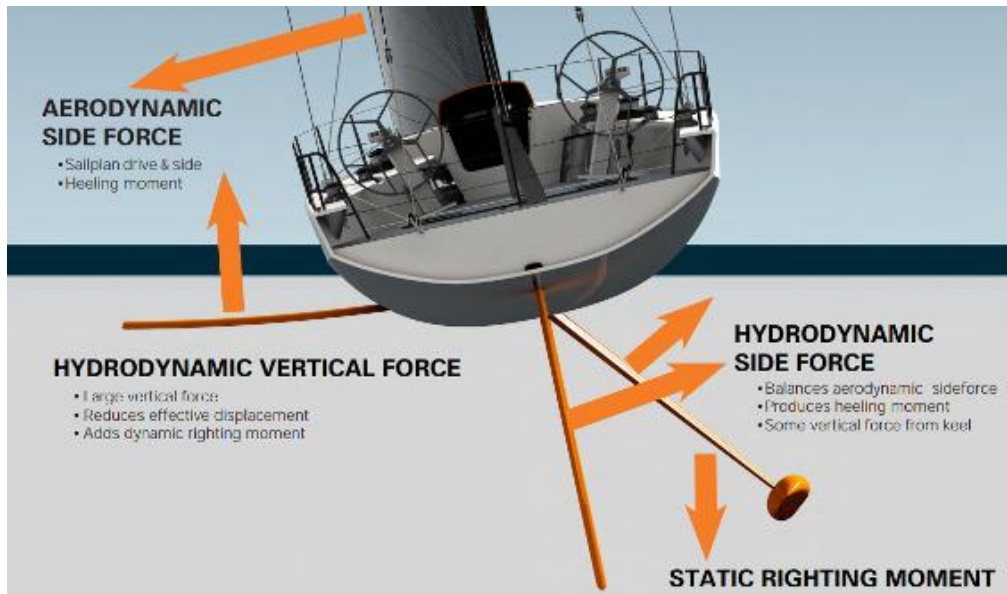


Figure 20: DSS foil - Flat shape - Section view [18].



Figure 21: DSS foil on Infiniti 36 racing yacht [19].

The DSS (Dynamic Stability System) foil is a retractable transverse foil that is deployed to leeward, creating lift to leeward and then increasing the righting moment to counter the heeling generated from the sails. Unlike the Figaro and Dali foils, the DSS only provides vertical lift force since it only has a straight shaft.

The stronger the wind, the faster the yacht, and the more lift and stability is generated, limited to small heel angles. In light wind condition, the DSS foil is retracted, leaving an easily driven hull to reduce drag. Compared to IMOCA 60 foils, the DSS foil is more "intelligent" because it can be totally retracted in the hull, and then does not generate any drag when the foil is not needed.

The *Infiniti 56C* equipped with DSS foils can be 10 to 30 percent faster than a comparable performance cruiser without DSS depending on the point of sail [2]. It reduces the heel by as much as 10 to 12 degrees, as well as the pitching moment, allowing a more comfortable cruise. It is expected to be more efficient when sailing downwind.

3. METHODOLOGY AND PLANNING

3.1. Content, Resources and Objectives

The master thesis is divided into two main subjects: the design of the foiling cruising yacht, and the hydrodynamic analysis based on experimental at acquired in the towing tank.

The first step is obviously to design the sailing yacht and the hydrofoils at full scale. The design has to follow the design spiral [20].

The second step is to adapt the design of the designed yacht equipped with foils from full scale to model scale, in order to build a hull model and hydrofoils models to be tested in towing tank. Finally, the results of the resistance test have to be extrapolated to full scale and analysed.

Hereafter is described the methodology, the main characteristics, the main issues of each part, and the resources needed for the design part and for the experimental part.

3.1.1. Design of a Foiling Cruising Yacht

The first step of the design is to define the main specifications of the vessel in as much details as possible. This step is called the Design brief or Design statement (Table 1).

Table 1: Design brief

Define the problem	The aim is to design a sailing yacht for cruising, equipped with hydrofoils.
Sailing programme	<ul style="list-style-type: none"> ▪ Cruising, few weeks, offshore (Mediterranean sea, Northern, Caribbean) ▪ Main cruising speed: 8 to 14 knots
Boat's type and main characteristics	<ul style="list-style-type: none"> ▪ Type: Sailing yacht, Monohull ▪ Design category: A category (Ocean category) [21] with ISO standards certification ▪ Length overall: LOA = 50 feet (i.e. 15 meters) ▪ Passengers: 6 ▪ General Arrangement: 1 configuration (3 cabins, 2/3 bathrooms, 1 kitchen and living room) ▪ Hull material: Fibreglass composite ▪ Sail and rig design: Sloop rig, aluminium ▪ Appendages: Lifting keel (3.6 m maximum draft, 2.1 m minimum draft), twin rudders, hydrofoils ▪ Powering: Saildrive engine

Hydrofoil option configurations	<ul style="list-style-type: none"> ▪ Dali moustache ▪ Chistera Figaro 3 ▪ Dynamic Stability System
Design restrictions and challenges	<p>The three different types of hydrofoil must be integrated within the same structure and interior design.</p> <p>Comfort must also be taken into consideration as it is a cruiser.</p>
Design tools	<ul style="list-style-type: none"> ▪ CAD (Computer Aided Design): AutoCAD [22], Maxsurf Modeler[23], Rhinoceros [24]. ▪ Delft Systematic Hull Yacht Series (DSHYS) [25] ▪ Scantling/Hull Structure: Hullscant [26] ▪ Resistance: Maxsurf Resistance [27] ▪ Stability: Maxsurf Stability [28] ▪ Velocity Prediction Programme: WinDesign VPP [29], Maxsurf VPP [30]
Rules and regulations	<ul style="list-style-type: none"> ▪ ISO 12215 Part 2 - Small Craft - Hull construction and scantlings - Materials: Core materials for sandwich construction, embedded materials [31] ▪ ISO 12215 Part 5 - Small Craft - Hull construction and scantlings - Design pressures for monohulls, design stresses, scantlings determination [32] ▪ ISO 12215 Part 9 - Small Craft - Hull construction and scantlings - Sailing Craft Appendages [33] ▪ ISO 12217 Part 2 - Small Craft - Stability and buoyancy assessment and categorization - Sailing boats oh hull length greater than or equal to 6 m [34] ▪ Nordic Boat Standard [20]

3.1.2. Hydrodynamic Analysis - Experimental Approach

As well as for the design part, Table 2 above defines the specifications and procedures that are used in order to achieve the experimental hydrodynamic analysis.

Before running the model in the towing tank for resistance tests, it has to be manufactured in Southampton Solent University's workshop. The manufacturing was a significant part of the internship, undertaken with the collaboration of the professors and students in Southampton Solent University.

Based on the design drawings, one hull model was built and tested in towing tank, to which three sets of 3D printed foils can be attached. See further detail and illustrations on the construction of the model in section 5.1.2.

Keeping the same hull model guarantees better results as the hull shape is always the same, and only the foils are changing. Five different configurations are tested in towing tank:

- the bare hull,
- the hull equipped with the keel,
- and the hull equipped with the keel and each hydrofoil are chosen for the study.

For each configuration, hydrodynamic results were measured on the model, and extrapolated to full scale (Figure 22).

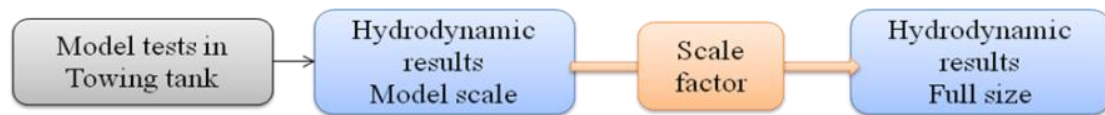


Figure 22: From model testing to full scale extrapolation. Own elaboration.

Table 2: Experimental approach brief

Definition of the problem	<p>The aim of the experimental approach is to test a model based on the full scale designed in the previous part: hull, keel and hydrofoils.</p> <p>The model is tested with and without foils in order to be able to deduce the impact of foils on sailing. The aim is to determine which foil is better for the boat, according to the owner's requirement.</p>
Manufacturing and materials of the model hull, keel and hydrofoils	<ul style="list-style-type: none"> ▪ Scale factor: $\lambda = 10$ ▪ Hull model length: 1.52 meters ▪ Hull model manufacture steps: 3D milled in Polystyrene, hand laminated with Fibreglass and Epoxy Resin, and painted with primer. ▪ Keel and bulb model manufacture steps: <ul style="list-style-type: none"> ○ Fin keel: Plywood laminates glued and sanded to the correct foiled section. ○ Bulb: 3D printed in Epoxy and painted with primer ▪ Hydrofoil models manufacture steps: 3D printed in Epoxy and vacuumed bagged with Carbon fibre and Resin. ▪ Attachment of the foils on the hull model: Threaded rods and nut system. ▪ Simulation of turbulent flow on the hull, keel, bulb and foils: Sand paper strips is installed to ensure transition is achieved in a similar location as on the real boat despite testing at a lower Reynolds number Re.
Towing tank testing	<ul style="list-style-type: none"> ▪ Number of runs: 402 (+144 for angle of attack comparison) ▪ 5 different model configurations: bare hull, hull with keel, hull with keel and foils (x3)

	<ul style="list-style-type: none"> ▪ 6 Froude numbers: from $Fr = 0.35$ to $Fr = 0.7$ ▪ 2 heel angles: $\theta = 10$ and 20 degrees ▪ 4 leeway angles: $\lambda = 0, 2, 4$ and 6 degrees
Challenges and expectations	<p>The manufacturing and towing tank testing are time consuming but are part of the process.</p> <p>The different experimental tests configurations should reproduce the real sailing conditions.</p> <p>According to the type of hydrofoil, it should provide lift, righting moment and side force during sailing. The addition of side force aims to supply the one of the keel during, and the lift will reduce the wetted surface area of the hull, and therefore the resistance.</p>
Computer software, companies and university facilities	<ul style="list-style-type: none"> ▪ Model hull and foils design: CAD (Computer Aided Design) software: AutoCAD, Maxsurf Modeler, Rhinoceros. ▪ Velocity Prediction Programme: VPP WinDesign, Maxsurf VPP ▪ Test matrix: Microsoft Excel ▪ Hull 3D printing: Monstercam company, Lee-on-the-Solent, UK, http://www.monstercam.co.uk/ ▪ Foils and bulb 3D printing: 3D printed by stereo lithography in ABS resin - Southampton Solent University 3D printing facility. ▪ Manufacturing: Southampton Solent university composite workshop, personal contribution to the manufacturing with the help of Pr. Soupez and Jack Cunningham-Burley ▪ Towing tank Test: Southampton Solent University Towing tank, personal contribution with the help of students and professors.
Regulatory frameworks: ITTC Recommended Procedure and Guidelines	<ul style="list-style-type: none"> ▪ ITTC 75-01-01-01 - Ship Models [35] ▪ ITTC 75-02-02-01 - Resistance Test [36] ▪ ITTC 5-02-02-02 - General guideline for uncertainty analysis in Resistance tests [37] ▪ ITTC 75-02-03-014 - 1978 ITTC Performance prediction method [38]

3.2.GANTT Diagram

The Figure 23 above shows briefly the different activities done during and after the internship in Southampton Solent University.

A Gantt diagram in APPENDIX A1: GANTT DIAGRAM details the time allowed for each activity.

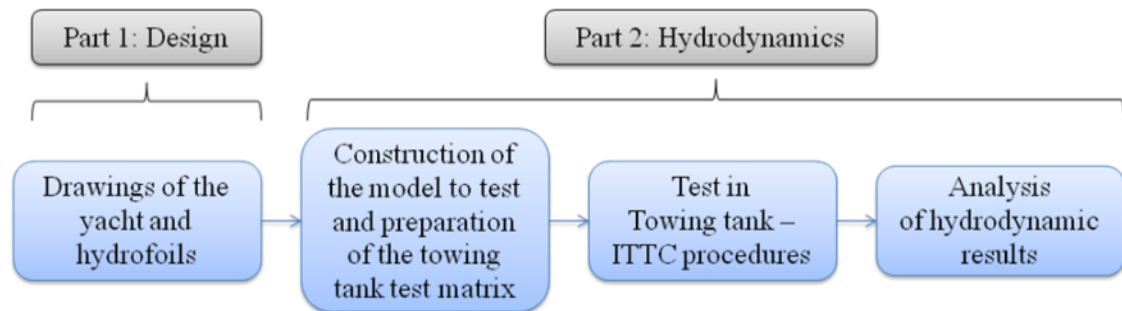


Figure 23: Activities done for the master thesis. Own elaboration.

4. PART 1: DESIGN OF A SAILING CRUISING YACHT WITH HYDROFOILS

The first part of the master thesis is to design the sailing yacht and the different types of hydrofoils. As stated in section 3.1.1, the main challenge on a design point of view is to integrate the different types of hydrofoil, having a minimum impact on the interior design, layout, and hull structure. The impact of the different foil configuration on the design will be evaluated and compared.

During all the design, the drawings have to be as flexible as possible, in order to be able to adapt the different mechanisms of foils.

The preliminary design and detailed design will be described in this part.

4.1. Preliminary Design

For the preliminary design, the following considerations have been made:

1. define the intended use and limits of the design in the Design Brief (Table 1),
2. complete a parametric study, collect and compare information of sailing monohulls and use the key design ratio to assess further dimensions on the preliminary layout and exterior of the yacht,
3. ascertain a first weight estimation,
4. compare the main dimensions of the yacht with the first estimation made with key design ratios and correct if necessary,
5. produce a preliminary design to work from.

The parametric study is the very beginning of the preliminary design. It consists in collecting the main dimensions of existing sailing yacht from builder website and magazines and from this analysis the following design ratios are defined:

- LOA / LWL ratio
- Length / Beam ratio
- Slenderness ratio (or Length to displacement ratio)
- Sail Area / Displacement ratio
- Ballast / Displacement ratio

See the definition and value of the key design ratios in Table 3.

In this master thesis, the cruising yacht has a length of 50 feet, so it was decided to study especially yachts having a length between 45 and 55 feet, with or without foils, racing or

cruising. The design ratio curves are shown in APPENDIX A2: KEY DESIGN RATIO FROM PARAMETRIC STUDY.

Table 3: Key design ratios

Item	Abbreviation	Value
Water length to length overall ratio	L_{WL} / L_{OA}	0.94
Length to Beam ratio	L_{WL} / B_{WL}	3.28
Beam to draft ratio	B_{WL} / T_k	1.25
Slenderness ratio	$L_{WL} / \Delta_c^{1/3}$	6.5
Sail area to displacement ratio	$SA / \Delta_c^{2/3}$	29
Ballast to displacement ratio	Ballast / Δ_c	0.3

Then, the preliminary dimensions to work from can be deduced (Table 4).

Table 4: First approximation for the dimensions of the sailing yacht

Item	Abbreviation	Value	Unit
Length overall	L_{OA}	15.22	<i>m</i>
Waterline length	L_{WL}	14.31	<i>m</i>
Beam Overall	B_{OA}	4.4	<i>m</i>
Maximum keel draft	$T_k \text{ max}$	3.5	<i>m</i>
Volume of the hull	V_c	10.66	m^3
Hull displacement	Δ_c	10930	<i>kg</i>
Upwind sail area	Upwind SA	140.49	m^2
Ballast	Ballast	3278.93	<i>kg</i>

4.2.Detailed Design

Then detail design is performed based on preliminary design main dimensions (Table 4), and following the design spiral (Figure 24). As said before, the main challenge of the design is to be able to install the three configuration of hydrofoils chosen for this master thesis on the same designed sailing yacht.

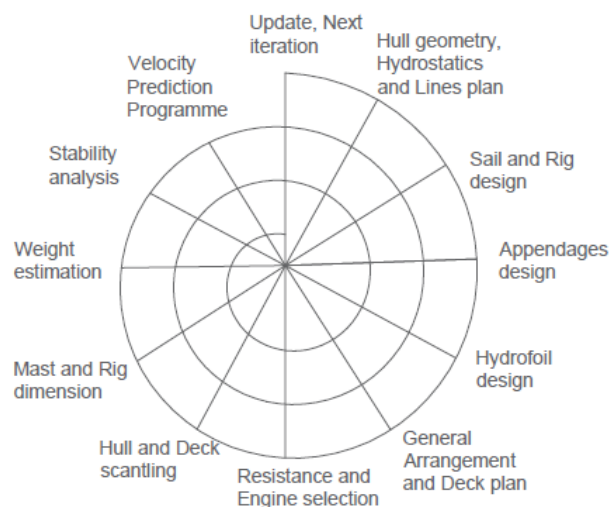


Figure 24: Design spiral. Own elaboration.

The hydrofoils design is performed in the same time as the keel and rudder design step. As mentioned in section 3.1.1, the aim of this master thesis is not to optimize the design of a foil, but to compare three existing shapes already used in racing. As a result, the designed shapes are issued from a parametric study and adapted to the dimensions of the cruising yacht. In this part, only the final versions are shown, the details are shown in the Appendices.

4.2.1. Hull Geometry, Hydrostatics and Lines Plan

In order to design the hull geometry, the software Maxsurf Modeler [23] was used. Taking the first dimensions from the preliminary design (Table 4), the general shape of the hull was enveloped, and rearranged as wanted, trying to keep the waterline length, beam and displacement as close as possible to the values defined in preliminary design. Table 5 shows the final dimensions and hydrostatics characteristics of the hull.

Table 5: Main dimensions and hydrostatics of the hull

Item	Abbreviation	Value	Unit
Length Overall	L_{OA}	15.22	<i>m</i>
Beam Overall	B_{OA}	4.72	<i>m</i>
Hull Depth	D	2.30	<i>m</i>
Length at waterline	L_{WL}	14.35	<i>m</i>
Beam at waterline	B_{WL}	3.43	<i>m</i>
Canoe body Draft	T_C	0.60	<i>m</i>
Displacement hull	Δ_C	11.5	<i>tons</i>
Longitudinal Centre of Buoyancy	LCB %	51.96	<i>from zero pt. (+ve fwd) % Lwl</i>
Longitudinal Centre of Floatation	LCF %	47.88	<i>from zero pt. (+ve fwd) % Lwl</i>
Prismatic coefficient	C_p	0.54	-
Midship area coefficient	C_m	0.71	-
Block coefficient	C_b	0.38	-
Total 3D true surface area		92.773	<i>m</i> ²
Total Above DWL 3D true surface area		54.116	<i>m</i> ²
Total Below DWL 3D true surface area		38.658	<i>m</i> ²

Since the 70's, TU Delft has used their towing tank to test over 73 sailboat hulls forming the Delft Systematic Yacht Hull Series (DSYHS) [25]. The DSYHS is a regression equations for wetted surfaces of the canoe body.

For the hull design, the hydrostatics may need to be checked against DSYHS, on the one hand to verify that principal dimensions are suitable values, and on the other hand to estimate the wetted surface of the canoe body, which is important for the prediction of viscous resistance R_v . This is particularly relevant to check it in this master thesis since the aim is to test the model of the yacht in towing tank for resistance analysis.

Table 6 shows that the main dimensions and hydrostatics of the hull complies to the standards of Delft series.

Table 6: DSYHS check

<i>Hull form parameters from Maxsurf</i>			<i>Range Delft series</i>	
Parameter	Abbreviation	Value	min	max
Length to beam ratio	L_{WL} / B_{WL}	4.18	2.76	5
Beam to draft ratio	B_{WL} / T_c	5.72	2.46	19.32
Slenderness ratio	$L_{WL} / V_c^{1/3}$	6.38	4.34	8.5
Longitudinal centre of Buoyancy	LCB	-7.45 %	0	-8.20%
Longitudinal centre of Floatation	LCF	-6.86 %	-1.80%	-9.50%
Prismatic coefficient	C_p	0.540	0.52	0.6
Midship area coefficient	C_m	0.713	0.65	0.78
Loading factor	$A_w / V_c^{2/3}$	6.860	3.78	12.67
Block coefficient	C_b	0.385	0.338	0.468

Hull lines drawings are presented in APPENDIX A3: HULL LINES GEOMETRY - BARE HULL.

4.2.2. Sailing Equilibrium: Sails and Appendages Design

4.2.2.1. Sail and Rig Design

From the initial parametric study, the maximum upwind sail area (SA) has been fixed to 140.49 m², as driven by the SA/disp. ratio of Table 4. However, this sail area can be seen as slightly low since most of the yacht taken in the parametric study does not take into account the additional forces provided by the hydrofoils. In the parametric study, the SA/D ratio for IMOCA 60 and Figaro racing yachts with and without foils have been compared and it has been found that, for Figaro yachts, the SA/D ratio is increased of 8% when there is foils, and for IMOCA 60, the SA/D ratio is increased of 11%. (Table 7).

Table 7: Parametric study SA/D ratio with and without foils

N	Yacht name	LWL (m)	Δ (kg)	V (m ³)	Upwind SA (m ²)	SA/D ratio
1	<i>Figaro Solo</i>	8.4	2400	2.34	56	31.8
2	<i>Figaro 2</i>	9.82	3050	2.98	68	32.9
Foil 3	Figaro 3	9	2900	2.83	70	35.0
Difference SA/D ratio with or without foils for Figaro =						+8%
1	Quéguiner – Leucémie Espoir	18.28	8000	7.80	300	76.2
2	Safran	18.28	8200	8.00	240	60.0
3	Maitre coq	18.28	7800	7.61	300	77.5
4	Le Souffle du Nord - Projet Imagine	18.28	7700	7.51	340	88.6
Foil 5	Safran II	18.28	6500	6.34	310	90.5
Foil 6	Hugo Boss	18.28	7500	7.32	340	90.2
Foil 7	Edmond de Rothschild	18.28	7600	7.41	290	76.3
Foil 8	Banque Populaire VIII	18.28	7600	7.41	300	78.9
Difference SA/D ratio with or without foils for IMOCA 60 =						+11%

It has been decided then to increase of 9.5% the initial SA/D ratio. Hence, the new SA/D ratio increases from 29 to 31.75 and the new upwind sail area (main sail and jib) is taken as 153.77 m².

It was decided in the design brief to have a sloop rig design, including a main sail, a head sail (or jib) and a spinnaker.

The overall sails and rigs parameter is shown in the Table 8 and Figure 25.

Table 8: Sails and rigs parameters

Item	Abbreviation	Value	Unit
Total sail area	SA _{total}	153.77	m ²
Main sail area	SA _{main}	88.56	m ²
Jib sail area	SA _{jib}	65.21	m ²
Spinnaker sail area	SA _{spin}	240.63	m ²
Mast height	H _{mast/ISP}	22.65	m
Main foot	E	7.19	m
Main luff	P	19.88	m
Jib foot	J	5.94	m
Jib leech	I	20.25	m
Jib luff perpendicular	LP	6.18	m
Boom above deck	BAD	2.10	m
Heigh of base of I	HBI	1.55	m

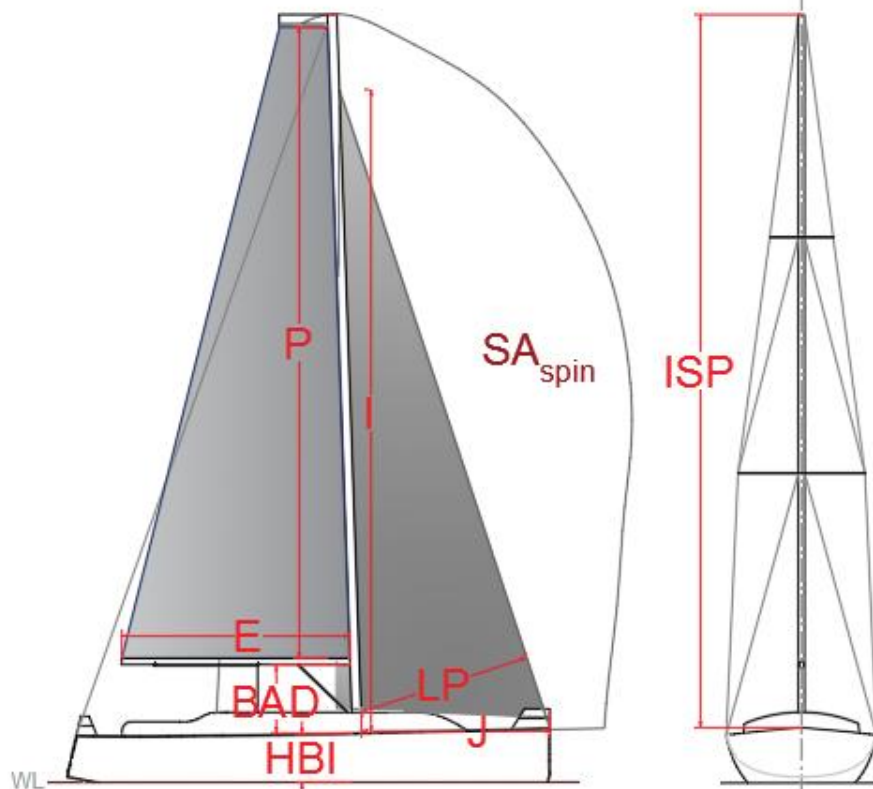


Figure 25: Sail and rig dimensions - Notation. Own elaboration.

The detailed rig dimensions will be described later on in section 4.2.7.

4.2.2.2. *Appendages Design*

First of all must be selected the suitable foil section for these appendages. It was decided that the sailing yacht has a twin rudder and a lifting keel with bulb. The lifting keel was chosen instead of a fixed keel because for a cruising yacht it is very convenient to be able to sail in shallow water. The keel can lift 1.5 m for this yacht, giving us a maximum keel draft $T_{k \max} = 3.6\text{m}$ and a minimum keel draft $T_{k \min} = 2.1\text{ m}$. The main purpose of the bulb is to lower the centre of gravity as much as possible. A twin rudder was selected because, when the boat heels, it is easier to manoeuvre.

The design was first based on the parametric study, and modified according to the keel and rudder area calculated before. The planform and the position of the keel and rudder for the balance also need to be selected.

Selecting a suitable foil section will depend on the required function of the foil. The main concerns are with keels and rudders, both these need to be symmetric sections, but their requirements are fundamentally different. Keels and rudders fulfil differing roles and slight differences in section characteristics are beneficial. Keels are required to generate high side force at low angles of attack with the least possible drag. Rudders are also required to produce high lift and low drag but at large angles of attack, enabling to delay stall. Since the lift curve slope is approximately straight until the onset of separation, the suitable sections are the one which exhibit separation onset at high angles of attack. This will allow the rudder to generate high lift before risk of stall.

Having said that, and according to [39] and [40], the following NACA sections are chosen for the yacht's appendages:

- **Twin rudder: NACA 0012**

4 digit NACA series are often used for rudders in sailing yacht design. The main advantages is that it has a good stall characteristics, a small centre of pressure movement across large speed range, a small effect to roughness [41] (less chance to have cavitation or vibration). Also, it is advised to have a very thin foil section (thickness not less than 9%) to avoid the loss of control, and also not a very thick section (thickness not more than 15%) to avoid high drag. Hence, 12% thickness to chord ratio was chosen. Consider the section C_D/C_L plots from Abbott & Von Doenhoff [40] on Figure 26.

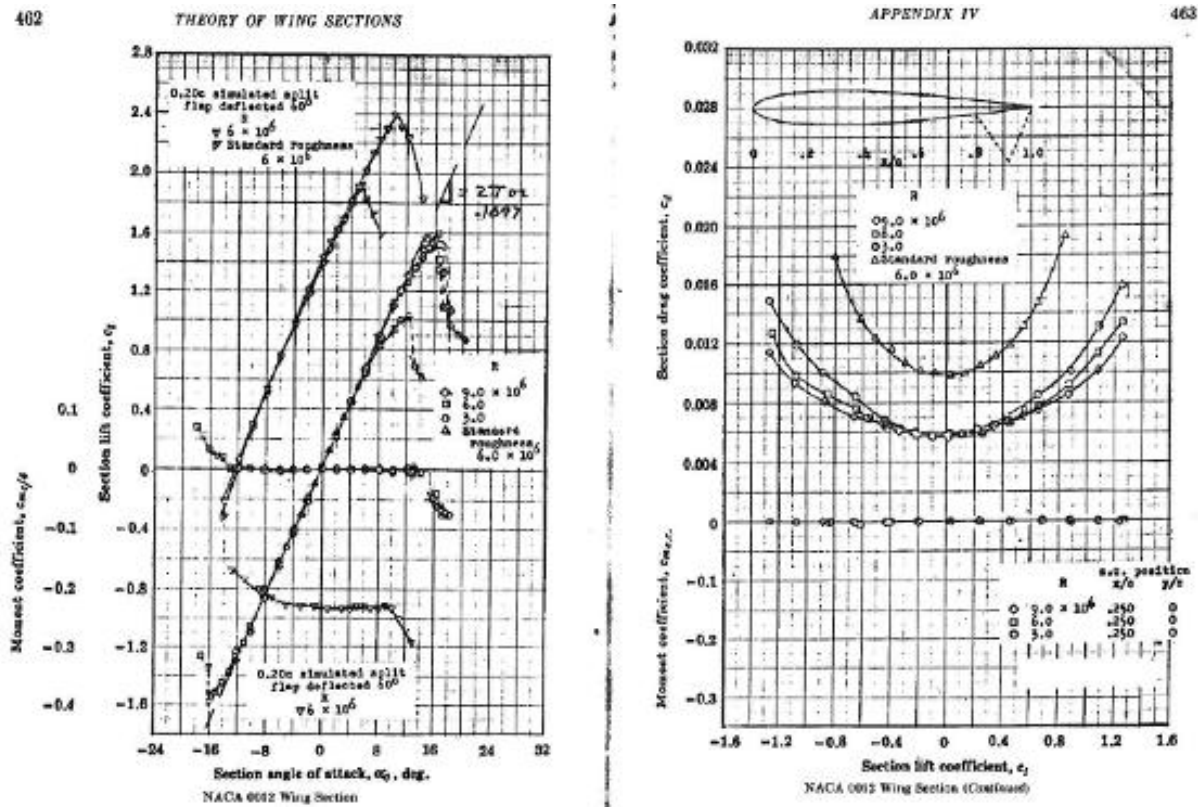


Figure 26: NACA 0012 Lift and Drag coefficient curves ($Re_{\text{rudder}} = 1.40E+06$) [40].

- **Keel fin: NACA 64-012**

For the keel fin, a 6 series NACA section is selected. The main advantages are the following: it has a high maximum lift coefficient, a very low drag over a small range of operating conditions, and it is optimized for high speed. The poor stall behaviour of the 6 digit series does not really matter since the keel never operates at these angles. Sections suitable for keels exhibit allow the drag coefficient (C_D) at small angles of attack and are sometimes referred to as ‘Drag Bucket’ sections, the term being derived from the characteristic of their C_D versus C_L graph. Nevertheless, outside of drag bucket the drag is higher than 00 series, so in this case at leeway greater than 3 deg, the keel drag is actually a handicap for the boat.

The NACA 64-012 foil section was chosen, meaning the location of the minimum pressure is located at 40% of the chord, and 12% thickness to chord ratio. Consider the section C_D/C_L plots from Abbott & Von Doenhoff [40] on Figure 27.

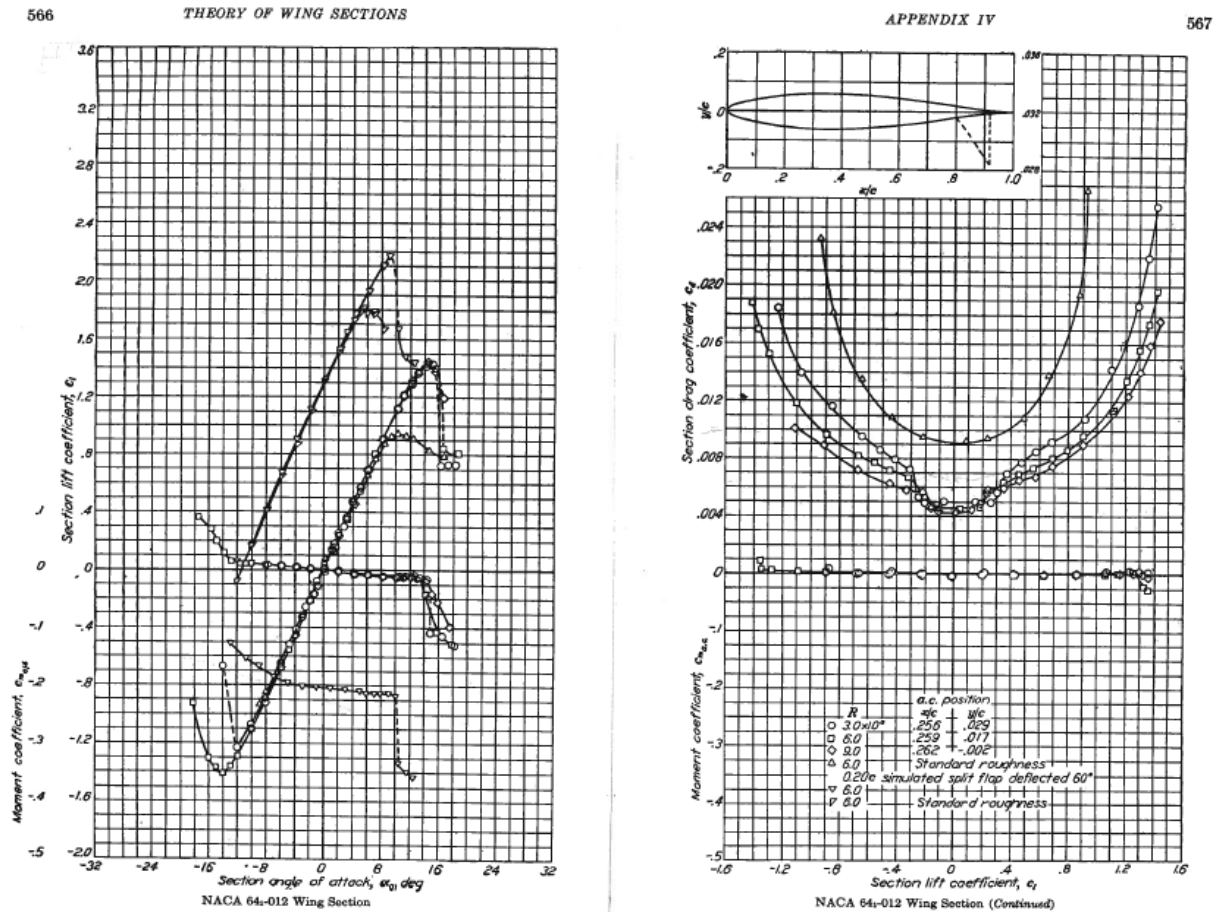


Figure 27: NACA 64-012 Lift and Drag coefficient curves ($Re_{keelfin} = 2.60E+06$) [40].

- **Keel T-bulb: NACA 65-012 / NACA 65-017**

As well as for the keel fin and rudders, the bulb needs a symmetrical section. Also, a 6 digit NACA section is selected, providing the same advantages as mentioned previously. The NACA 65 is often selected for the bulb of the keel because gives lower drag.

The keel bulb, in lead material, is the ballast of the keel and thus the dimensions are selected according to the weight and volume needed.

Before the weight estimation of the boat was made, a first estimation of the geometry was made according to the parametric studies, taking the NACA 65-015, with 15% of thickness to chord ratio (Figure 28). In the next steps of the design process, the weight of the yacht was estimated and thus, the ballast weight could be identified (30% of the weight of the yacht), and the volume of the keel bulb was computed. An optimization of the bulb geometry was made and the final NACA sections 65-012 (vertical) and 65-017 (horizontal) were selected. A larger thickness to chord ratio was selected on the horizontal direction to flatten the shape of the bulb and thus to lower the centre of gravity of the yacht, which was found a little bit too high after the weight estimation.

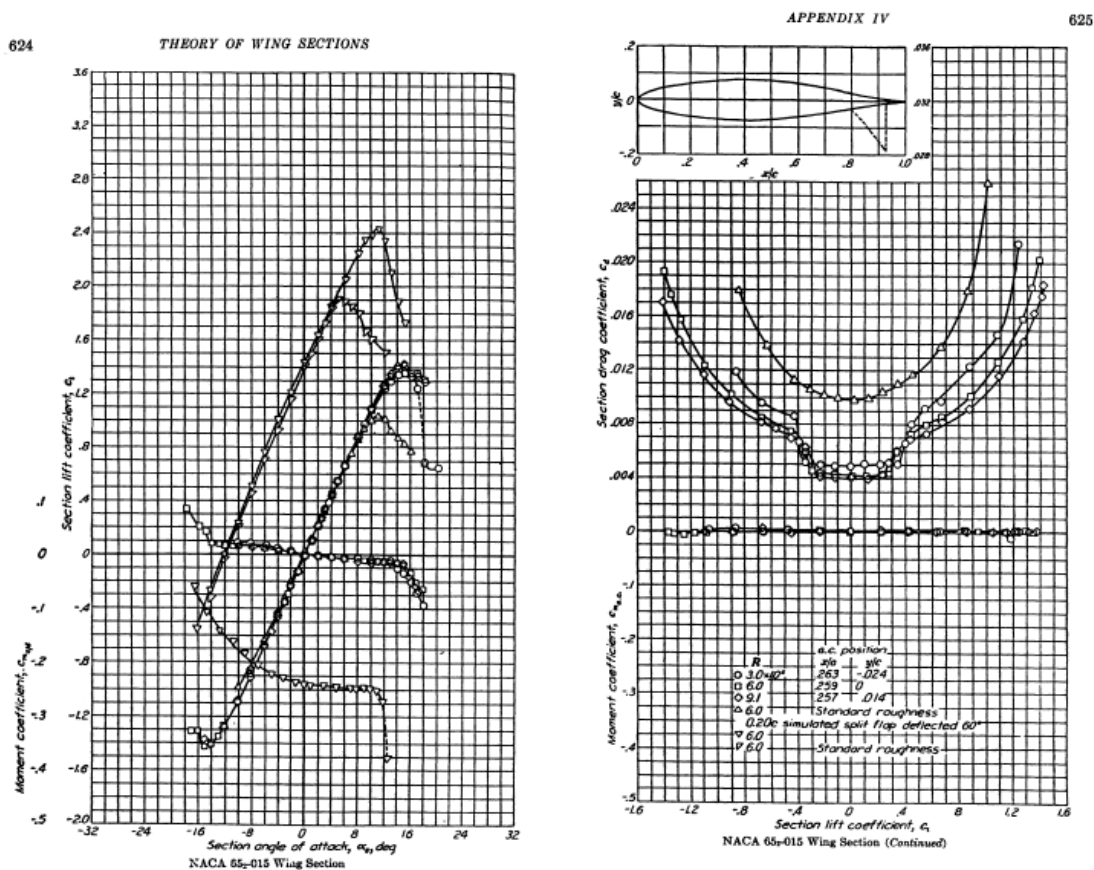


Figure 28: NACA 65-015 Lift and Drag coefficient curves ($Re_{bulb} = 1.91E+07$) [40].

One of the most difficult problems in the design is to find the longitudinal position of the sail plan relative to the underwater body. If the sails are too far aft, the yacht will require a considerable weather helm to go on a straight course, while lee helm will be required with the sails too far forward. That is why determination of appendages geometry and position is really complex. The process was based on Principles of Yacht Design book [20].

If a yacht sails with all degrees of freedom constant, it is said to be in equilibrium: all the forces and moments balance each other.

According to basic 2D lift theory, both the sails, keel and rudders are considered as a foil section, which produces lift and drag forces. The lift is perpendicular to the free stream, and the drag parallel to the free stream.

The aerodynamic forces and hydrodynamic forces balance each other, as shown on Figure 29. Sail forces are treated as aerodynamic lift and drag and are measured relative to the apparent wind direction, these are then resolved into sail side force and sail drive which are measured relative to the boat course. Hull forces are treated as hydrodynamic resistance and side force and are measured relative to the course of the yacht.

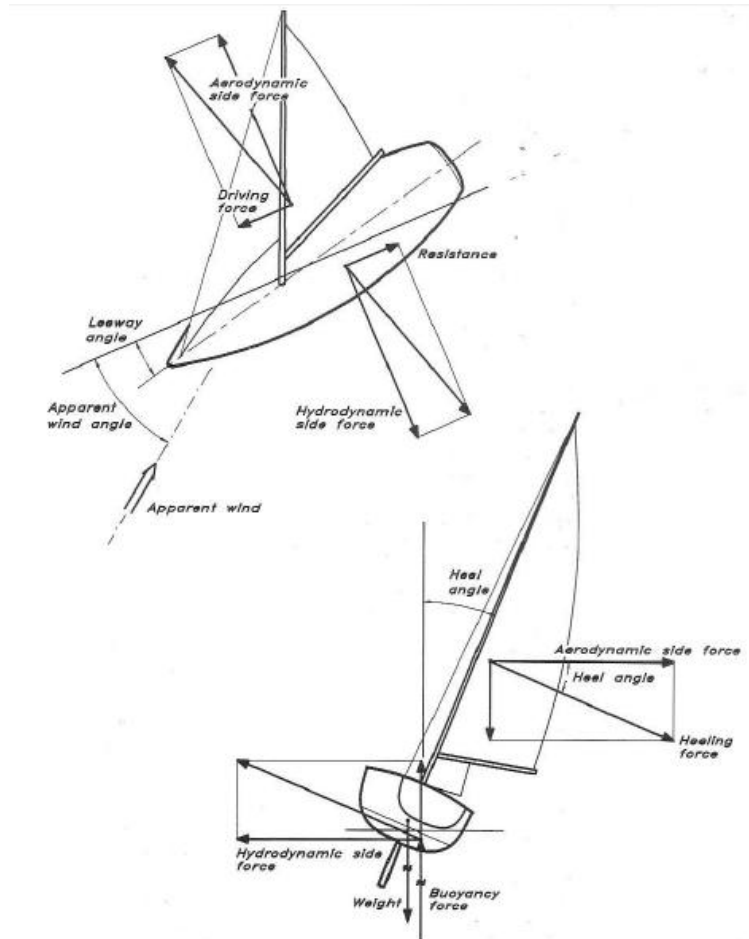


Figure 29: Aerodynamic and hydrodynamic forces acting on a sailing yacht [20].

In order to calculate the area of the keel and rudder, the Sail Side Force (SSF) and then the Keel Side Force (KSF) must be found first (see APPENDIX A4: SAIL SIDE FORCE AND KEEL SIDE FORCE CALCULATION for detail). Results are presented in Table 9.

Table 9: Sail side force and Keel side force results. From APPENDIX A4

Item	Abbreviation	Value	Unit
Sail Side Force	SSF	2112.02	N
Keel Side Force (keel and rudders)	KSF	1900.82	N

Assuming the keel generates 75% of the side force and the rudders 25%, the keel area K_A and rudder area R_A can be calculated as follow with Eq. 5 and Eq. 6:

$$K_A = 0.75.KSF / (1/2.\rho.V_B^2.C_L) \quad \text{Eq. 5}$$

$$R_A = 0.25.KSF / (1/2.\rho.V_B^2.C_L) \quad \text{Eq. 6}$$

where:

- KSF is the keel side force
- V_B is the speed of the boat

- C_L is the lift coefficient of the rudder or keel (taken from NACA graph at 4 degree leeway angle)
- ρ is the density of the water

Finally, the keel and rudder area are the following (Table 10):

Table 10: Keel and Rudder area

Parameter	Abbreviation	Value	Unit
Keel Lift coef from NACA graph at 4 degree leeway angle	C_L	0.5	-
Keel fin area	KA	2.55	m^2
Rudder Lift coef from NACA graph at 4 degree leeway angle	C_L	0.4	-
Rudder area	RA	1.31	m^2

The keel fin and rudder planform will be a standard planform (Figure 30) with straight leading and trailing edge, and a leading edge sweepback angle.

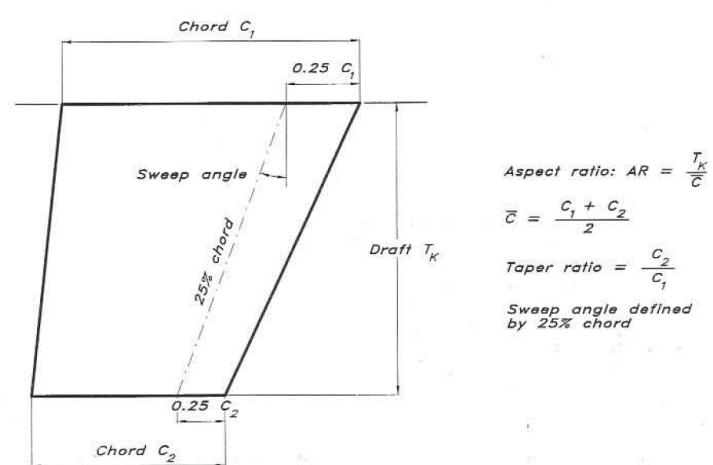


Figure 30: Standard planform chosen for the keel and rudders [20].

The final dimensions for the keel, bulb and rudders are shown below in Table 11, Table 12 and Table 13, and a 3D drawings from Rhinoceros is shown in Figure 31.

Table 11: Twin rudder geometry

<i>Foil section: NACA 0012</i>			
Item	Abbreviation	Value	Unit
Planform area (one rudder)	A_{rudder}	0.58	m^2
Draft rudder	T_r	1.6	m
Thickness to chord ratio	t/c	0.12	
Chord root	c_1	0.5	m
Chord tip	c_2	0.2	m
Mean chord	\bar{c}_{rudder}	0.35	m
Geometric Aspect ratio	AR_G	4.41	-
Taper ratio	TR	0.4	-
Sweep angle	α	11	deg
Wetted surface one rudder	WSA_{rudder}	1.16	m^2
Volume one rudder	V_{rudder}	0.017	m^3

Table 12: Keel fin geometry

Keel fin section: NACA 64 012			
Item	Abbreviation	Value	Unit
Planform area keel fin	$A_{\text{keel_fin}}$	1.92	m^2
Draft keel fin	T_k	2.85	m
Thickness to chord ratio	t/c	0.12	
Chord root	c_1	0.75	m
Chord tip	c_2	0.6	m
Mean chord	$\bar{c}_{\text{keel_fin}}$	0.675	m
Geometric Aspect ratio	AR_G	4.23	-
Taper ratio	TR	0.80	-
Sweep angle	α	3	deg
Wetted surface area	$WSA_{\text{keel_fin}}$	3.94	m^2
Volume	$V_{\text{keel_fin}}$	0.104	m^3

Table 13: Keel bulb geometry

Keel Bulb sections: NACA 65 012 (vertical) and NACA 65 017 (horizontal)			
Item	Abbreviation	Value	Unit
Planform area bulb	A_{bulb}	0.92	m^2
Bulb length	L_b	2.7	m
Horizontal Thickness to chord ratio	t/c_H	0.17	
Vertical Thickness to chord ratio	t/c_V	0.12	
Chord Horizontal	\bar{c}_H	0.46	m
Chord Vertical	\bar{c}_V	0.325	m
Horizontal Aspect ratio	AR_H	5.87	
Vertical Aspect ratio	AR_V	8.31	
Wetted surface area	WSA_{bulb}	2.26	m^2
Volume	V_{bulb}	0.171	m^3

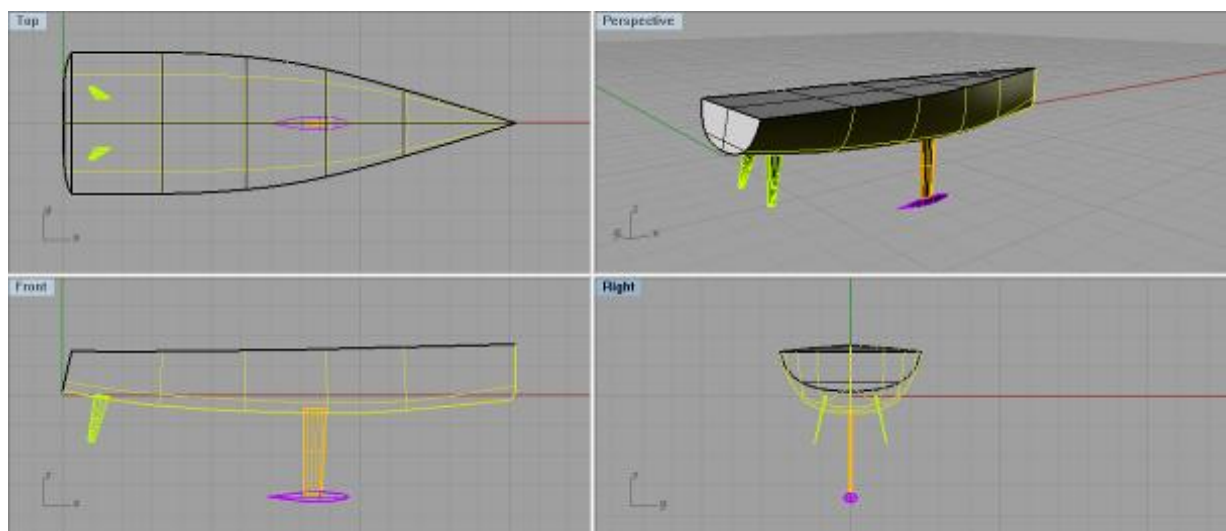


Figure 31: 3D Rhinoceros representation of the hull with bulbous keel and twin rudder. Own elaboration.

For a foil section (keel, rudder, hydrofoil), Reynolds number is calculated with the following Eq. 7. Results are shown in Table 14.

$$Re = (\rho \cdot V_B \cdot c_{foil}) / \mu \quad \text{Eq. 7}$$

For a bulb, Reynolds number is calculated with the following Eq. 8:

$$Re = (\rho \cdot V_B \cdot l_{bulb}) / \mu \quad \text{Eq. 8}$$

with:

- c_{foil} , the average chord of the wetted surface area of the foil, in meter,
- l_{bulb} , the length of the bulb, in meter
- V_B the velocity of the boat, here taken as 16 knots or 8.23 m/s.

Table 14: Reynolds number appendages

Item	Abbreviation	Value	Unit
Velocity of the boat	V_B	8.23	m/s
Keel fin average chord	c_{keel}	0.675	m
Length of the bulb	l_{bulb}	2.7	m
Rudder Average chord	c_{rudder}	0.35	m
Reynolds number	Re_{keel}	4.79E+06	-
	Re_{bulb}	1.91E+07	-
	Re_{rudder}	1.40E+06	-

4.2.2.3. Balance

In parallel with the geometry of the sails and appendages, the balance or sailing equilibrium of the yacht is checked. The balance is the relative position of the centre of effort of the sails CE and the centre of lateral resistance CLR of the underwater body, or the lead.

The method suggested by Larsson [20] was used to calculate the lead of the boat. The centre of effort CE is simply taken as the geometrical centre of area of the mainsail and headsail, and the centre of lateral resistance CLR is a combination of the keel CLR (centre of area projected on the 1/4 chord line) and the rudder CLR (centre of area projected onto the 1/4 chord line), see Figure 32. The lead represents 10% of the waterline length (Table 15), which is just above the range values suggested by Larsson, between 5 and 9% L_{wl} for a masthead rigged sloop of this kind for a bulbous keeled boat.

Table 15: Balance and geometric centres

Item	Abbreviation	Value	unit
Longitudinal Centre of effort from Lwl	CE_L	7.21	m
Vertical Centre of effort from waterline	CE_v	10.42	m
Longitudinal Centre of Lateral resistance from Lwl	CLR_L	5.60	m
Vertical Centre of Lateral resistance from waterline	CLR_v	-1.53	m
Lead 0 to 20% Lwl		10	%
Heeling Arm upright	HA	11.95	

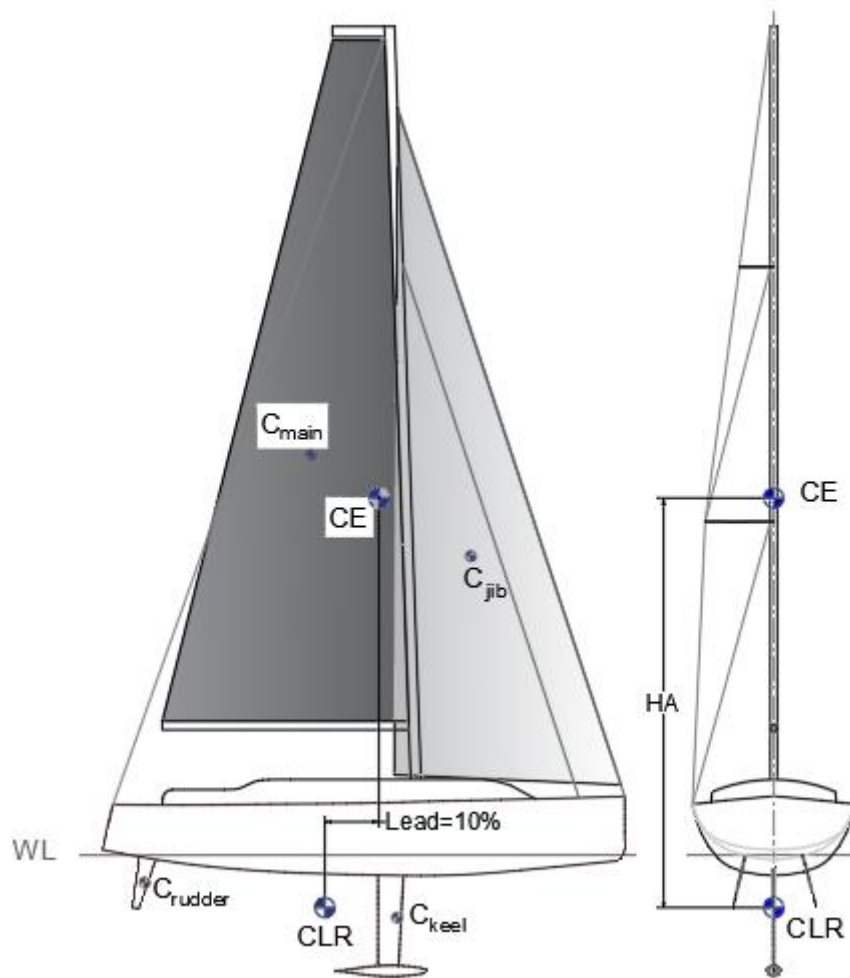


Figure 32: Balance and geometric centres representation. Own elaboration.

4.2.3. Hydrofoil Design

Since hydrofoils are optional in sailing condition (i.e. for safety conditions, the boat should be able to sail without hydrofoil in case it breaks), the design can be done independently from the appendages design and independently from the sailing equilibrium. Hydrofoils contribute in providing lift (L) to the boat, to increase the Righting Moment (RM), and in some cases, to provide an additional Side Force (SF) to the keel and rudder. See Table 16.

As the aim of the master thesis is not to optimize the shape of the hydrofoil, the planform effect is of most interest. Hence, the general shape of each hydrofoil will be taken from a parametric study, based on three existing boat equipped with foils (see part 2.3):

- IMOCA 60 Safran II for the Dali moustache foils,
- Figaro III Bénéteau for the Chistera foils,
- Infiniti 56 (Far Yacht design) for the DSS foil.

The first restrictions will be to follow the general geometry and location on the yacht, keeping in mind that the main concern in the design is to adapt the shape and dimensions to the hull design, and to fit within the General Arrangement.

Table 16: Hydrofoils characteristics from parametric study

Nb	Foil Name	Yacht	General shape	Longitudinal position	Additional forces provided to the yacht		
					L (N)	SF (N)	RM (N.m)
1	Dali Moustache	IMOCA 60 (Safran II)	V shape	In front of the mast	Yes	Yes	Yes
2	Chistera	Figaro 3 Bénéteau	Upside down V shape	In front of the mast	Yes	Yes	Yes
3	DSS	Infiniti 56	Flat Shape	Behind the keel and the mast	Yes	NO	Yes

Regarding the selection of the foiling section, it was hard to find information in books, articles or websites about the exact section used for each existing foiling yacht. The aim of the master thesis is to compare the hydrodynamics between the three types of foil, hence, the most relevant thing to do is to choose the same NACA section for all the foils. From literature and websites, it was decided to take the NACA 63-412 foiling section (Figure 33), which is a common section used for *Moth* sailing yacht.

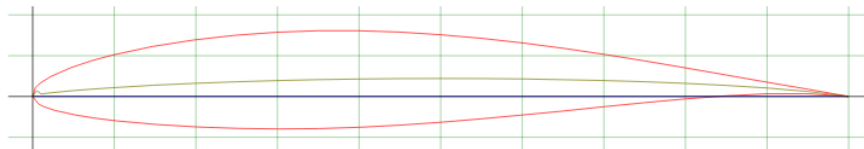


Figure 33: NACA 63-412 section geometry [42].

NACA 63-412 is a 6 series section, and is designated as low-drag, section.

It has minimum pressure 30% of the chord back, has an optimal lift coefficient of 0.4, and a maximum thickness to chord ratio of 12% [42].

The advantages and drawback of this NACA section are detailed in Table 17.

Table 17: Advantages and drawbacks of NACA 63-412 section

	Advantages	Drawbacks
NACA 63-412	<ul style="list-style-type: none"> - Uniform velocity from the leading edge back to a specified location (maintains laminar flow to the 30 percent chord point) - High maximum lift coefficient ($C_L \text{ max} = 1.4$) 	<ul style="list-style-type: none"> - High drag outside the optimum range of operating conditions - High pitching moment - Poor stall behaviour (maximum stall angle $\alpha_{\text{max}} = 15$ degree) - Very susceptible to roughness (drag

	<ul style="list-style-type: none"> - Very low drag over a small range of operating conditions - Optimized for high speed - 12% relative thickness, an adequate one 	bucket nonexistent for low Reynolds number)
--	---	---

As said in section 4.2.2.2, the Reynolds number a foil section (keel, rudder, hydrofoil), is calculated with the following equation Eq. 9:

$$Re = (\rho \cdot V_B \cdot c_{foil}) / \mu \quad \text{Eq. 9}$$

with:

- c_{foil} , the average chord of the wetted surface area of the foil,
- l_{bulb} , the length of the bulb,
- V_B the velocity of the boat, here taken as 16 knots.

Results are shown in Table 18.

Table 18: Hydrofoil Reynolds number

Item	Abbreviation	Value	Unit
Velocity of the boat	V_B	8.23	m/s
DSS average chord	C_{DSS}	0.7	m
Figaro 3 average chord	C_{F3}	0.45	m
Dali average chord	C_{DALI}	0.45	m
Reynolds number	Re_{DSS}	4.96E+06	-
	Re_{F3}	3.19E+06	-
	Re_{DALI}	3.19E+06	-

Figure 34 shows the lift and drag coefficient curves for a Reynolds number $Re = 5.0E+06$.

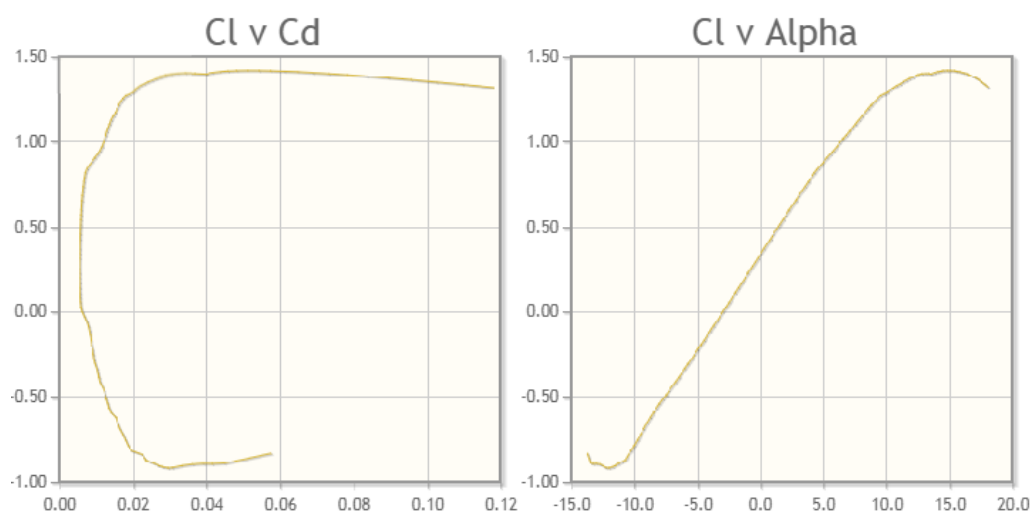


Figure 34: NACA 63-412 Lift and Drag coefficient curves for $Re=5.0E+06$ [42].

The general shape of each foil, based on the hydrofoils presented in part 2.3 is shown in Figure 35, Figure 36 and Figure 37:

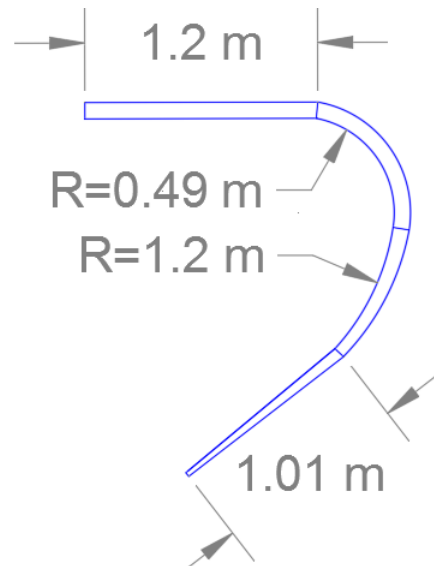


Figure 35: Figaro 3 general shape. AutoCAD design. Own elaboration.

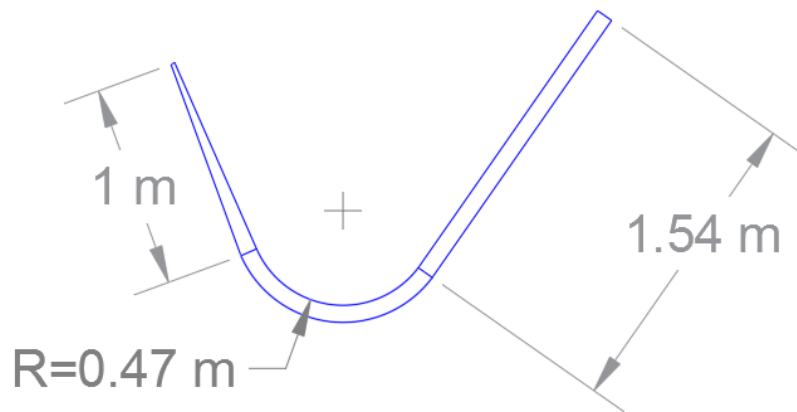


Figure 36: Dali moustache general shape. AutoCAD design. Own elaboration.

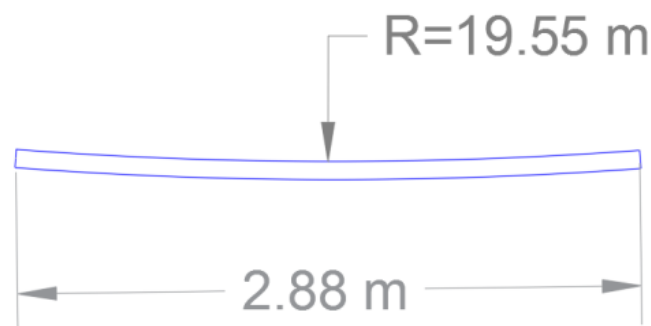


Figure 37: DSS general shape. AutoCAD design. Own elaboration.

4.2.4. General Arrangement and Deck Plan

The next step in the design process is to do the interior and deck layout. The GA (General Arrangement) will be based on a current cruising yacht design GA configuration. As seen in the Design Brief (Table 1), it must provide comfort and also be able to integrate the three types of foils.

The general layout and deck plan are shown in APPENDIX A5: GENERAL ARRANGEMENT AND DECK PLAN DRAWINGS.

The main considerations when designing the interior layout are that there should be sufficient headroom at the foils emplacement. As said in the Table 16, the Figaro 3 foils and Dali Moustache foils are longitudinally positioned in front of the mast, and the DSS is positioned behind the lifting keel (Figure 38). That means in the designed GA, the DSS is positioned in the floors of the living room, the Dali moustache is in the main cabin, diagonally, and the Figaro 3 is also in the main cabin, in the ceiling (Figure 39).

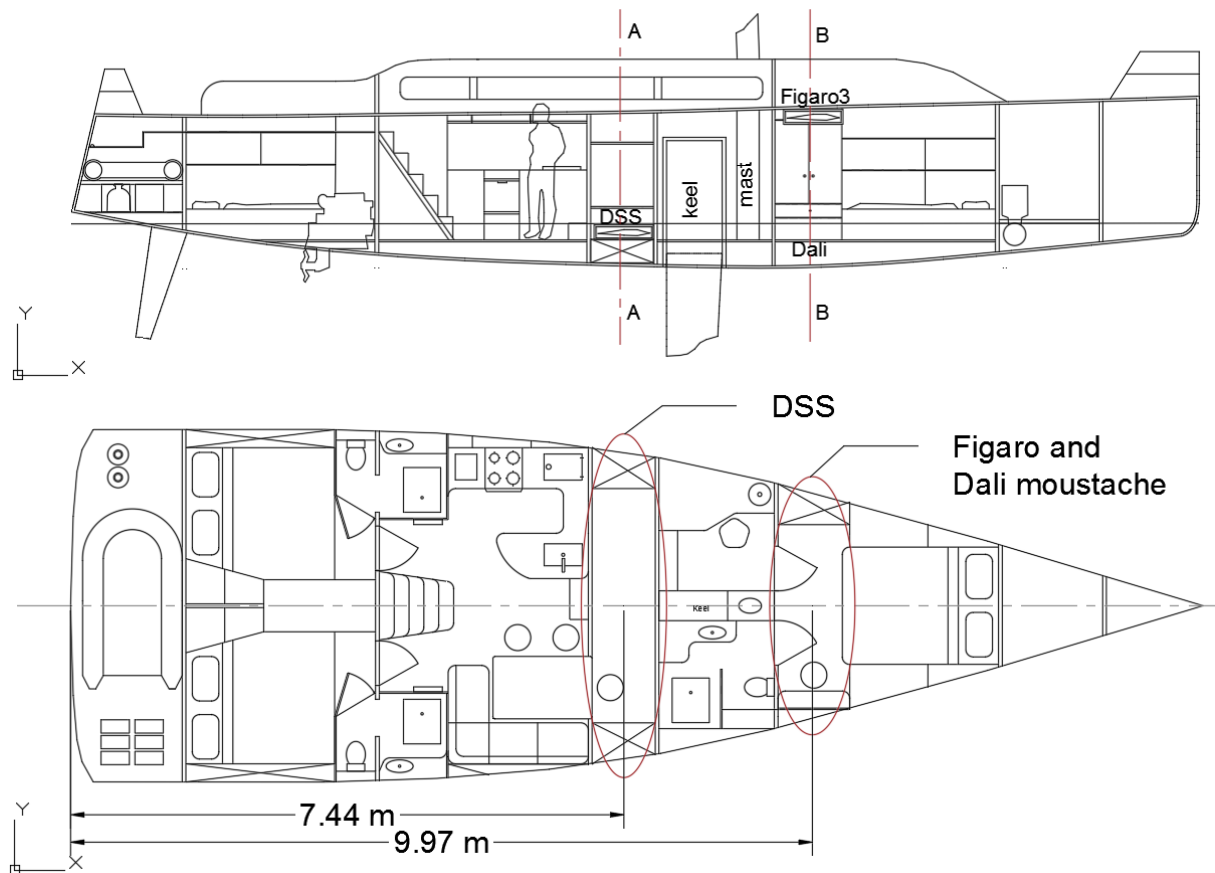


Figure 38: Longitudinal position of the foils and integration in the GA. AutoCAD design. Own elaboration.

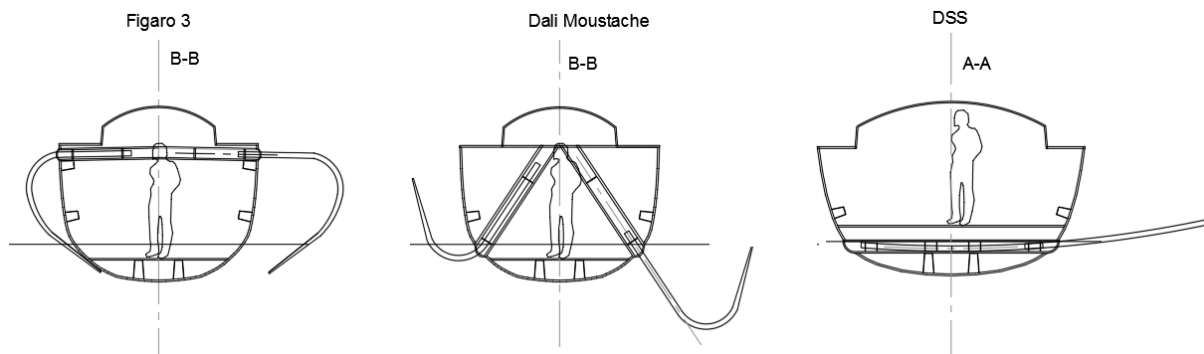


Figure 39: Transversal sections with hydrofoils. AutoCAD design. Own elaboration.

Also, Figure 39 outline one restriction when designing the foils. The curve of the foil should fit more or less the section shape of the hull in order not to add too much resistance when the foil is not used (in retracted position). This criteria is relevant for the Figaro 3 foil.

Those figures confirm that it is hard to make one generic GA that can comply with all three types of foils. The criteria of the headroom is determinant to say whether the foil is suitable for the yacht or not. An "ergoman" of 1.85 m is taken as reference based on standard ergonomic and anthropometric consideration [43]. Here the DSS is the most suitable configuration for our GA. If a step of 450 mm is added in the middle of the living room, there is still sufficient headroom. Also, the Figaro 3 foils can be integrated easily, it would just require the sailor to incline the head 300 mm to go to the bed or to the bathroom. In the contrary, the Dali Moustache foil would not be convenient at all for our GA configuration. It requires too much space and would not allow the sailor to move in the cabin. On a design point of view, this foil configuration will not be taken into consideration.

Also, in this master thesis, as this study is turned to hydrodynamics topic, the mechanisms for the lifting keel and foils will not be discussed due to a lack of time, but can be considered for future studies.

4.2.5. Resistance and Engine Selection

In order to select the engine for our boat, the resistance of the hull should be evaluated. It will be first estimated with the initial weight of the boat, and will be adjusted later on a second design loop after the weight calculation of the boat.

The resistance is done on Maxsurf Resistance [27], which is based on Delft III methods, and taking 60% efficiency (see resistance curves on Figure 40). The sailing yacht resistance

prediction with Delft III use the regression based on either Gerritsma et al (1991) or Gerritsma et al (1992) (Refer to APPENDIX A6: MAXSURF HULL RESISTANCE RESULTS).

In the towing tank, the upright resistance of the hull has also been tested. In section 5.2.1, the comparison of the hull resistance between the theory (Maxsurf results studied in section 4.2.5 and VPP results studied in section 4.2.10) and the experimental results will be done. This will allow further discussion on uncertainty.

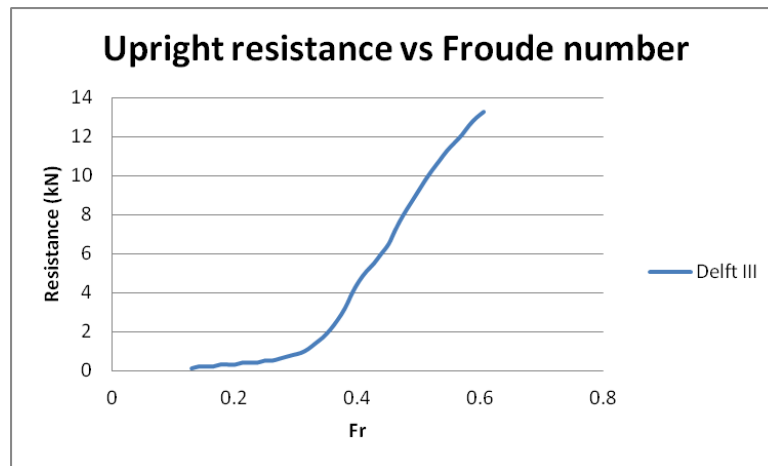


Figure 40: Resistance curves comparison from Maxsurf Resistance.

Once the resistance curve and the resulting power needed on Maxsurf Resistance is known, the engine can be selected by estimating the maximum power needed for the boat.

According to Dave Gerr's formula (Eq. 10) [44], the displacement hull speed was estimated at 9.2 knots.

$$V_S [Kts] = 1.34 \cdot \sqrt{L_{WL}} \quad \text{Eq. 10}$$

Hence, for a speed of $V_S = 9.2$ kts ($Fr = 0.39$), the Sail power is estimated by Maxsurf Resistance at 30 kW (Figure 41).

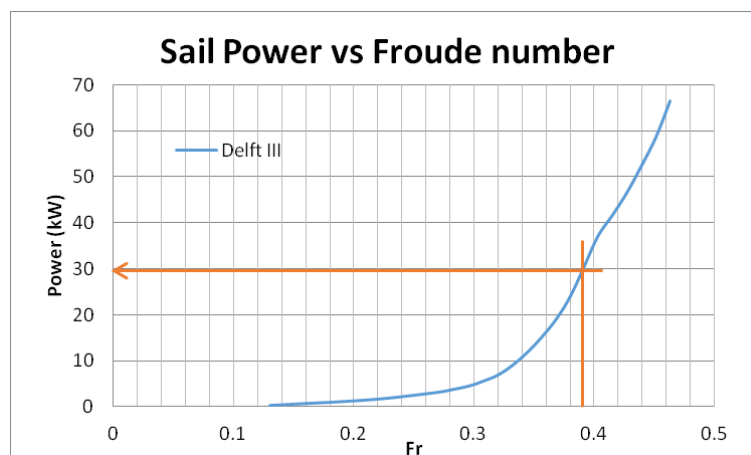


Figure 41: Sail power versus Froude number. Maxsurf resistance.

However, this sail power does not take into account the efficiency of the powering or safety factor.

Dave's Gerr formula [44] can be used in order to estimate the Sail power (Eq. 11).

$$SHP = \Delta \cdot L_{WL} / ((2.3 - SL \text{ Ratio}) \cdot 8.11)^3 \quad \text{Eq. 11}$$

where SL Ratio is calculated with Eq. 12:

$$SL \text{ Ratio} = 8.26 / (\Delta / (0.01 \cdot L_{WL})^3)^{0.311} \quad (SL \text{ Ratio} \geq 1.34) \quad \text{Eq. 12}$$

with L_{WL} the Length at water line (meters), and Δ the displacement in tons.

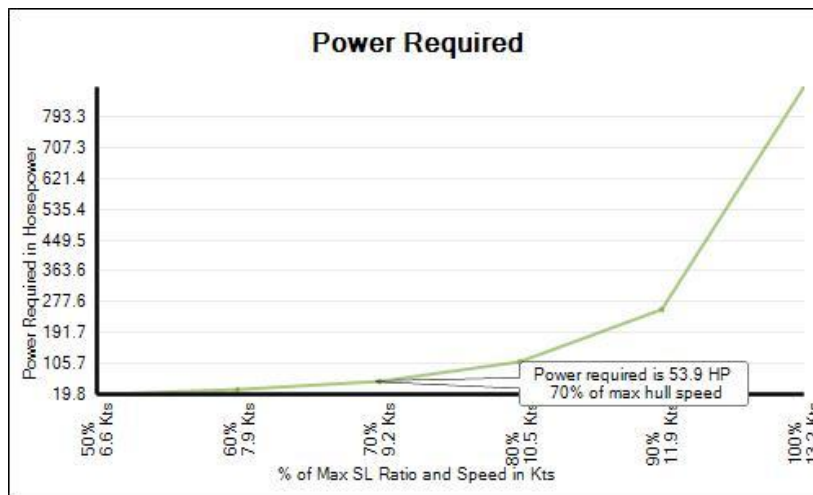


Figure 42: Power required for the engine [45].

The power required is estimated at 40 kW (i.e. 53.9 HP) for 9.2 knots (or 70% of the max hull speed) as shown on Figure 42. Hence, a sail-drive engine Volvo Penta of 44 kW crankshaft power was selected, assuming an efficiency. See the main engine data in APPENDIX A7: ENGINE VOLVO PENTA CHARACTERISTICS.

Once the engine has been selected, the fuel consumption can be calculated. The average speed was estimate at 9 knots, that gives a consumption of 11.5 L/h. But actually, as the time of use and speed of the engine is not exactly know, the maximum fuel consumption (15.5 L/h) and 24 hours of journey will be considered for calculations. Finally, the amount of fuel needed for 24 hours at full capacity is estimated at 400 L (taking a 10% margin), see Table 19, which is more than enough compared typical fuel capacity for cruising yachts.

Table 19: Fuel Consumption Estimation (Fuel tanks)

Description	Amount	Unit	
Max Consumption	15.50	L/ hour	
Hours Travelling	24.00	hours	
Estimated Amount of Fuel	372.00	L	Margin 15% 409.20 L

4.2.6. Hull and Deck Scantling - Structural Design

The next step of the design is to define the scantling on the hull and deck, that is to say the plate thickness, the panel size, the bulkheads, frames and stiffeners dimensions and location, and the material composition are going to be selected. To do so, HullScant, which is a Wolfson Unit's Hull Scantlings programme, will be used. HullScant is used to evaluate the scantlings for motor and sailing vessels under 24 metres. The program calculates the actual scantling structural properties of a vessel and can compare this with the requirements set out in the ISO standard 12215, Part 5 [32], which deals with pressures and scantling equations for fibre reinforced plastic, metal and wood monohull boats.

As most of the cruising yacht of this size are in composite, it was decided that the hull and deck will be in composite too, and more precisely in sandwich construction or cored FRP (Fibre Reinforced Plastic) composed of an epoxy matrix, carbon fabrics and foam cores (PVC for stiffeners or SAN for plates). A bank list of composite material was studied before using HullScant, based on *Gurit* material supplier's website, and ISO 12215, Part 2 standard for core materials for sandwich construction [31].

Table 20: Composite material input in Hullscant.

Product	Layer	Scantling use	Location	Type	Size sheet Width x Length	Density (kg/m ³)	Density (g/m ²)
XC611	Fiber	All	Hull	45° Bi Carbon Fabric	1270x50 mm		611
XCT411	Fiber	All	Deck	Tapes Bi Carbon	140x50 mm		411
GURIT® PVC80	Core	Stiff	Hull	Cross-linked PVC foam	1020x2180 mm	80	
GURIT® PVC60	Core	Stiff	Deck	Cross-linked PVC foam	1020x2180 mm	60	
UT-C500	Fiber	All	Hull	Uni Carbon Fabric	500x100 mm		500
UT-C300	Fiber	All	Deck	Uni Carbon Fabric	500x125 mm		300
GURIT® Corecell M100	Core	Panels	Hull	SAN structural foam	1130x2275 mm	107.5	
GURIT® Corecell M80	Core	Panels	Deck	SAN structural foam	1220x2440 mm	85	

The first thing to do is to define the different areas on the hull, deck and superstructure, in order to find the most critical areas regarding the load applied on each part of the boat. According to ISO 12215 Part 5, the general division is as follow:

- the bottom of the hull, which is under the waterline and where hydrostatic and hydrodynamic pressure loads are applied,
- the side of the hull, which is above the waterline, where the pressure load is lower than on the bottom,
- the deck,
- and the superstructure.

Also forward bottom and side shell needs to be stronger than the aft bottom and side shells; where high slamming loads is expected.

Most precisely, some local point on the boat are more loaded compared to others, and need to be carefully studied when doing the scantling (framing has to be increased) and choosing the materials:

- the keel attachment on the bottom area,
- the rudder attachment on the bottom area,
- the hydrofoil attachment on the bottom for the DSS and on the side for the Figure 3,
- the mast on the deck,
- the rigging attachment on the deck area (chain plate, stay fitting, winches, etc...)
- the slamming area on the bow of the hull,
- the engine bed on the bottom area,
- the windows on the side and on the deck,
- etc...

Taking all of this into account, a first scantling geometry, stiffening dimensions (Figure 43), panel size (Figure 44) and curvature (Figure 45), and laminate layers composition was defined, and the design pressure on the critical areas was calculated with HullScant. Some pressure adjusting factors are defined automatically in the software regarding the category of the boat (in this case Category A) [32]. The most critical situation were tested in order to comply with the requirements ISO 12215 Part 5. HullScant results are presented in APPENDIX A8: HULL AND DECK SCANTLING RESULTS WITH HULLSCANT.

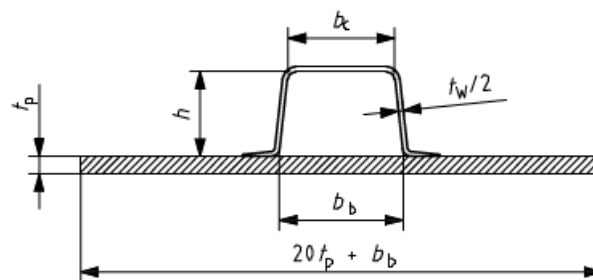


Figure 43: "Squat" top-hat stiffeners dimensions*. Available from [32].

**with 'h' the top hat height, 'b_b' the base width, 'b_c' the top width (flange), 't_p' the plate thickness, 't_w' the stiffener thickness.*

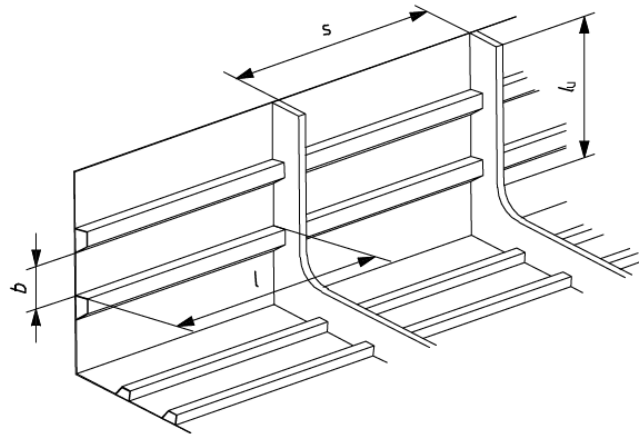


Figure 44: Panel size** [32].

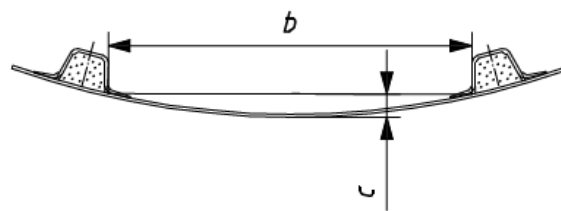


Figure 45: Panel curvature** [32].

***with 'b' the shorter dimension of the plate panel, 's' the stiffener or frame spacing, 'l' the longer dimension of plate panel, 'c' the crown of a curved panel.*

Having a compliant result with the software is however not always enough since the theory behind the rule is not always logical. For instance, in some cases, a plate thickness can be found compliant to the rule even though it is very thin. Therefore, some adjustments need to be made in order to be closer to the reality.

Also, the programme has another limit since it can only calculate the critical forces for the hull and deck shell and stiffeners, but cannot calculate the reinforcement of the keel, rudder and hydrofoils. Indeed, the ISO requirements used for the sailing craft appendages reinforcement calculation is the ISO 12215 Part 9 [33] and is not taken into consideration into the programme. A detailed calculation for the keel, rudder and hydrofoils reinforcement is however out of the scope of study, but should be considered for future studies.

The final Hull and Deck scantling are shown in APPENDIX A9: HULL AND DECK STRUCTURAL ARRANGEMENT.

4.2.7. Mast and Rigging Dimensions

This part deals with the dimensioning and construction of the mast and rig. It was calculated according to the Nordic Boat Standard (NBS), which is explained in Principles of Yacht Design book [20].

As mentioned, a sloop rig configuration has been chosen. The sloop rig has a good all-around aerodynamically, especially on the wind, and need a special off-the-wind sails (Spinnaker sail). It also has a higher centre of effort and higher yacht centre of gravity.

The designed rig is a masthead with double spreaders (see Table 21 and Figure 46).

It is composed of:

- diagonal and vertical shrouds (D1, D2, D3, V1, V2)
- a forestay
- an inner forestay
- a backstay
- a C-shape section mast
- a B-shape section boom

Table 21: Rig loads and dimensions

Item		Material	Dimensioning Load (kg)	Diameter (mm)	Compliance factor
Shroud	D1	Aluminium	8709	11	1.13
	D2	Aluminium	4866	9	1.26
	D3	Aluminium	12369	13	1.11
	V1	Aluminium	6564	10	1.15
	V2	Aluminium	12380	13	1.11
Forestay		Aluminium	8772	13	1.12
Inner Forestay		Aluminium	7018	10	1.08
Backstay		Aluminium	6890	10	1.10
Mast C245		Aluminium	525	245/127	
Boom B200		Aluminium	561	200/117	

Rigging material properties for the wire diameters were taken from Principle of Yacht Design book [20] and typical sections for mast and boom were taken from *Sedenmast* supplier's website [46] and [47].

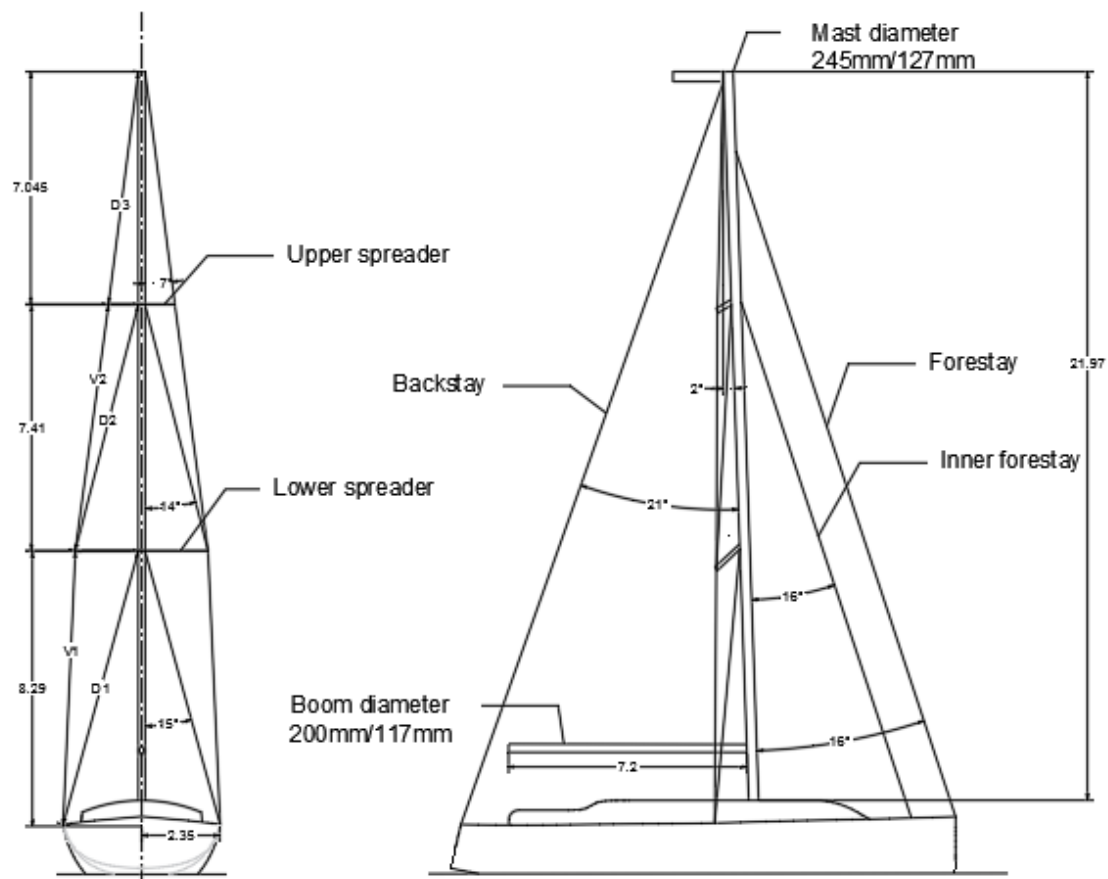


Figure 46: Sloop rig design and dimensions (meters). AutoCAD drawings. Own elaboration.

The detailed loading cases calculated with Nordic Boat Standard is shown in APPENDIX A10: MAST AND RIG CALCULATION SPREADSHEET (NBS).

4.2.8. Weight Estimation

To judge the possible performance and stability of the yacht, using the elements designed in the previous parts, and suppliers and manufacturers data, a full weight estimate of the yacht was carried out.

The centre of gravity of the yacht will be deduced and the stability check can be carried out in Maxsurf Stability in section 4.2.9.

There are several cases to study since the yacht has a lifting keel and different types of foils. As said in part 4.2.3, the case of the Dali moustache foil will not be considered since it is not relevant in a design point of view. Therefore, the total weight estimation and centre of gravity calculation is carried out for four different configurations: DSS keel up and keel down, and Figaro 3 keel up and keel down in Lightship configuration (Figure 47).

[-][Top][2D Wireframe]

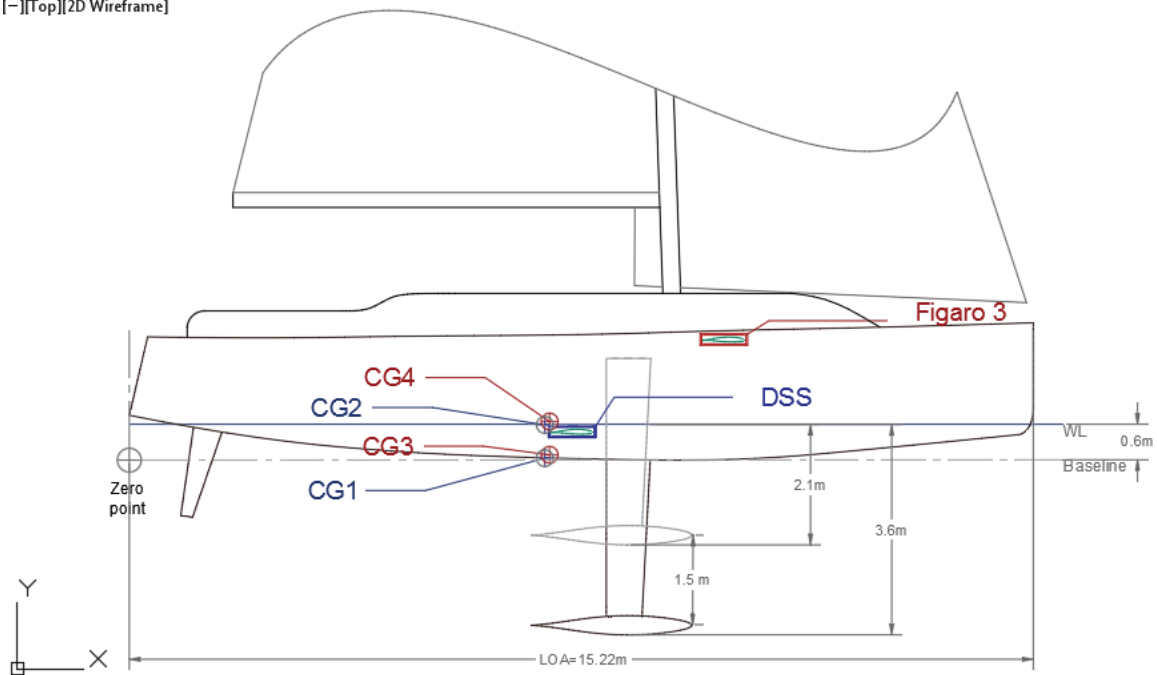


Figure 47: Centre of gravity Lightship for configuration 1, 2, 3 and 4. AutoCAD drawings. Own elaboration.

Considering the different tankage loading (for fresh water, grey water and fuel), Table 22 shows the total weight:

- Lightship: All tanks and consumable empty
- Full load: All tanks and consumable full
- Starting condition: Fuel and fresh water full, Grey water tank empty
- Half load at mid-voyage: All tanks at 50%
- End of voyage: Fuel and Fresh water 10% and Grey water 100%

Refer to APPENDIX A11: TANK LOADING for the tanks loading.

Table 22: Weight estimation for different configurations

<i>Configuration 1 (DSS, lifting keel down)</i>			
Loadcase	Displacement	LCB	VCG
	<i>t</i>	<i>m</i>	<i>m</i>
Light ship	11.27	6.92	0.04
Full load	11.72	6.88	0.05
Start	11.65	6.88	0.05
Half load	11.49	6.9	0.04
End	11.37	6.91	0.04

<i>Configuration 3 (Figaro 3, lifting keel down)</i>			
Loadcase	Displacement	LCB	VCG
	<i>t</i>	<i>m</i>	<i>m</i>
Light ship	11.55	7.07	0.12
Full load	12	7.02	0.13
Start	11.94	7.02	0.13
Half load	11.78	7.04	0.13
End	11.66	7.06	0.13

<i>Configuration 2 (DSS, lifting keel up)</i>			
Loadcase	Displacement	LCB	VCG
	<i>t</i>	<i>m</i>	<i>m</i>
Light ship	11.27	6.92	0.59
Full load	11.72	6.88	0.58
Start	11.65	6.88	0.58
Half load	11.49	6.9	0.59
End	11.37	6.91	0.59

<i>Configuration 4 (Figaro 3, lifting keel up)</i>			
Loadcase	Displacement	LCB	VCG
	<i>t</i>	<i>m</i>	<i>m</i>
Light ship	11.55	7.07	0.67
Full load	12	7.02	0.65
Start	11.94	7.02	0.66
Half load	11.78	7.04	0.66
End	11.66	7.06	0.66

The weight estimation is carried out step by step, considering the main following elements:

- Hull and deck structure and superstructure
- Tank loading
- Crew
- Painting and fairing
- Machinery
- Deck outfitting
- Rig and Sail
- Accommodations
- Appendages

Refer to APPENDIX A12: WEIGHT ESTIMATION IN LIGHTSHIP CONDITION for detailed weight estimation.

4.2.9. Stability Analysis

Maxsurf Stability [28] was used to plot the GZ curves for the most critical configurations (i.e. with foils and keel up) and for the two tank loadcases imposed by ISO 12217 Part 2 [34]: Lightship (0%), and End of voyage (10%).

The Stability index (STIX) was checked following the ISO 12217-Part 2 requirements.

The STIX is a way of representing the ‘seaworthiness’ of a design. It is an assessment of the ability of a monohull boat to resist and to recover from a knockdown or inversion. It scores a vessel’s stability on a scale of 1 to 100 using the vessel’s length as a prime factor adjusting this by seven other factors including the assessment of a vessel:

- Ability to withstand a capsize by considering the area under the GZ curve.
- Recovery from inversion by looking at the vessel’s PVS.
- Recovery from knockdown by overcoming water in the sails.
- Displacement-length factor recognizing problems associated with topside flare and excessive beam.
- Wind moment representing the risk of flooding due to a gust and
- The risk of down flooding in a broach or knockdown.

Downflooding requirements are to ensure that the level of watertight integrity appropriate to the design category is maintained. By defining the downflooding openings such as hatches and windows. The minimum downflooding angle is shown in Figure 48. The design category A is taken here.

Table 3 — Required minimum downflooding angle

Design category	A and B	C	D
Required downflooding angle, $\phi_{D(R)}$	40°	35°	30°

Figure 48: Required minimum downflooding angle. Available from [34]

The Figure 49 shows the model to be run on Maxsurf Stability: the hull with the deck, the cockpit and the roof, and with the keel up.

Moreover, all the input parameters according to the ship weight estimation, the fuel, fresh water and grey water tank position and downflooding key point position are presented in Table 23, Table 24 and Table 25.

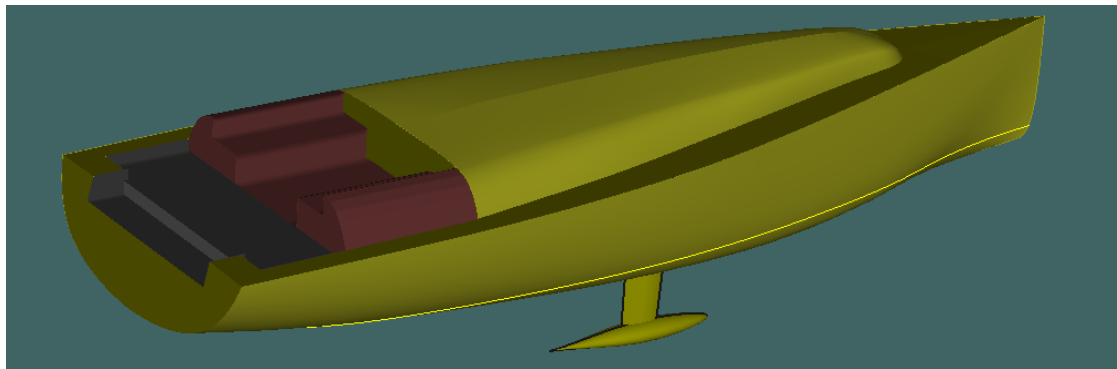


Figure 49: Model for Stability analysis - Hull with keel up, roof and cockpit. Maxsurf Modeler.

Table 23: Loadcase configurations - input parameters in Maxsurf Stability

Loadcase	FOIL	KEEL	TANK	Weight (t)	LCG*(m)	VCG**(m)
1	DSS	UP	0%	11.27	6.92	-0.01
2	DSS	UP	10%	11.37	6.91	-0.01
3	FIGARO 3	UP	0%	11.55	7.07	0.07
4	FIGARO 3	UP	10%	11.66	7.06	0.06

*from the aft; **from waterline

Table 24: Tank location - input parameters in Maxsurf Stability

Name	Density (kg/m ³)	Fluid type	Aft (m)	Fore (m)	Port (m)	Starboard (m)	Up (m)	Down (m)
FUEL	0.9443	Fuel Oil	5.11	6.11	-0.3	0.3	-0.24	-0.48
FW_PORT	1	Fresh Water	5.18	6.02	-0.89	-0.49	-0.24	-0.47
FW_STB	1	Fresh Water	5.18	6.02	0.49	0.89	-0.24	-0.47
GW	1	Grey Water	6.3	6.7	-0.33	0.33	-0.25	-0.51

Table 25: Downflooding point - input in Maxsurf Stability

	LONGI (m)	OFFSET (m)	HEIGHT (m)
STAIRS	4.09	0.75	1.24

Water and Fuel tanks positions, zero point, downflooding key point and centre of gravity are represented on Figure 50.

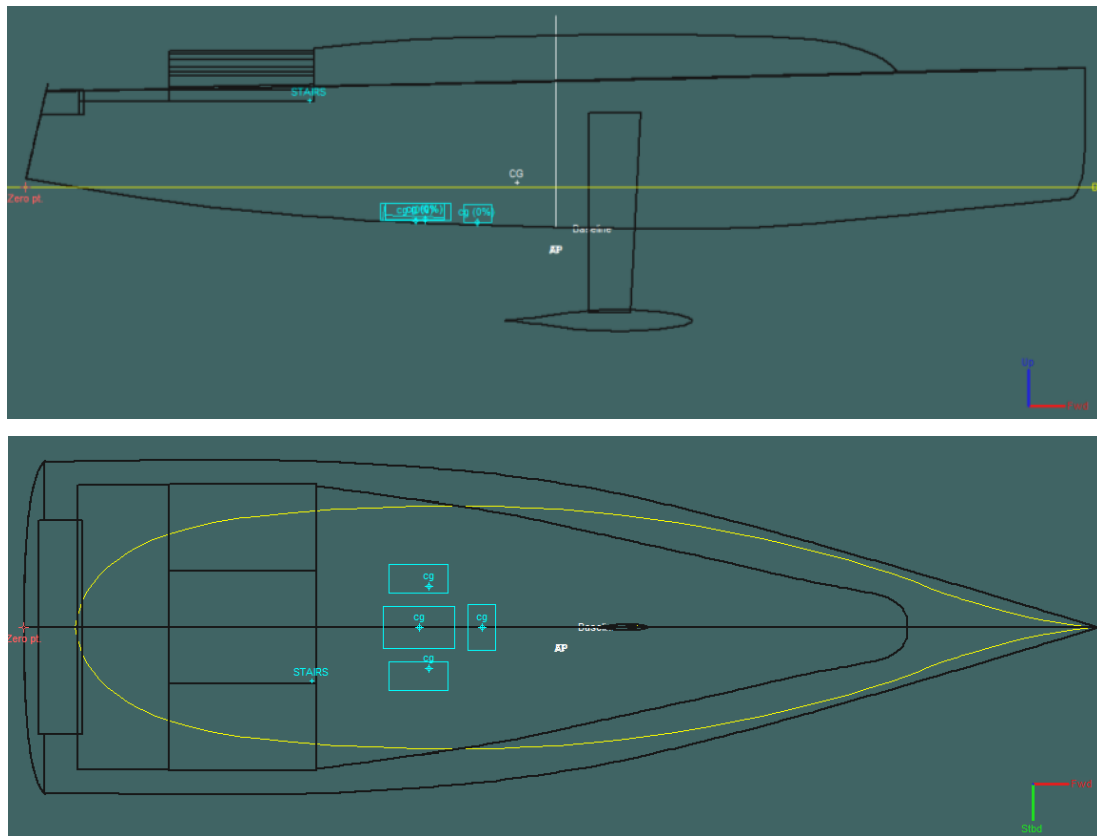


Figure 50: Centre of gravity, tank position and zero point for loadcase N°3 (Figaro 3 Lightship) - Maxsurf Stability display.

Finally, GZ curves are displayed in Figure 51 and the maximum GZ was found around 55° of heel for all configurations, which is a reasonable value.

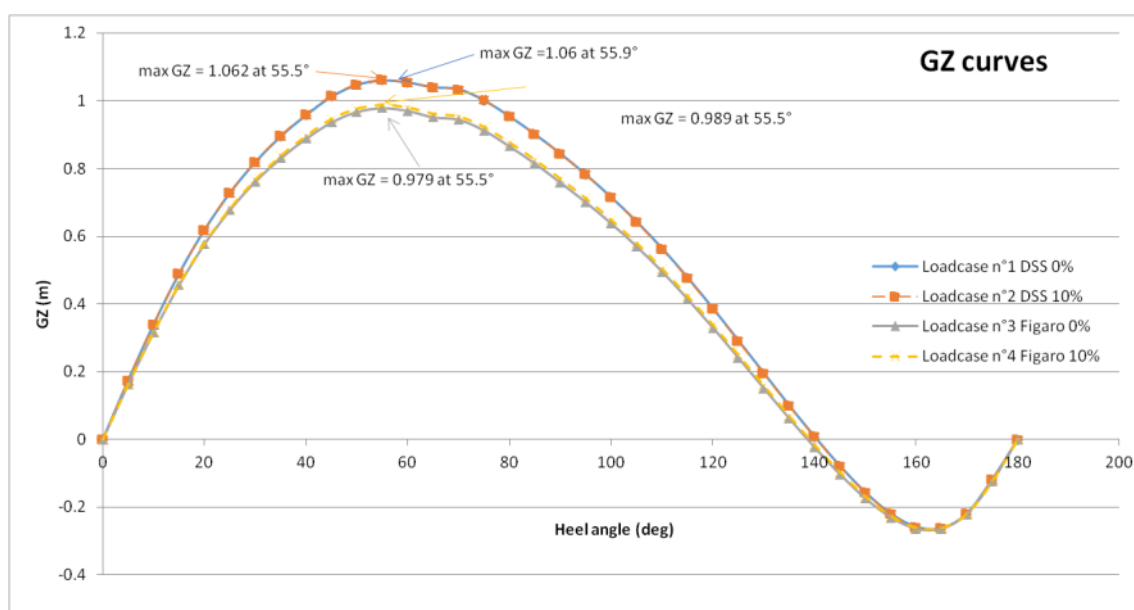


Figure 51: GZ curves for loadcases N°1, 2, 3 and 4 (defined in Table 23) - Maxsurf Stability results.

4.2.10. Velocity Prediction Programme (VPP)

In practice sailing is a very dynamic activity. Just about all of the variables from the true wind speed and upwards are changing continuously and the helmsman and crew are trying to adjust the boat to obtain the best performance all the time. No mathematical solution can ever reflect this. However for each true wind speed (TWS) and true wind angle (TWA), a VPP can provide a snap shot solution assuming a condition based on sailing equilibrium. The VPP attempts to solve all of the aerodynamic and hydrodynamic forces involved in sailing equilibrium.

WinDesign VPP [29] was developed by Wolfson Unit for the analysis of towing tank and wind tunnel tests on conventional sailing vessels. This type of study is best suited to the preliminary design stage, where various options may be evaluated quickly.

First of all, hydrodynamic inputs (dimensions of the hull with rudder and keel) and aerodynamic inputs (rig and sail plan, Figure 52) are referenced in the software.

Then, some scenarios are displayed such as:

- Sail inventory (Table 26), which gives the area, span and fluttering factor AF_x of the Main sail (Main), Fore sail (Jib) and Spinnaker (Spin),
- Sail Sets (Table 27), which gives the sail configuration for upwind and downwind conditions,
- Operation Sets (Table 28), which gives the range of TWA and TWS for upwind and downwind point of sail.

Table 26: Sail inventory

Name	Area	Span	Base Ht	AF _x		Aero	Base
	m^2	m	m	-			
Jib	65.209	20.25	0	1		Jib_0	HEAD
Main	88.564	19.88	2.1	1		Main_0	MAIN
Spin	240.625	22.62	0	0.75		Spin_0	SPIN

Table 27: Sail sets

Upwind	Downwind
Jib	Spin
Main	Main

Table 28: Operation sets

Name	SailSet	Sail area	TWS-Low	TWS-High	TWA-Low	TWA-High
		m^2	<i>knots</i>	<i>knots</i>	<i>deg</i>	<i>deg</i>
Ops_Down	Downwind	329.19	4	25	80	180
Ops_Upwind	Upwind	153.77	4	25	0	130

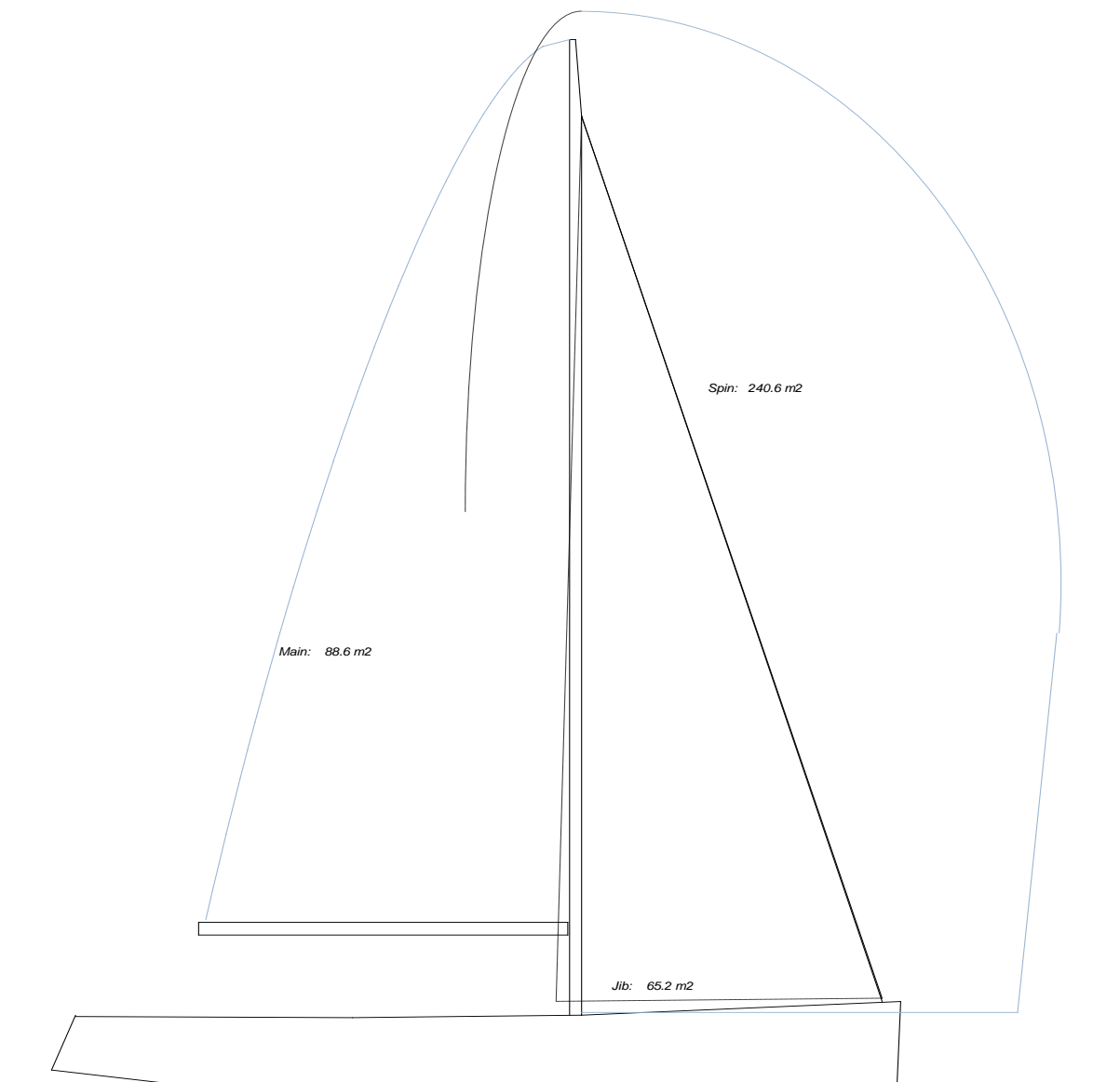


Figure 52: VPP Rig and Sail plan - WinDesign VPP representation.

The interesting results, relative to the true wind speed and true wind angle, are:

- the Boat speed V_S (in knots and Froude number),
- the Heel angle β (in degree),
- the Leeway angle L_α (in degree).

See the results APPENDIX A13: VPP TABLES FOR BEST SPEED, HEEL ANGLE, LEEWAY ANGLE.

The speed polar plot for downwind and upwind conditions is presented in Figure 53.

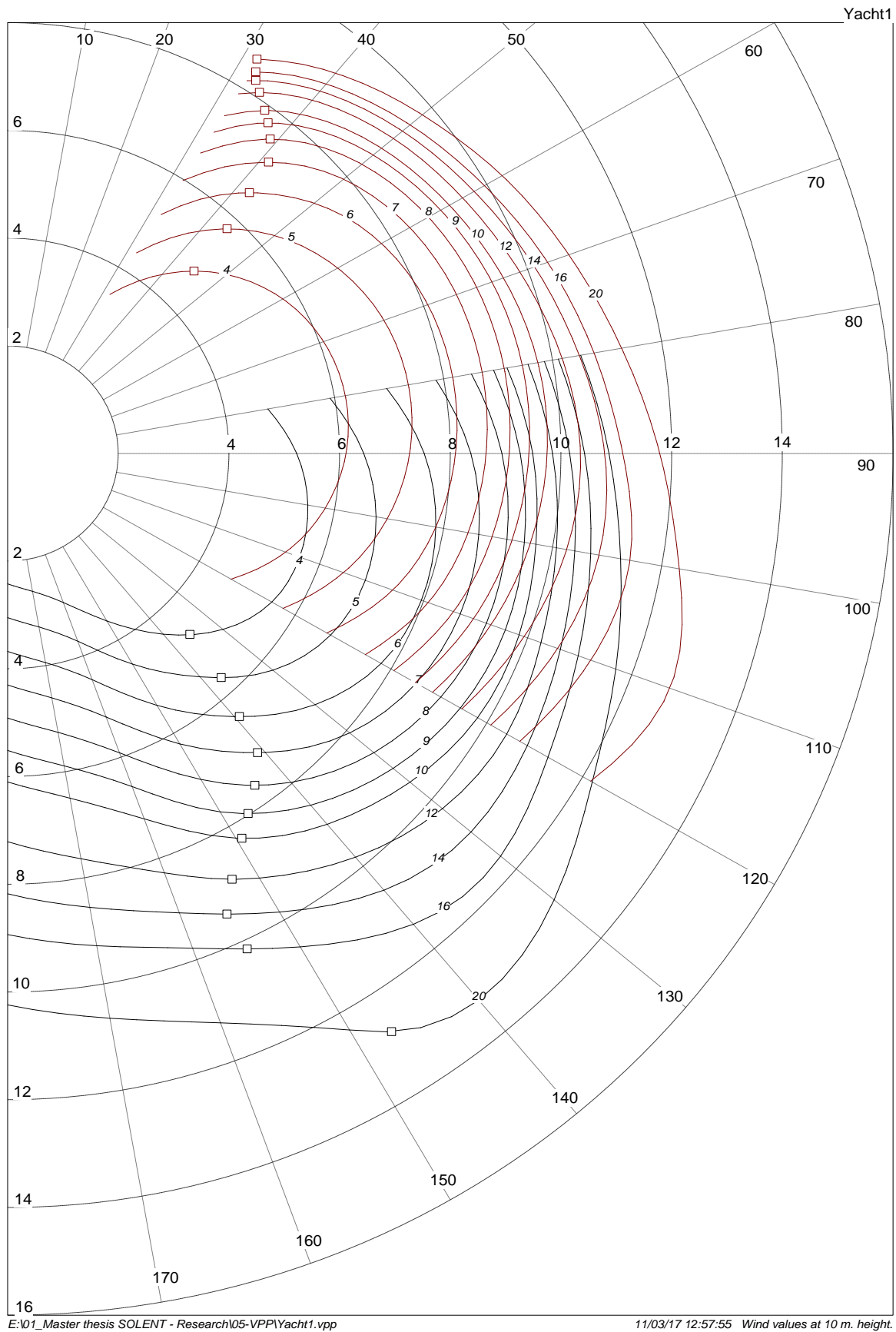


Figure 53: Speed Polar Plot (knots) for Upwind (red curves) and Downwind (black curves) conditions- WinDesign VPP results.

5. PART 2: HYDRODYNAMIC ANALYSIS BY AN EXPERIMENTAL TANK TESTING APPROACH

The second part of the master thesis is to analyse the hydrodynamic resistance of the sailing yacht with hydrofoils, following ITTC guideline procedures [36] for resistance model testing. In order to carry out the hydrodynamic analysis, the full size design of hull and appendages have to be adapted to model scale. Based on the sailing yacht designed in section 4, the model has been manufactured and tested in a towing tank. In a pure hydrodynamic analysis, the model was tested in a towing tank with the three types of hydrofoils: the DSS, the Figaro 3 and also the Dali Moustache foil, even if the latest one is not relevant for applications to cruising boat in this instance due to the lack of volume.

The drag force, side force, heave and trim were measured during the tank testing. All those hydrodynamic results at model scale were gathered in a test matrix and scaling up to full size, according to Froude similarity approach.

The first tests to be run were the model bare hull in order to determine the resistance coefficient of the basic form. The model was later on tested with appendages, first with the keel, and then with each foil, in order to determine the increase in resistance coefficient due to appendages. Other parameters such as the generated side force will also be outlined.

The different configurations were analysed and compared, and their impact on hydrodynamic performance outlined. From a hydrodynamic point of view, it is expected to have less drag force resistance with the hydrofoils. Also, the hydrofoil is expected to improve the efficiency of side force or "effective draft". The effective draft concept will be explained in more detail in sections 5.1.3.5 and 5.2.4. An improvement in lifting force in certain wind conditions should also be observed during experiment.

All the results will be showed in a polar plot to outline the best hydrofoil shape according to the point of sail or to the application, or owner's requirement. The VPP estimation carried out in section 4.2.10 is very important in order to choose the best and realistic sailing conditions for the hydrodynamic analysis.

As the impact on hydrodynamic performance is compared in this part, the effect of the foils on stability and seakeeping is beyond the scope of this investigation and is to be considered for further studies.

5.1. Experimental Tank Testing Approach

5.1.1. Model Dimensions

5.1.1.1. Scaling Rules and Hull Model Dimensions

According to ITTC guidelines procedures for Ship Model [35] the basic requirement is that the model should be geometrically similar to the ship wherever it is in contact with the water.

The model is built geometrically similar to the full scale designed yacht (section 4), with the linear dimension scale factor λ (Eq. 13):

$$\lambda = L_{ship} / L_{model} > 1 \quad \text{Eq. 13}$$

The other conversion formula are shown in Eq. 14, Eq. 15 and Eq. 16:

$$\text{Area:} \quad A_{model} = A_{ship} / \lambda^2 \quad \text{Eq. 14}$$

$$\text{Volume \& force:} \quad V_{model} = V_{ship} / \lambda^3 \quad \text{Eq. 15}$$

$$\text{Time \& Velocity:} \quad T_{model} = T_{ship} / \sqrt{\lambda} \quad \text{Eq. 16}$$

Careful consideration needs to be made to choose the scale factor of the model, taking into account the towing tank dimensions (Table 29). The main concern are:

- the side wall effect: condition where the waves reflect to the side walls of the tank and make the test data less reliable. The beam should not be too big relative to the width of the tank,
- the blockage effect: condition where the flow in the towing tank is partially blocked by the model. The blockage becomes more critical and test data become less reliable as the cross section of the model (beam and draught) increases relative to tank cross section (width and depth),
- the model maximum speed: relative to maximum speed of the carriage,
- the model maximum build weight: relative on the one hand, to the weight requirement so the model can be ballast to the waterline, and on the other hand, relative to the 100N limit of the drag and side force measurement,
- the model maximum length and keel draft, relative to the length of the carriage and depth of the basin.

On the contrary, because of high accuracy requirements, scale effects are critical regarding appendages. Small appendages are severely prone to Reynolds scaling errors. That is why the scale factor shall not be too low in order to use as large models as possible.

Table 29: Towing tank dimensions and restrictions for the model

Towing tank dimensions:		
Item	Value	Unit
Length	60	m
Width	3.7	m
Depth	1.8	m
Restrictions:		
Item	Value	Unit
Model maximum length	2	m
Model maximum weight	50	kg
Carriage top speed	6	m/s

The scale factor $\lambda = 10$ was chosen in order to comply with the restrictions mentioned above.

Table 30 shows the ship and model dimensions for the hull.

Table 30: Hull ship and model dimensions

Ship hull dimensions				Model hull dimensions			
Length overall	L_{OA-S}	15.22	m	Length overall	L_{OA-M}	1.52	m
Waterline length	L_{WL-S}	13.42	m	Waterline length	L_{WL-M}	1.34	m
Beam	B_S	4.7	m	Beam	B_M	0.47	m
Draught	T_{c-S}	2.3	m	Draught	T_{c-M}	0.23	m
Draft keel	T_{k-S}	3.7	m	Draft keel	T_{k-M}	0.37	m
Waterline	DWL	0.6	m	Waterline	DWL	0.06	m
Wetted surface area	WSA_{ship}	36.28	m ²	Wetted surface area	WSA_{model}	0.36	m ²
Water plane area	$A_{waterpl-S}$	34.33	m ²	Water plane area	$A_{waterpl-M}$	0.34	m ²
Surface area	SA_{ship}	160.00	m ²	Surface area	SA_{model}	1.60	m ²
Displacement	Δ_S	11500	kg	Displacement	Δ_M	11.5	kg
Longitudinal centre of buoyancy	LCB_S	6.984	m	Longitudinal centre of buoyancy	LCB_M	0.698	m
Longitudinal centre of floatation	LCF_S	6.536	m	Longitudinal centre of floatation	LCF_M	0.654	m
Max speed to test	V_S	16	kts	Max speed to test	V_M	5.06	kts
Max speed to test	V_S	8.23	m/s	Max speed to test	V_M	2.60	m/s
Max Froude number	Fr	0.717	-	Max Froude number	Fr	0.717	-

5.1.1.2. *Hydrofoils and Keel Model Dimensions*

Having the scale factor, the model dimensions of the keel fin, keel bulb and hydrofoils, keeping the same geometry that was defined for full scale can be obtained (Table 31). The NACA sections will be preserved for the 3D drawings at model scale, even if the Reynolds number dependency is masked in the tank due to the scale. However, as the hydrofoils will be 3D printed, a small modification has been made in the section. The trailing edge has been rounded because it is quite difficult for the 3D printed machine to print sharp edges at this scale.

Table 31: Appendages dimensions model size

Keel		Bulb		Foil DSS		Foil Dali Moustache		Foil Figaro 3	
λ	10	λ	10	λ	10	λ	10	λ	10
C_{av}	6.8 cm	l_b	27 cm	c	7 cm	c_1	7 cm	c_1	7 cm
b	28.5 cm	C_H	4.6 cm	b	23.4 cm	b_1	15.4 cm	b_1	17.4 cm
WSA	400 cm ²	C_v	3.3 cm	WSA	310 cm ²	c_2	6.4 cm	c_2	4.7 cm
t/c	0.12	WSA	230 cm ²	t/c	0.12	b_2	14.2 cm	b_2	16.1 cm
$(1+k)$	1.252	t/c_{av}	0.145	$(1+k)$	1.252	C_{av}	6.7 cm	C_{av}	5.9 cm
		$(1+k)$	1.218			WSA	410 cm ²	WSA (upright)	400 cm ²
						t/c	0.12	t/c	0.12
						$(1+k)$	1.252	$(1+k)$	1.252

5.1.2. *Manufacturing Process and Towing Tank Preparation*

5.1.2.1. *Workshop Manufacturing Process*

First of all, the hull 3D numerical model designed in Rhinoceros was sent to a company (MonsterCam, Lee-on-the-Solent, UK) to be CNC machined. The hull model was made in polystyrene.

Once the model in polystyrene was delivered to the University, it was necessary to add a composite coating in order to strengthen it. This step was done in the workshop, by hand laminate with two layers of fiberglass woven roving fabric (100 gsm and 200 gsm bi-directional orientation) and epoxy resin (mixed with hardener, ratio 100:28, Ampreg 22, Gurit), with the help of Jack Cunningham-Burley (Figure 54).

After the hand laminate, high viscosity resin (resin mixed with SP micro balloons) was applied on the model to cover the bumps (Figure 55).

It was then sanded to make the surface smoother and make a nice finish. It was finally painted with Primer.



Figure 54: Hand lay-up process in the workshop. Own picture.



Figure 55: Resin and micro balloons paste covering. Own picture.

In addition to the hand lay-up process, it was mandatory to think about the installation of the appendages and post on the hull. The longitudinal position of each appendages, heel fitting and post and ballast weight openings is shown in Figure 56 and Figure 57.

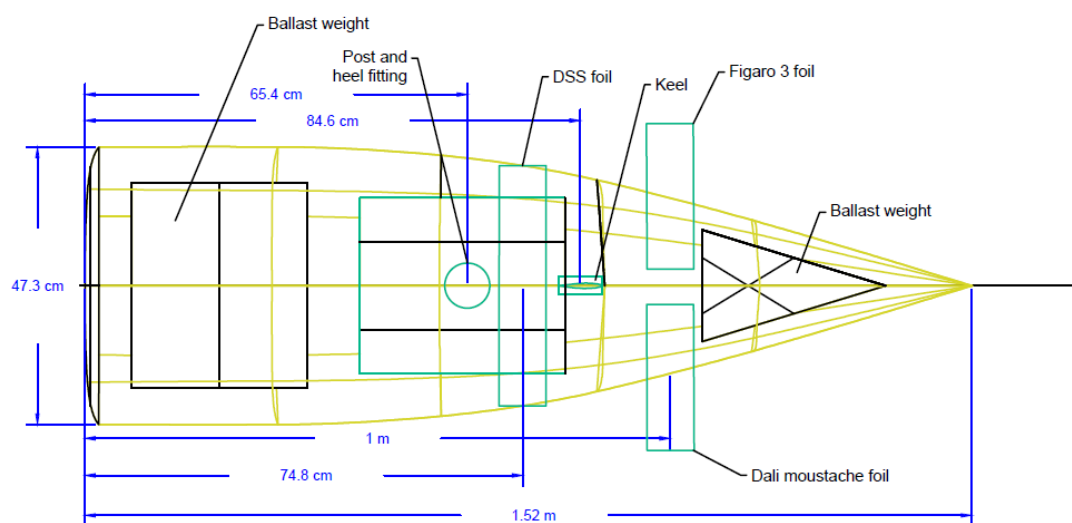


Figure 56: Longitudinal position of appendages and post. Rhinoceros. Own elaboration.

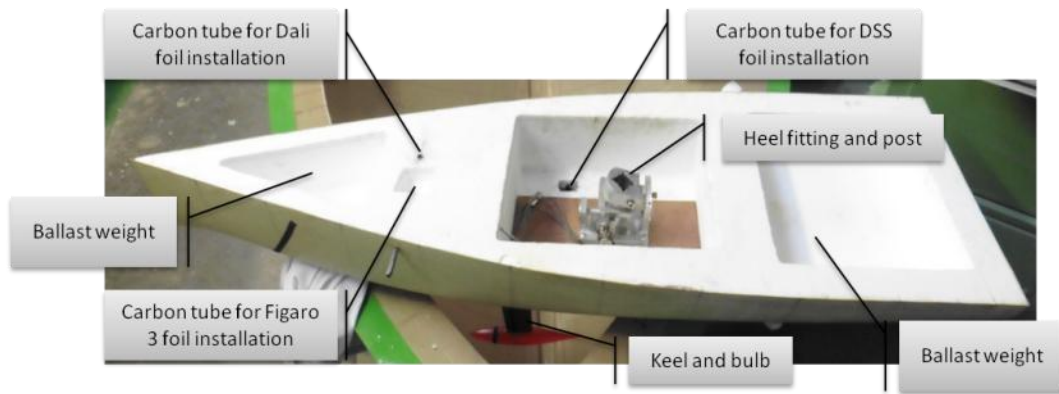


Figure 57: Appendages and post installation on the hull model. Own picture.

First of all, the tow force should be applied at the LCF to avoid trim effect [35]. Hence the heel fitting and post of the carriage will have to be installed at LCF on the hull model.

Then, both keel and hydrofoils should be rigidly attached to the hull and accurately aligned to the center line. A problem, especially with high aspect ratio keel or foil is ensuring that the scaled section are stiff enough, as they can become highly loaded in testing and will easily flex and flutter giving unsteady side force results.

According to ITTC [35]:

- Appendages should be built to the full external shape as designed.
- The manufacturing tolerances of appendages should be within ± 0.2 mm.
- Surface finish should be at least as good as that recommended for the hull model.
- Appendages should be located within ± 0.5 mm of their design position [35].

The three types of foils were attached on the hull with a system of threaded rod and nut, hence, some carbon tubes were inserted in the hull after drilling into the model.

Because of matters of installation on the hull, all the foils could not be attached on the same side of the model. Hence, the DSS and Dali were installed on starboard side, and the Figaro was installed on port side (Figure 58).

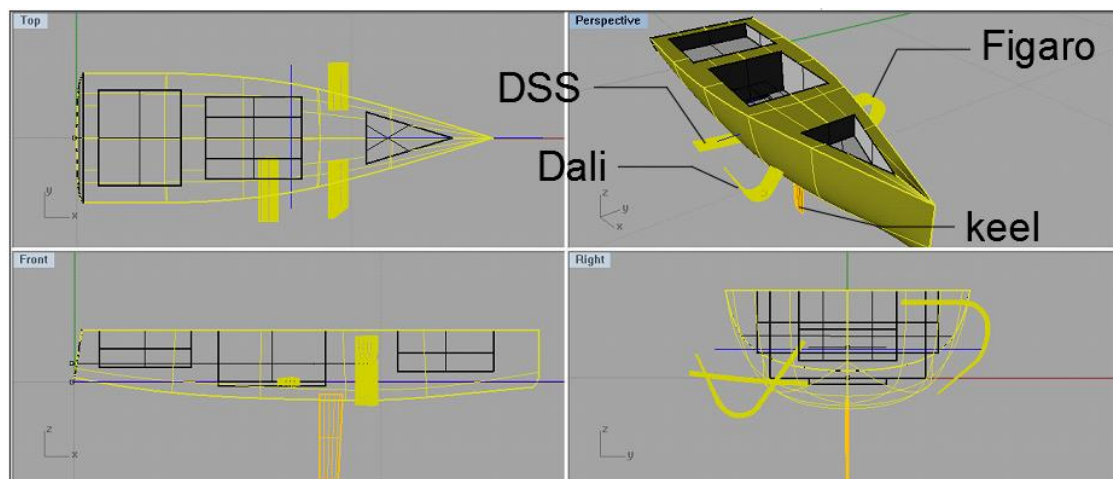


Figure 58: 3D representation of the model with appendages and foils. Rhinoceros. Own elaboration.

Photos of the foils installed on the model in the towing tank are shown in Figure 59, Figure 60 and Figure 61.

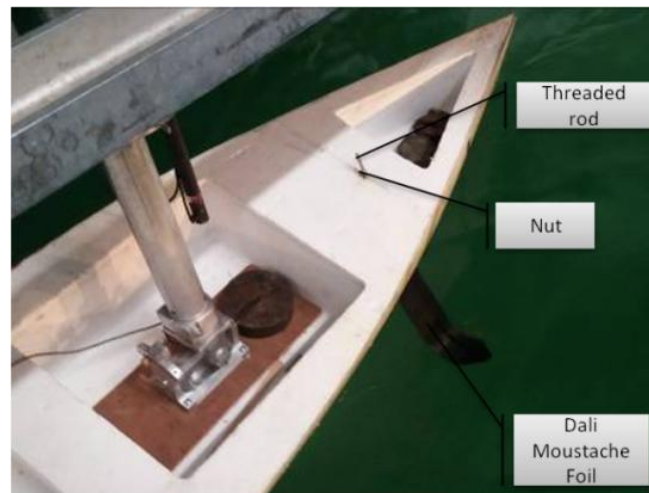


Figure 59: Dali foil attachment on the hull (Starboard). Own picture.

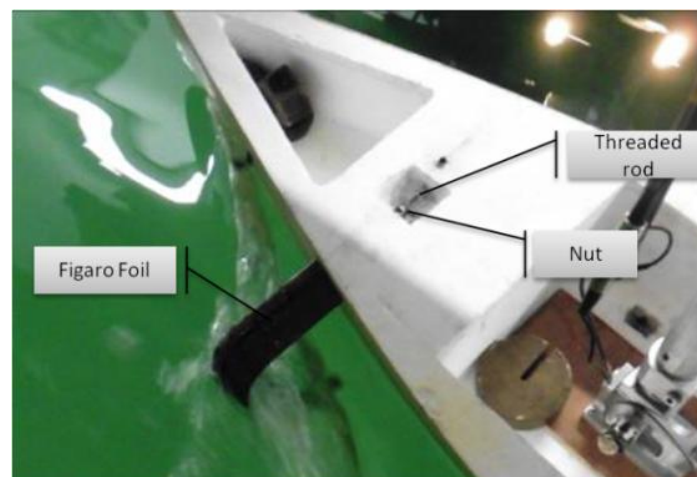


Figure 60: Figaro 3 foil attachment on the hull (Port). Own picture.

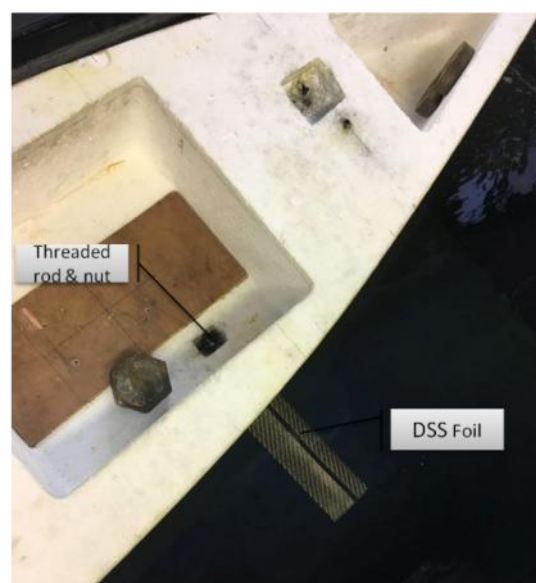


Figure 61: DSS foil attachment on the hull (Starboard). Own picture.

Then, the next in the workshop was to build the keel fin. It was manufactured by assembling plywood laminates, and then sanded to the correct foiled section (Figure 62).



Figure 62: Keel fin plywood laminates. Half of the sanding process. Own picture.

Then, the bulb and hydrofoils were 3D printed in Southampton Solent University. It was 3D printed by stereolithography or SLA (Figure 63) in epoxy resin (ABS). As shown on Figure 64, the Dali and Figaro hydrofoils had to be printed in two pieces in order to fit in the 3D printer (maximum 28 cm).



Figure 63: 3D printers in Southampton Solent University. Own picture.



Figure 64: Plywood keel fin, bulb and hydrofoils after 3D printing. Own picture.

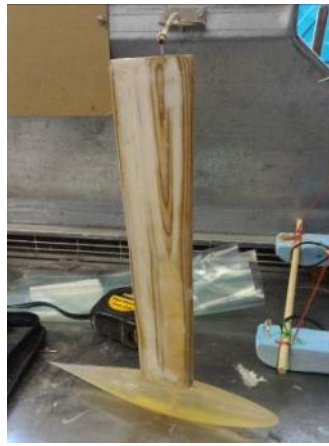


Figure 65: Keel fin and keel bulb. Own picture.

After the bulb and hydrofoils were 3D printed, the bulb was attached to the keel fin (Figure 65), without any other process needed (apart from a little sanding), however the hydrofoils needed to be assembled and then coated with carbon fibre in order to be able to withstand the forces generated. After inserting a threaded rod inside of the foil for future attachment to the hull, the carbon fibre fabric was applied on the foil by vacuum bagging in the workshop (Figure 66).



Figure 66: Vacuum bagging process (DSS foil). Own picture.

Figure 67 shows the foils after all process of bag vacuum, sanding, resin coating, surface finish, and varnish application.

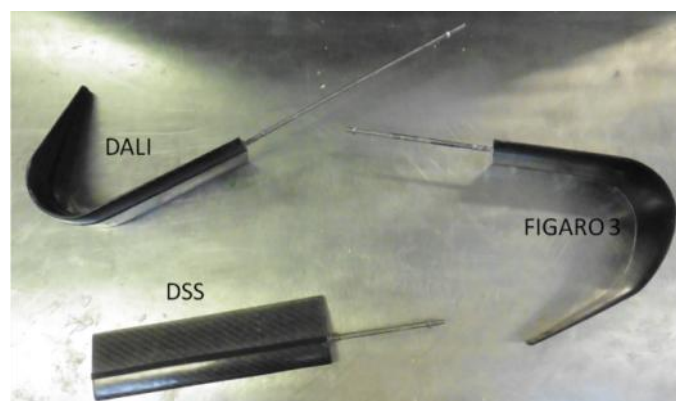


Figure 67: Hydrofoils with threaded rod, after vacuum bagging and finish coating. Own picture.

5.1.2.2. *Turbulent Flow Simulation*

Sand paper strips is installed to ensure transition is achieved in a similar location as on the real boat despite testing at a lower Reynolds number Re .

Roughness strips used for turbulence stimulation will typically comprise backing strips/adhesive of 5 mm to 10 mm width covered with sharp edged sand with grain size around 0.50 mm., with its leading edge situated about 5% L_{PP} aft of the FP [35].

Another method to verify the 5% L_{PP} aft of the FP is to consider that having the critical Reynolds number for a flat plate of $Re_{cr} = 5.E+06$ [3], the distance of the leading edge of the roughness strip can be calculated with Eq. 13 (see Table 32):

$$Re_{cr} = (\rho_w V_s d_s) / \mu \quad \text{Eq. 17}$$

Table 32: Location of the roughness strip calculation for the hull model

Item	Abbreviation	Value	Unit
Critical Reynolds number	Re_{cr}	5 000 000	
Length of the ship full scale	L_{WL}	15.22	m
Density water	ρ_w	1025	kg/m^3
Dynamic viscosity	μ	0.00119	$Pa.s$
Velocity full scale kts	V_s	14	$knots$
Velocity full scale	V_s	3.09	m/s
Distance aft of the FP ship	d_s	0.806	m
Distance aft of the FP model	d_m	0.081	m

The 5% L_{PP} is actually verified: $d_s / L_{WL} = 5.3\%$.

The appendages will additionally have turbulence stimulators situated typically at one third of the bulb length from its fore end [35].

5.1.2.3. *Ballasting*

The model should be loaded to give the correct volume displacement at model scale. This typically involves calculation of the full-scale volume displacement from knowledge of the full-scale weight and the appropriate water density; scaling of the volume displacement to model scale using the adopted scale factor; calculation of the model-scale weight using the water density appropriate for the tank; finally ballasting of the model to the calculated weight. The model weight should be correct to within 0.2% of the correct calculated weight displacement.

In order to estimate the weight of the ballast that need to be placed on the model (Table 33) during the tests, Eq. 18 is used:

$$m_{ballast} = m_{tot} - m_{keel} - m_{barehull} - m_{foil} - m_{post\&heelfitting} \quad \text{Eq. 18}$$

Table 33: Model size ballast and weightage estimation

Item	Abbreviation	Value	unit
Full size ship displacement	Δ_{ship}	11.5	t
Model displacement	Δ_{model}	11.5	kg
Bare Hull	$m_{barehull}$	3.35	kg
Heel fitting & Post weight	m_{post}	2.25	kg
Keel and bulb weight	m_{keel}	0.35	kg
Foil weight (for Figaro 3)	m_{foil}	0.3	kg
Total target weight	m_{tot}	11.50	kg
Ballast weight	$m_{ballast}$	5.55	kg

For the towing tank test, ballast weights were added to the model so that the waterline conformed to the theoretical one.

5.1.3. Towing Tank Testing Theory

5.1.3.1. Model Test Measurement

The towing tank in Southampton Solent University (Figure 68) is used for testing hydrodynamic lift and drag components for sailing and motor craft, and incorporates a wave motor. The basin is 60 m in length, 3.7 m wide and 1.8 m deep. The carriage top speed is 4.6 m/s. The basin is also equipped with a computer-controlled wave generator, and is able to test wave and tidal renewable energy devices. It can be used for instrument calibration.

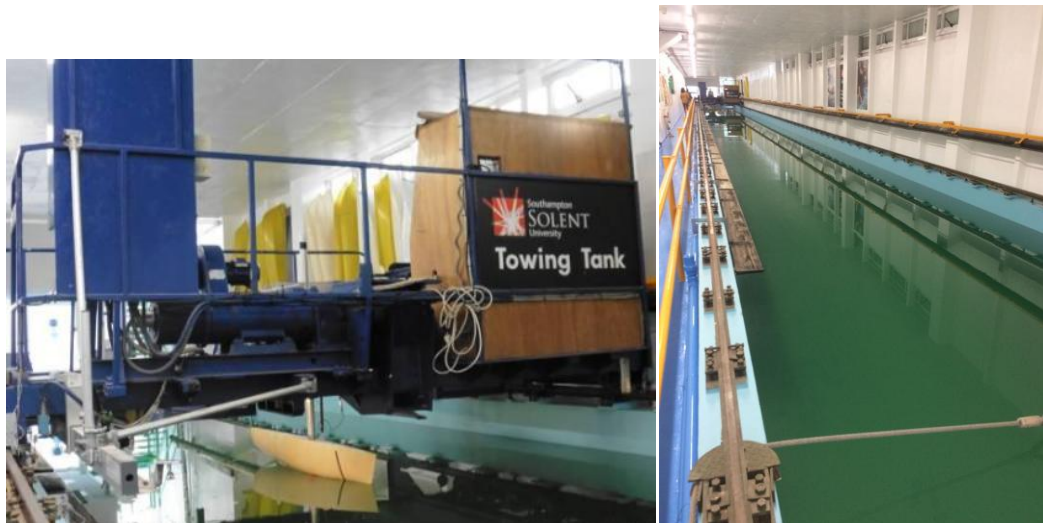


Figure 68: Model in Southampton Solent university's towing tank and towing tank. Own pictures.

Measurement in the towing tank will be performed with the dynamometers and captors (Figure 69). The resistance dynamometer measures the horizontal tow force speed of the towing carriage.

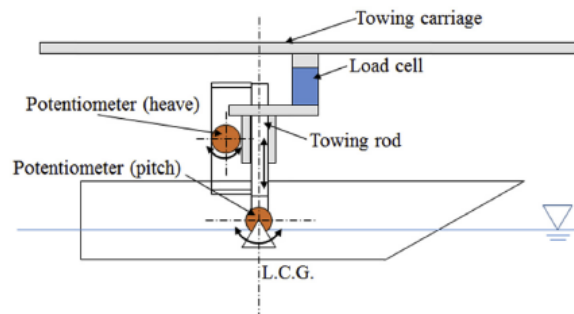


Figure 69: Schematic diagram of the towing mechanisms [48].

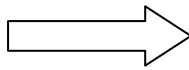
Before the test, it takes time to ballast the model, rig it up, align it, calibrate the dynamometer [36] and install the appropriate foil.

The method that is used to measure the response of the yacht model is called matrix method.

The process is as followed:

Control:

- Speed (Froude number)
- Heel angle
- Yaw angle
- Foil angle of attack



Measure:

- Heave
- Trim
- Drag force
- Side force

In order to determine the speed, heel angle and yaw angle to be configured for the control of the towing tank, the VPP analysis done in section 4.2.10 helps selecting the range of boat speed, heel angle and leeway angle configurations to be tested in towing tank (Table 35 Table 35).

However, careful consideration should be given here. For the towing tank tests, all the combination were tested in order to build the test matrix. But, in order to be consistent and bring the results closer to real sailing conditions, some logic statements may be mentioned when analysing the results in section 5.2. These conjectures are based on the VPP analysis performed in section 4.2.10. As stated in Table 28, upwind conditions correspond to a range of true wind angle between 0 and 130 degree, and downwind conditions corresponds to a range of true wind angle between 80 and 180 degree.

The best configurations to analyse later on are the following (based on Table 34):

- Regarding the boat velocities, the following speeds are referred as upwind conditions when compared to a real sailing condition: $Fr = 0.35, 0.4, 0.45$.
For downwind conditions, the higher speeds will be analysed: $Fr = 0.5, 0.6$ and 0.7 .
- The heel angle is more likely to be close to 20 degree when the boat sails upwind and most likely not more than 10 degrees when it sails downwind.
- Regarding the leeway angle, in upwind condition, the highest leeway angle was found 3 degree and for downwind conditions it was found close to 0 degree.

Table 34: Best speed, heel angle and leeway angle from VPP analyse

	TWS (kts)	4	5	6	7	8	9	10	12	14	16	20
Boat speed (Knots)	Upwind	4.78	5.76	6.54	7.22	7.58	7.8	7.95	8.17	8.32	8.45	8.66
	Dnwind	4.7	5.67	6.43	7.16	7.61	7.97	8.3	8.88	9.43	10.18	12.96
Boat speed (Fr)	Upwind	0.20	0.24	0.28	0.31	0.32	0.33	0.34	0.35	0.35	0.36	0.37
	Dnwind	0.20	0.24	0.27	0.30	0.32	0.34	0.35	0.38	0.40	0.43	0.55
Heel angle (degree)	Upwind	5.39	7.33	9.43	12.03	15.07	17.55	18.58	20.15	21.3	21.56	21.53
	Dnwind	2.42	3.12	3.56	4.02	3.98	3.84	3.71	3.56	3.71	4.6	10.38
Leeway angle (degree)	Upwind	2.25	2.3	2.41	2.53	2.77	2.92	2.93	2.93	2.94	3	3.13
	Dnwind	0.66	0.62	0.57	0.53	0.46	0.39	0.34	0.28	0.26	0.29	0.42

Table 35: Number of runs estimation and real

Item	Nbr	Detail
Models	6	<ul style="list-style-type: none"> Bare Hull Hull and bulbous keel [x2] (Heeling Starboard and Port)* Hull, keel and DSS foil (Heeling Starboard) Hull, keel and Dali foil (Heeling Starboard) Hull, keel and Figaro 3 foil (Heeling Port) <p>*As the foils are not all installed on the same side of the model, the hull with the keel on both heeling side must be run in order to see if the resistance is not too different and to compare the foils resistance (if it is, it means that the model is not symmetrical or that the keel was not correctly aligned). During the tests, the difference was found negligible (less than 5%).</p>
Velocity (Fr)	6	<p>$Fr = 0.35, 0.40, 0.45, 0.5, 0.6, 0.7$</p> <p>The range of Froude numbers from the VPP analyse corresponds to speeds in knots from 8 to 14 knots ($Fr=0.35$ to 0.6). However, as the VPP was run without foils, it was decided to go until 16 knots (which corresponds to $Fr = 0.7$)</p>
Heel angle	2	<p>$\beta = 10$ and 20°</p> <p>Initially, 10, 15 and 20 degree were selected. However, after few first runs, the difference between 10 and 20 was negligible. It was decided to continue the tests only with 10 and 20 degree of heel.</p>

Yaw angle	4	$L_\alpha = 0/2/4/6^\circ$ From VPP prediction, the maximum leeway angle was found 3 degree. However, the effective draft graph will be compared in the results, and the effective draft curve is known to be linear. The leeway angle can be doubled in order to have more precise values.
1 st estimation	288 runs	
Prohaska tests	+ 48 runs	In order to determine the form factor for each heel angle, Prohaska tests must be run at low Froude number prior to the other runs.
Total 1st estimation	336 runs	
Actual number of run	402 runs	Some tests were to be done again due to uncertainty of measurement or mistakes in the installation.
Additional runs for comparison of the foil angle of attack	+ 144 runs	Only one optimum angle of attack for each foil was tested during the internship. This is however interesting to compare the resistance when running the model with different angle of attack. Additional runs were performed after my internship by Charles Kitting, a 3 rd year student in Southampton Solent University who is doing a similar study on hydrofoils for his final year dissertation [49].

The 402 runs were performed during two weeks. A series of 10 runs would take approximately 1 hour, taking into account the necessary waiting time for the tank to settle between each run, and without taking into account the installation time.

The towing tank testing is therefore quite time consuming for a hydrodynamic analysis.

5.1.3.2. *Reminding of Sailing Yacht Resistance for Towing Tank Testing*

Just like any other craft travelling in the air/water interface, the total resistance of a sailing yacht can be broken down into wave making and frictional resistance components, and scaled up to full size using the ITTC 1978 method [38] which is based on Froude number similarity for wave resistance for both model and full size wave resistance scaling. The frictional resistance is calculated separately based on the two very different Reynolds numbers the model and full size yacht are tested at.

Basic testing measures the ship drag as a function of speed. The non dimensional quantities of Froude number, Reynolds number and total drag coefficient are in Eq. 19, Eq. 20 and Eq. 21:

$$Fr = V_S / \sqrt{g.L} \quad \text{Eq. 19}$$

$$Re = V_S.L / \nu \quad \text{Eq. 20}$$

$$C_T = R_T / (1/2.\rho.V_S^2.WSA) \quad \text{Eq. 21}$$

where:

- V_S is the ship velocity (in m/s),
- g is the gravity (in m/s²),
- ν is the kinematic viscosity (in m²/s),
- ρ is the mass density of fresh water (in kg/m³),
- R_T is the total resistance of the ship (in N),
- L is the length of the ship (in m),
- and WSA is the wetted surface area (in m²).

In addition to the above, there must also be an induced drag term of the hull, keel and rudder due to their side force generation, which is required for sailing. There will also be some changes in resistance due to heel. Thus the resistance of a sailing yacht can be broken into the following components in Eq. 22:

$$R_{TOTAL} = R_U + R_H + R_I \quad \text{Eq. 22}$$

The sailing yacht resistance is composed of:

- R_U the upright resistance (consisting of frictional and wave making resistances)
- R_H the heel resistance (when the boat is heeled, it will contain the resistance of component due to heeling)
- R_I the induced resistance (the drag due to total side force generated by hull/appendages - associated to Froude number)

5.1.3.3. Upright resistance calculation R_U

The upright resistance of the yacht R_U comprises two main components, which are calculated separately. In tank testing terms, they are split into the viscous resistance R_V and the wave resistance R_W .

The viscous resistance R_V is the sum of the friction and the form drag for the hull and each appendage such as keels, rudders and keel bulb.

The friction coefficient is calculated using standard ITTC 57 friction line formulae (Eq. 23).

$$C_F = 0.075 / (\log Re - 2)^2 \quad \text{Eq. 23}$$

This formulae was originally derived from tests on ship hulls which tend to have parallel mid bodies. Yachts tend not to, and consequently, actual friction coefficients for yachts tend to be slightly higher than that predicted using the ITTC 1957 formulae. Hence, for traditional long keel yachts, the characteristic length of the waterline used in the Reynolds number component is normally taken as 70% of the waterline length (L_{WL}) as shown in Eq. 20.

$$Re_{hull} = (0.7 L_{WL} V_S) / \nu \quad \text{Eq. 24}$$

However, for modern hull, 100% L_{WL} may be taken instead of 70%. In the experiment, it will just result to a higher form factor.

For appendages on modern shaped, the Reynolds number is taken on the average chord of the foiling section in question or in the case of the bulb, use the bulb fore-aft length. This is justified considering the length of an average streamline, unlike along conventionally shaped hull (Figure 70):

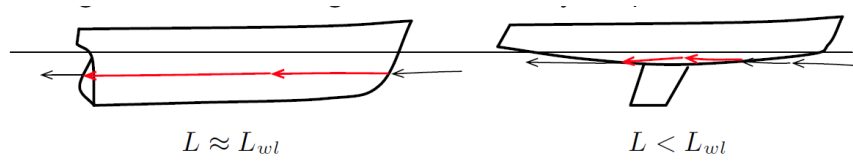


Figure 70: Modern sailboat hull particularity [50].

This lead us to this relation: $Re_{hull} \gg Re_{appendages}$. To sum up, Eq. 25, Eq. 26 and Eq. 27 are used to calculate the Reynolds numbers.

$$Re_{hull} = (L_{WL} \cdot V_S) / \nu \quad \text{Eq. 25}$$

$$Re_{foil} = (c \cdot V_S) / \nu \quad \text{Eq. 26}$$

$$Re_{bulb} = (l_{bulb} \cdot V_S) / \nu \quad \text{Eq. 27}$$

When tank testing, it is usual to establish the form factor $(1+k)$ so as to establish the viscous pressure drag for the hull, and also the appendages.

First of all for the hull, the form drag is a fixed percentage of the 2D friction drag (i.e. $\text{drag} = k\% \times \text{Friction drag}$). Then, the viscous drag is $(1+k) \cdot R_F$ or in coefficient terms, $C_V = (1+k) C_F$. Thirdly, the wave drag coefficient is $C_W = a Fr^n$, where a is a constant and n is 4.

Hence, from the basic rules where $C_T = C_V + C_W$, and $C_T = (1+k) \cdot C_F + a Fr^4$, equation Eq. 28 is obtained:

$$C_T / C_F = (1+k) + a (Fr^4 / C_F) \quad \text{Eq. 28}$$

The form factor can be obtained in the usual way using the Prohaska plot technique (The intercept of a linear regression through a plot of Fr^4 / C_F against C_T / C_F) [36]. An example of Prohaska plot from the results of the bare hull model run upright (no heel, no yaw) in the towing tank is shown in Figure 71 and APPENDIX A14: PROHASKA PLOT BARE HULL shows the other Prohaska plot when the model is heeled.

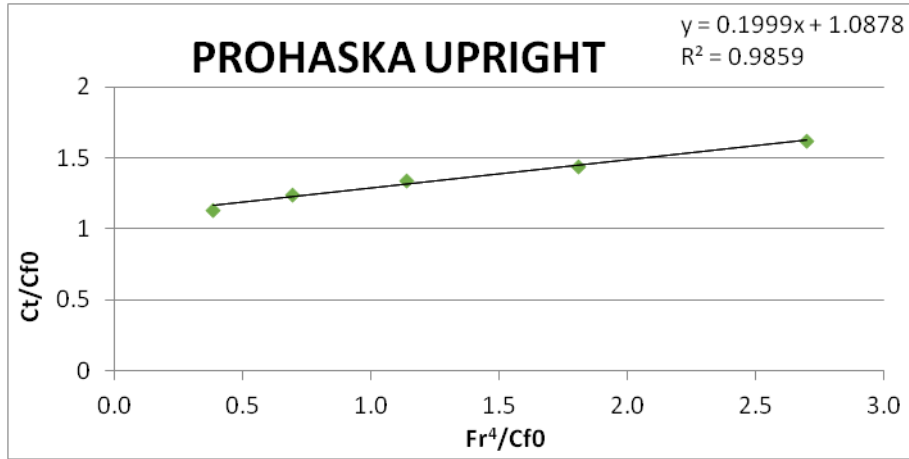


Figure 71: Prohaska plot from the towing tank test matrix. Upright (no leeway angle, no heel angle).

For appendages, two different formula are used, one specific for foiled section and another for bulbs. The tank testing is not necessary to estimate the form factor for those appendages.

For any foiling section (keel fin, rudder or hydrofoil), form factor can be estimated with Eq. 29, formulae proposed by S.F. Hoerner deduced by testing in wind tunnel [51]:

$$(1+k)_{foil} = 1 + 2.(t/c) + 60.(t/c)^4 \quad \text{Eq. 29}$$

where c is the average chord of the foiling section.

For bulbs, form factor is estimated with Eq. 30 proposed by Hoerner [51]:

$$(1+k)_{bulb} = 1 + 1.5 (t/c) \quad \text{Eq. 30}$$

where (t/c) is the average thickness to chord ratio (in the case of elliptical shaped bulb).

Finally, the friction coefficient C_F and viscous coefficient C_V are calculated as follow in Eq. 31 and Eq. 32:

$$C_F = 0.075 / (\log_{10} Re - 2)^2 \quad \text{Eq. 31}$$

$$C_V = C_F (1+k) \quad \text{Eq. 32}$$

Then, the wave resistance coefficient C_W can be calculated. Assuming the yacht is towed with no heel angle or leeway angle (upright, zero yaw) with a keel and bulb and hydrofoil attached, then the measured total drag R_T for a particular speed (or Fr) is in equation Eq. 33.

$$C_T = R_T / (1/2 \cdot \rho \cdot V_S^2 \cdot WSA) \quad \text{Eq. 33}$$

Then, for that Froude number, the bare hull wave drag coefficient $C_{W \text{ model}}$ is calculated as in Eq. 34.

$$C_{T \text{ model barehull}} = C_{T \text{ total measured}} - C_{V \text{ keel}} - C_{V \text{ foil}} - C_{V \text{ bulb}} \quad \text{Eq. 34}$$

This is referred to as stripping out the appendages drag (Eq. 35).

$$C_{W \text{ model barehull}} = C_{T \text{ model barehull}} - C_{V \text{ model barehull}} \quad \text{Eq. 35}$$

Then, $C_{W \text{ ship}}$ at full scale is equal to the $C_{W \text{ model}}$ (Eq. 36)

$$C_{W \text{ model barehull}} = C_{W \text{ ship barehull}} \quad \text{Eq. 36}$$

To obtain $C_{T \text{ ship}}$ at full size, recalculate all of the appendages and hull friction coefficient (as the Reynolds number will have increase) and multiply each recalculated C_F by their respective unchanged form factor $(1+k)$ to give the full size viscous drag coefficients (Eq. 37).

$$C_{T \text{ ship}} = C_{W \text{ ship}} + C_{V \text{ (hull, keel, bulb, foil) ship}} \quad \text{Eq. 37}$$

NB: This is important to note that this is true for no leeway (hence no lift and no induced drag) and no heel angle (no assymetricity and no change in wetted surface area).

5.1.3.4. Heel resistance calculation R_H

Calculating the viscous resistance at set heel angles is necessary to improve the accuracy of wave coefficients. As heeled, the yacht experiences changes to the upright resistance due to changes in wave making resistance, the waterline length and the hull wetted surface area.

As seen in section 5.1.3.3, the wave resistance is dependent of the form factor $(1+k)$, the waterline length L_{WL} and the wetted surface area WSA.

For the bare hull, the approach is to update the form factor $(1+k)_{\text{hull}}$ by Prohaska method, for each heel angle to be tested. Also, the wetted surface area and waterline length will be predicted using Maxsurf programme [28]. It will predict any changes in waterline length whilst heeled, which may lead to changes in Reynolds number for a particular speed.

For the appendages, the form factor, wetted surface area and average chord will be estimated the same as in upright position since the bulbous keel and hydrofoils (except for the Figaro 3) are completely in the water. The only difference in the wetted surface area and waterline length exists for the Figaro 3 foil. However, since the difference is not significative at model scale, the assumption made for the hydrodynamic analysis is that the maximum wetted surface area will be taken (for 20° heel).

5.1.3.5. Induced drag resistance calculation R_I : The Effective Draft Concept

When a yacht is sailing or in the case of towing tank tests, towed at a yaw (or leeway) angle both the hull and its appendages will contribute to the generation of lift, or side force. A consequence of side force generation is that there will be an additional drag associated with lift generation which is called induced drag (D_I) according to 3D foil theory. The Induced drag is proportional to the lift or side force generated by the appendages squared (SF^2) (Eq. 38) and may be determined from towing tank data.

$$C_{DI} = C_L^2 / (\pi \cdot AR_G) \quad \text{Eq. 38}$$

with AR_G , the geometric aspect ratio.

Combining Eq. 38 and the basic formula of lift and drag Eq. 39 and Eq. 40,

$$C_L = L / (1/2 \cdot \rho \cdot S \cdot V_S^2) \text{ or } C_L = SF / (1/2 \cdot \rho \cdot S \cdot V_S^2) \quad \text{Eq. 39}$$

$$C_{DI} = D_I / (1/2 \cdot \rho \cdot S \cdot V_S^2) \quad \text{Eq. 40}$$

the equation for the Induced Drag D_I is deduced (Eq. 41):

$$D_I = SF^2 / (1/2 \cdot \rho \cdot S \cdot V_S^2 \cdot \pi \cdot AR) \quad \text{Eq. 41}$$

where S is the planform area Eq. 42 and AR is the geometric aspect ratio Eq. 43:

$$S = \text{span} \times \text{average chord} \quad \text{Eq. 42}$$

$$AR_G = \text{span}^2 / S \quad \text{Eq. 43}$$

Thus, for a lifting surface (Eq. 44):

$$S \cdot AR_G = (\text{span} \times \text{average chord}) \times (\text{span} / \text{average chord}) = \text{span}^2 \quad \text{Eq. 44}$$

The 3D foil theory is based on a foil of finite span with tips at either end, the geometric aspect ratio of the foil is expressed in terms of the total span as $AR_G = \text{span}^2 / S$. However, the keel and hydrofoils, whilst clearly acting as foils, only have one tip, the other end of the foil being the bounded of the hull. If the hull provided a perfect mirror effect boundary at one end, the keel could be seen as one half of the 3D foil, whose effective aspect ratio was twice that of the actual keel for elliptical spanwise loading (no tip vortex). In the case of the foils tested in this master thesis, the value will be closer to 1.8. Hence, the effective aspect ratio is $A_E = 1.8 \times A_G$. Also, the equivalent span of the hull and keel combination is referred to as effective draft T_E .

Hence, for a sailing yacht sailing in air/water interface, the formula is Eq. 45:

$$S \cdot AR_E = (T_E \times \text{average chord}) \times (1.8 \cdot T_E / \text{average chord}) = 1.8 \cdot T_E^2 \quad \text{Eq. 45}$$

Then, the induced drag is calculated with Eq. 46:

$$D_I = 0.9.SF^2 ./ (T_E^2 \cdot \pi \rho . V_S^2) \quad \text{Eq. 46}$$

where:

- D_I is the induced drag in N
- SF is the side force in N
- T_E is the effective draft in m
- V_S is the boat speed in m/s
- ρ is the water density in kg/m^3

Finally, if the dynamometer measures the generated side force SF and the induced drag is subtracted and identified from the total drag of a heeled and yawed model, then the effective draft could be calculated as in Eq. 47:

$$T_E = \sqrt{(0.9.SF^2 ./ (D_I \pi \rho . V_S^2))} \quad \text{Eq. 47}$$

Hence, a first comparison can be made to select the best foil in terms of generating lift. For a particular heel angle, the effective draft T_E against Froude numbers is plotted. In the instance of Figure 72 for 20 degree of heel, the DSS configuration is the most efficient one in terms of generating lift until Froude number 0.6. For the highest speed, the Dali moustache is the best configuration.

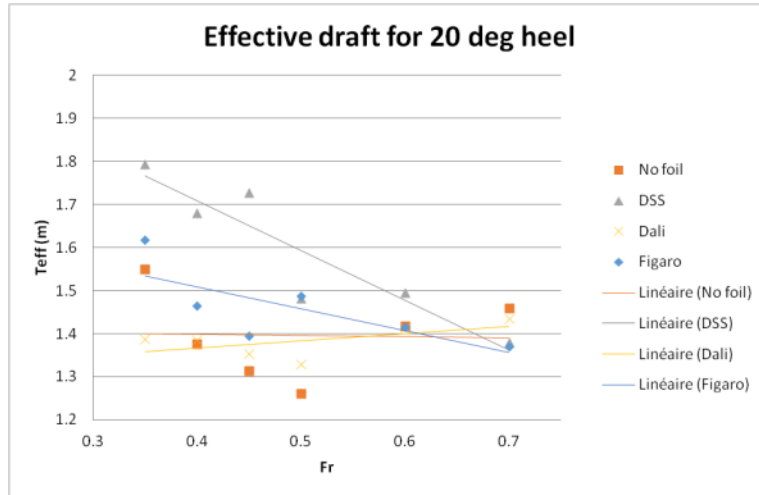


Figure 72: Effective draft against Froude number comparison for 20 degree of heel.

Considering the slope of a straight line plot of the SF^2 (x axis) versus the total drag (y axis) which is plotted for a fixed yacht speed (or Froude number) and fixed heel angle, for a range of incremented yaw angles (see Figure 73), then the slope of that line is Eq. 48.

$$y/x = D_I / SF^2 \quad \text{Eq. 48}$$

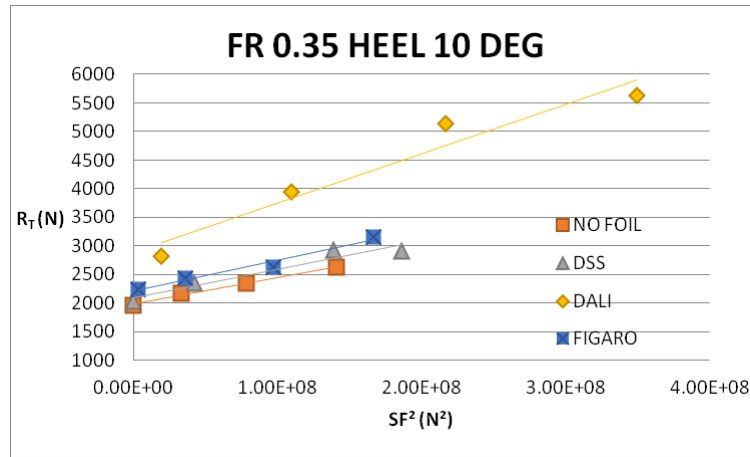


Figure 73: Effective draft graph from the tank test matrix. Comparison between the model without foil, with DSS foil, and with Figaro foil at Froude number 0.35 and 10 degree of heel.

Hence, for a particular boat speed and heel angle, different model configurations can be compared and the most efficient one in terms of the lowest resistance can be selected by determining the lowest value. In the instance of Figure 73, the model without foils is the best, and if we compare between the three foils, the model equipped with DSS foil is the most efficient.

5.1.3.6. Scaling to Full Size - Test Matrix

From measurement, the following data output will be obtained at model scale, and have to be scaled to full size:

- the resistance drag (in N),
- the side force (in N),
- the heave (in mm),
- the trim (in degree)
- and also the speed (in m/s).

The scaling of the results to full size was carried out in a Test Matrix in Excel.

Froude similarities implies that the Froude number and the wave resistance coefficient are equal: $Fr_M = Fr_S$, and $C_{W,M} = C_{W,S}$ as shown in Eq. 49.

$$V_{model} / \sqrt{(g \cdot L_{model})} = V_{ship} / \sqrt{(g \cdot L_{ship})} \quad \text{Eq. 49}$$

Therefore, the speed of the full scale ship is calculated with Eq. 50:

$$V_{ship} = V_{model} \cdot \sqrt{\lambda} \quad \text{Eq. 50}$$

For the drag, as explained in section 5.1.3.3, will use model test to find the total resistance of the model $R_{T,M}$ and $(1+k)$ for each configuration, and then extrapolate it to full scale model in order to find the real resistance of the ship.

Also, the side force is scaled as follow (Eq. 51):

$$SF_{ship} = SF_{model} \cdot \lambda^3 \cdot (\rho_{seawater} / \rho_{tankwater}) \quad \text{Eq. 51}$$

And the heave and trim are scaled as follow (Eq. 52 and Eq. 53):

$$Heave_{ship} = Heave_{model} \cdot \lambda \quad \text{Eq. 52}$$

$$Trim_{ship} = Trim_{model} \quad \text{Eq. 53}$$

5.1.3.7. *Uncertainty of measurements*

As for every tests, the results from measurements have chances to be less precise due to measurement uncertainty. The uncertainty sources can be:

- Model geometry
- Model installation
 - Hull positioning (Yaw angle)
 - Alignment of the keel on the centre line and symmetry of the keel fin and bulb
 - Angle of attack of the foil installation
- Instrument Calibration
- Instrumentation measurement

The quoted bias accuracies are for indicative purposes only. Uncertainty analysis should be used to derive the actual requirements.
- Water temperature

5.2. Hydrodynamic Analysis

5.2.1. Upright Hull Resistance Comparison

First, the bare hull model is towed at no heel and no leeway in order to determine the upright resistance of the basic form.

From these results, a first basic analysis that can be made to compare the hull upright resistance from experiment against the upright resistance calculated with Maxsurf Resistance [27] and WinDesign VPP [29].

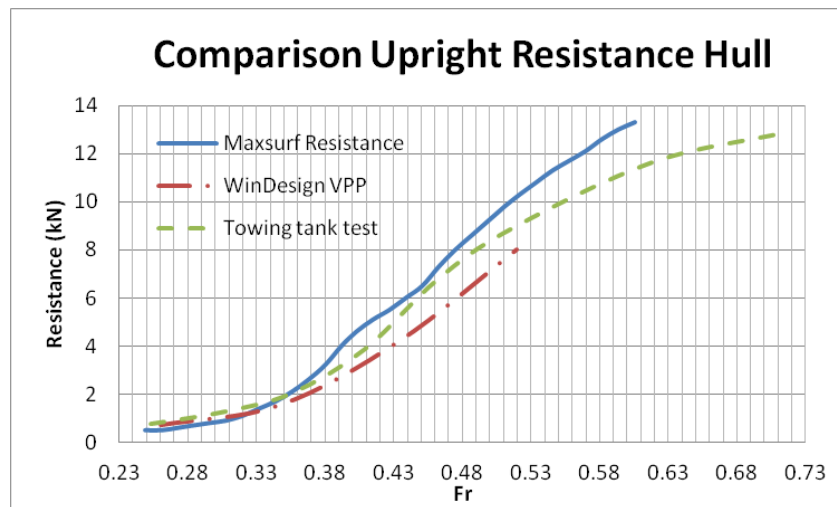


Figure 74: Upright resistance comparison between software prediction and towing tank tests.

Looking at Figure 74, the upright resistance calculated with Maxsurf Resistance, WinDesign and the tank test results have a similar pattern. However, after $Fr = 0.33$, the resistance calculated with Maxsurf Resistance using Delft series III seems to be less accurate since it is less regular (rises suddenly at $Fr = 0.33$, drops back at $Fr = 0.4$ and rises again at $Fr = 0.45$).

Also, the resistance predicted with WinDesign VPP is the lowest one, it seems that the Wolfson Unit calculation underestimates the resistance from $Fr = 0.4$ to $Fr = 0.5$ compared to Delft Series method or experimental measurement. This means the VPP will be very optimistic as a lower resistance has been assumed. Hence the actual speeds would be lower than those of the VPP.

Finally, the resistance measured in the towing tank seems to be in between the two predictions and the curve increases progressively.

In the next parts, the model will be run heeled and yawed, with and without hydrofoils. Additional resistance will be present: induced drag due to leeway and drag due to heel.

5.2.2. Resistance, Lift, Heave and Trim Comparisons

First of all, it should be noted that the model was tested only with one foil in the case of Figaro and Dali moustache, since when it is heeled windward, only one foil is deployed. In the case of the model having 10 degree of heel, the Figure 75 shows that the foil which is retracted does not impact too much, only in the case of Figaro we have a more wetted surface area in the water, leading to more resistance. Moreover, it was in a matter of cost since one foil was expensive to manufacture and also in a matter of installation on the model. The Figaro and Dali being on the same longitudinal position it could not have been possible to install two pairs of foils on the model. It can simply be said that in the case of Figaro, more resistance is expected when reading the hydrodynamic results.

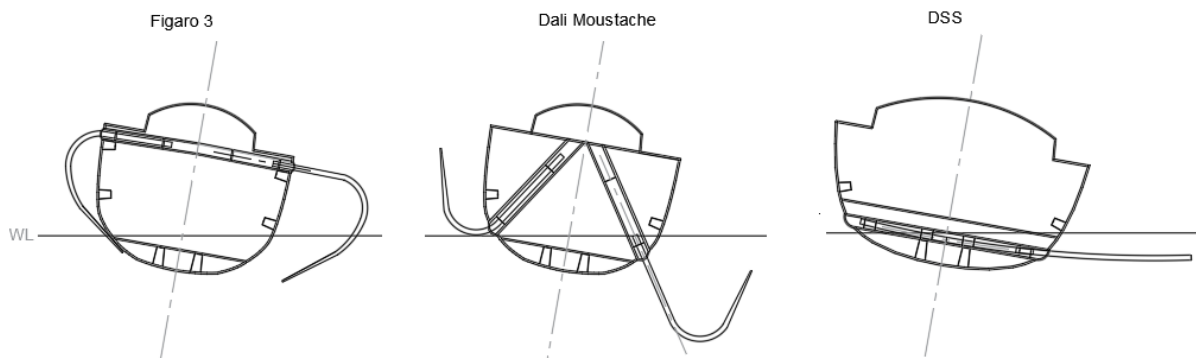


Figure 75: Model with foils heeled at 10 degree.

As shown on Figure 76, the 402 runs during the experiment are controlled by the velocity, the heel angle, the leeway angle and the angle of attack of the foil (see section 0).

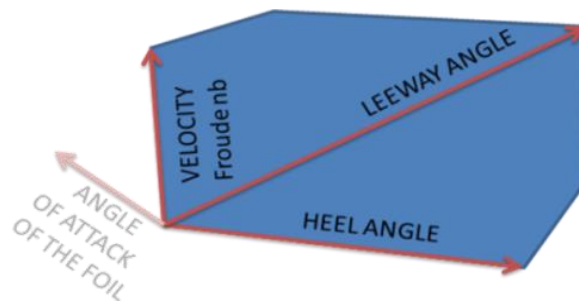


Figure 76: Influence of the parameters on the Resistance Prediction. Own elaboration.

The drag, side force, heave and trim against Froude number graphs at full scale were plotted at all leeway and heel angles in the test matrix (see APPENDIX A15: DRAG, SIDE FORCE, HEAVE AND TRIM GRAPHS). A first overview of the drag, side force, heave and trim results for 20 degree of heel and 4 degree of leeway is shown in Figure 77, Figure 78, Figure 79 and Figure 80.

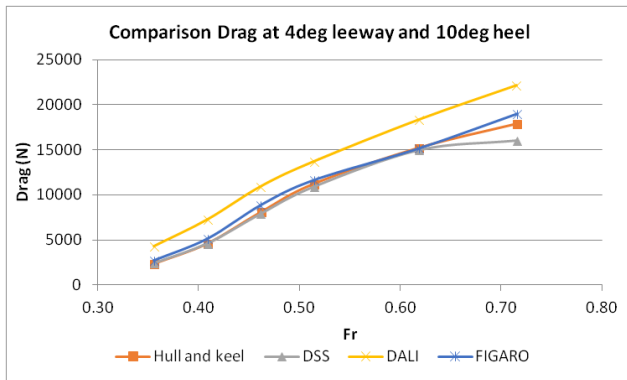


Figure 77: Drag force at leeway 4° and heel angle 20°

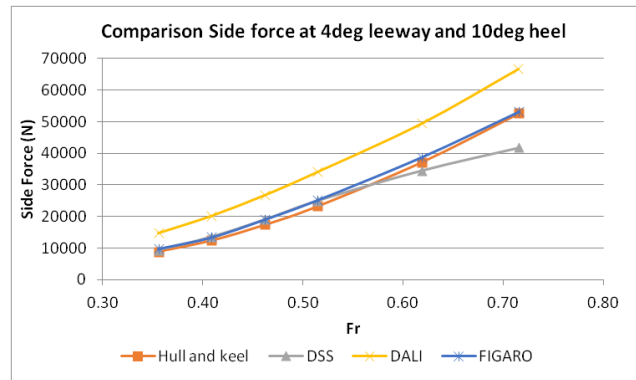


Figure 78: Side force at leeway 4° and heel angle 20°

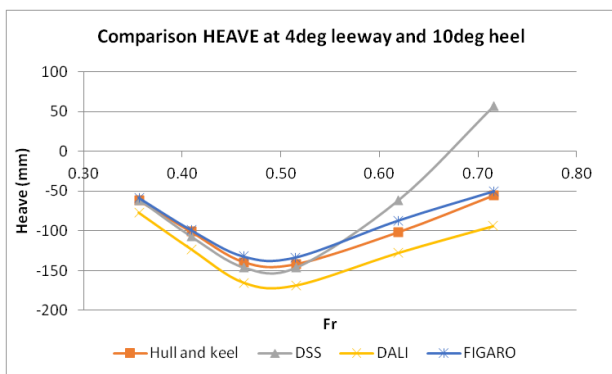


Figure 79: Heave at leeway 4° and heel angle 20°

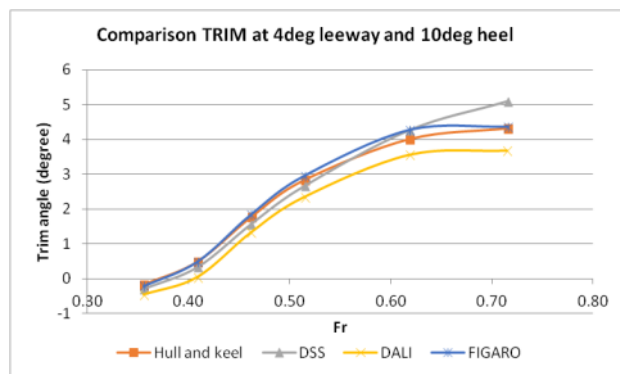


Figure 80: Trim at leeway 4° and heel angle 20°

Figure 77 shows that, in terms of pure resistance, foils are not reducing the drag since the hull only always has the lowest resistance. So the benefit of the foils is not in the resistance decrease, and would most likely be in the stability (increased RM) or seakeeping.

Looking at the test results for each foil, it has been noticed that for the same model, there is less resistance when the model is tested with a reduced heel angle. Hence, the interest of having foils is in the increased RM, that enables to reduce the heel and the resistance.

Refer to APPENDIX A16: RESISTANCE COMPARISON BETWEEN LOW AND HIGH HEEL ANGLE FOR EACH FOIL AT DIFFERENT LEEWAY ANGLE for the resistance graphs comparisons.

In term of pure hydrodynamics, it is however still important to us to find out which foil would be best suited to which condition. The Dali moustache foil generates the more drag as expected since it has the most wetted surface area compared to the two other foils (Table 36).

Table 36: Wetted surface area of each foil at 20 degree of heel in calm water at full scale

	DSS	Dali	Figaro
WSA at 20 degree of heel without waves (m ²)	2.04	3.71	1.73

The Dali generates the more drag but also the more side force (Figure 78). It is also noticed that the DSS generates less drag than the Figaro, which is not expected when looking at the WSA, but which is explained by observation during the experiment. At 20 degrees of heel, the vortices generated by the bow of the hull at high speeds (usually from $Fr = 0.45$) interfered with the Figaro foil, and the foil starts to aspirate the water around and sprays water around (Figure 81). All of this contributes in generating more resistance.



Figure 81: Vortex generation from the bow and interference with Figaro foil at high speeds in the tank. Own picture.

This observation is the proof that the theory and the experiment does not always meet the same conclusion. Hence, Eq. 54 using the wetted surface area cannot be used to calculate the resistance with Figaro 3 foil.

$$R_{DI} = 1/2 \cdot \rho \cdot WSA \cdot V^2 \cdot C_{DI} \quad \text{Eq. 54}$$

Careful consideration should be made when reading the results of Figaro 3 foils, and one solution is to use Gerritsma formula (Eq. 55):

$$R_{DI} = 1/2 \rho S V^2 C_L^2 / (\pi \cdot AR_G) \quad \text{Eq. 55}$$

with:

- The planform area: $S = \text{span} \times \text{average chord}$,
- The geometric aspect ratio: $AR_G = \text{span}^2 / WSA = \text{span} / \text{average chord}$ (The average chord is taken instead of the WSA in the geometric aspect ratio)

Looking at the heave on Figure 79, the general observation that can be made is that the hull sinks from $Fr = 0.35$ to $Fr = 0.5$ (the heave decreases) and then rises up (the heave increases). Also, the drag of the DSS drops at higher speeds. It is explained by the fact that the hull is

lifted out of the water looking at the heave (Figure 79), hence less wetted surface area, hence less resistance. However, the side force generated by the DSS is the lowest (Figure 78).

It can also be noticed on Figure 80 that the foil generating the less trim angle is the Dali moustache (3.5 degree at maximum speed), as predicted in section 2.3.1. It even decreases the trim by one degree compared to the model without foils. The worst configuration regarding the trim angle is the Figaro (5.2 degree at maximum speed).

Table 37: Drag and Side Force contribution of each foil compared to the results without foils. Heel 20 degree and leeway 4 degree.

	No foil		DSS		Dali		Figaro		Foil Addition in Drag			Foil Addition in SF		
Fr	Drag	SF	Drag	SF	Drag	SF	Drag	SF	DSS	Dali	Figaro	DSS	Dali	Figaro
	N	N	N	N	N	N	N	N	N	N	N	N	N	N
0.35	2267	7455	2217	8815	4492	14455	2779	8841	-50	+2225	+512	+1360	+6999	+1386
0.4	4757	10642	4728	11738	7735	19646	5462	12065	-29	+2978	+705	+1096	+9004	+1423
0.45	8424	15723	8486	17931	11613	27359	9997	19035	+62	+3188	+1573	+2209	+11636	+3313
0.5	11887	22001	12057	24691	14928	35614	13240	25564	+170	+3041	+1354	+2690	+13612	+3562
0.6	16804	37357	15993	37694	20364	53950	17889	41400	-810	+3560	+1085	+336	+16593	+4043
0.7	19576	52321	17901	44995	25583	73413	21490	55351	-1675	+6007	+1915	-7325	+21092	+3031

Before comparing the results with the effective draft method in section 5.2.4, Table 37 shows a quick overview of the contribution of each foils in term of drag and side force at 20 degree of heel and no leeway. It is obvious that the DSS brings the less drag, at the highest speed, there is even less drag than without foils. However, there is a huge drawback regarding the side force since the contribution is very small, and especially for $Fr = 0.6$ and 0.7 .

As predicted, the Dali moustache foil contributes the most in Side force but the huge drawback is the resistance.

For a boat heeling at 20 degree and 4 degree of leeway, the Figaro seems to be a good compromise between the DSS and the Dali since it provides sufficient additional side force to the keel and add some resistance in a reasonable amount.

5.2.3. Influence of Angle of Attack

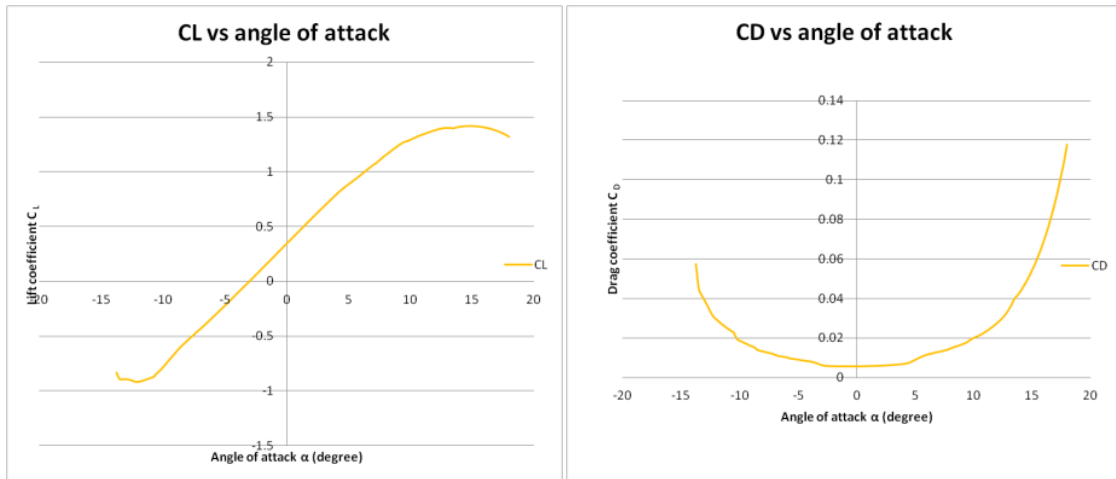


Figure 82: Lift and Drag coefficient against angle of attack for NACA 63 412 at $Re=5.0 \text{ E}+06$ [42].

For a fixed Reynolds number $Re = 5.0 \text{ E}+06$ for each foil, the lift and drag coefficient curves against the angle of attack (Figure 82) were selected from [42].

Once C_L and C_D against α is known, the lift and drag force can be calculated with Eq. 56 and Eq. 57 and compared to experiment:

$$L = C_L \cdot \frac{1}{2} \cdot \rho \cdot WSA \cdot V_S^2 \quad \text{Eq. 56}$$

$$D = C_D \cdot \frac{1}{2} \cdot \rho \cdot WSA \cdot V_S^2 \quad \text{Eq. 57}$$

Induced drag can also be calculated and compared to experiment with Eq. 58:

$$R_{DI} = \frac{1}{2} \cdot \rho \cdot WSA \cdot V_S^2 \cdot \frac{C_L^2}{\pi \cdot AR_G} = 1.8 \cdot \left(\frac{1}{2}\right) \cdot \rho \cdot (\text{average chord})^2 \cdot V^2 \cdot C_L^2 / \pi \quad \text{Eq. 58}$$

Careful consideration should be done to select the correct angle of attack since it should not be higher than the stall angle, the concern is mostly important for the DSS foil since it has a flat shape and that its main hydrodynamic contribution is the lift.

On Figure 82, the stall angle is $\alpha_{\text{stall}} = 14$ degree.

Also, as the trim angle of the model increases with speed during the test in the towing tank, the angle of attack of the foil is also increased. This should also be taken into account when choosing the angle of attack of the foil.

Finally, it was decided to test Dali foil with the angle of attack at 0 degree and 16 degree (Figure 83), Figaro foil with the angle of attack at 0 degree and 8 degree (Figure 84); and DSS foil with the angle of attack at 0, 4 and 8 degree (Figure 85).

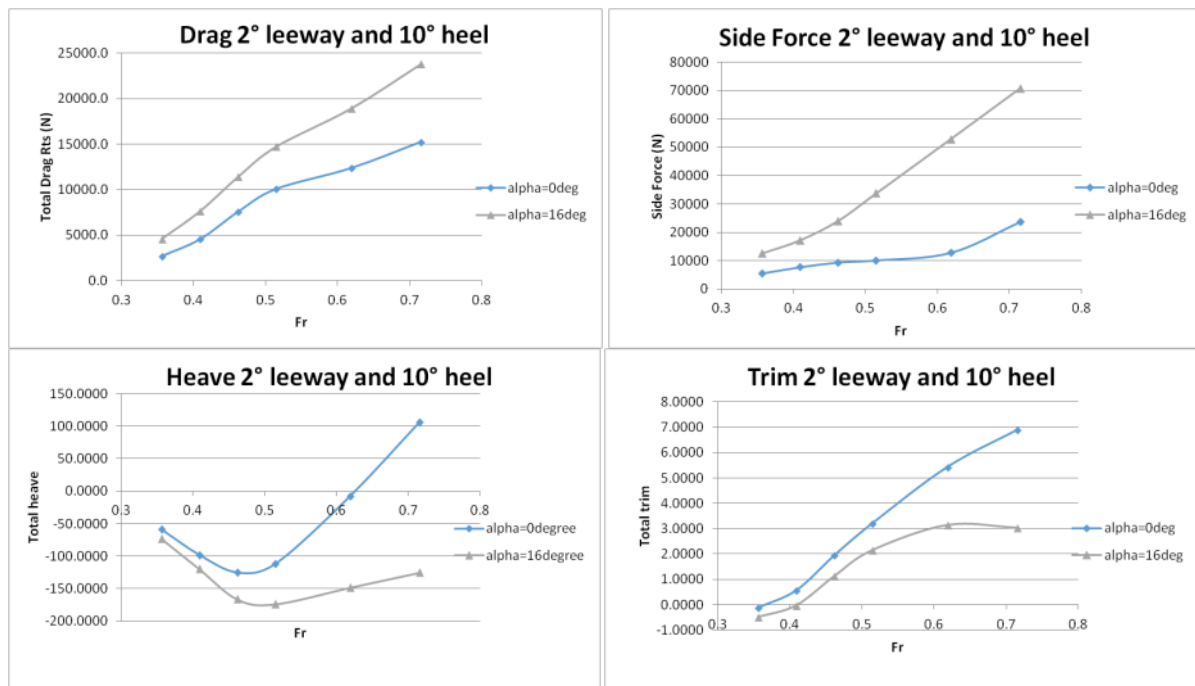


Figure 83: Drag, Side Force, Heave and Trim comparison for different angle of attack with Dali foil

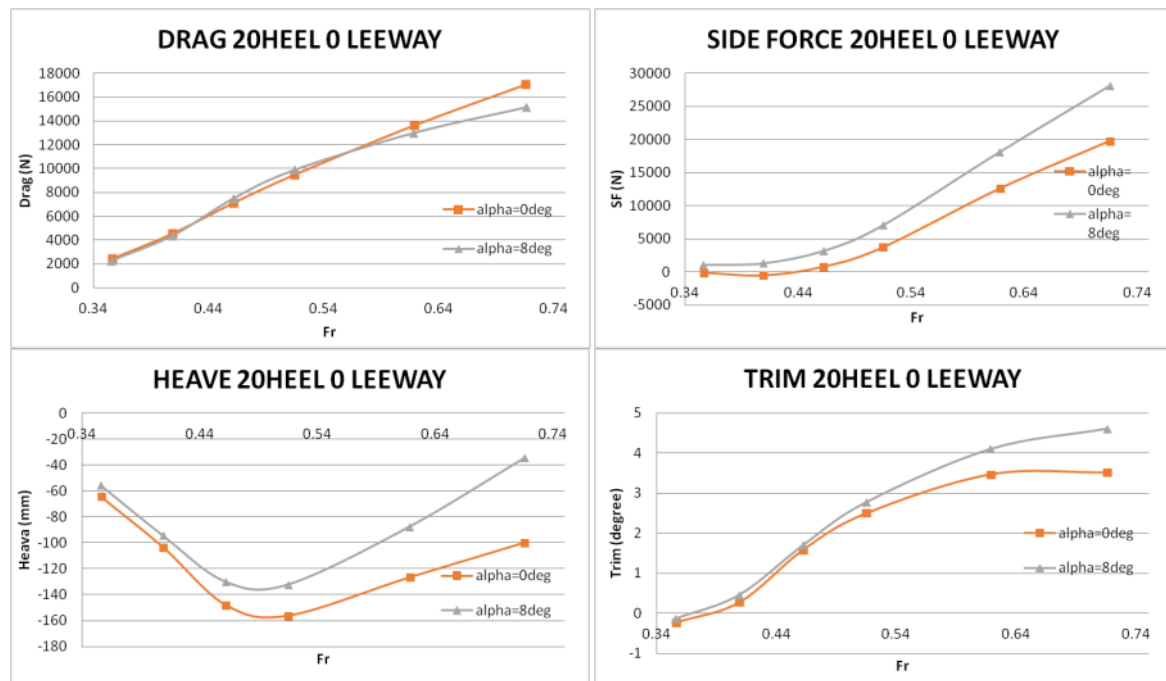


Figure 84: Drag, Side Force, Heave and Trim comparison for different angle of attack with Figaro foil

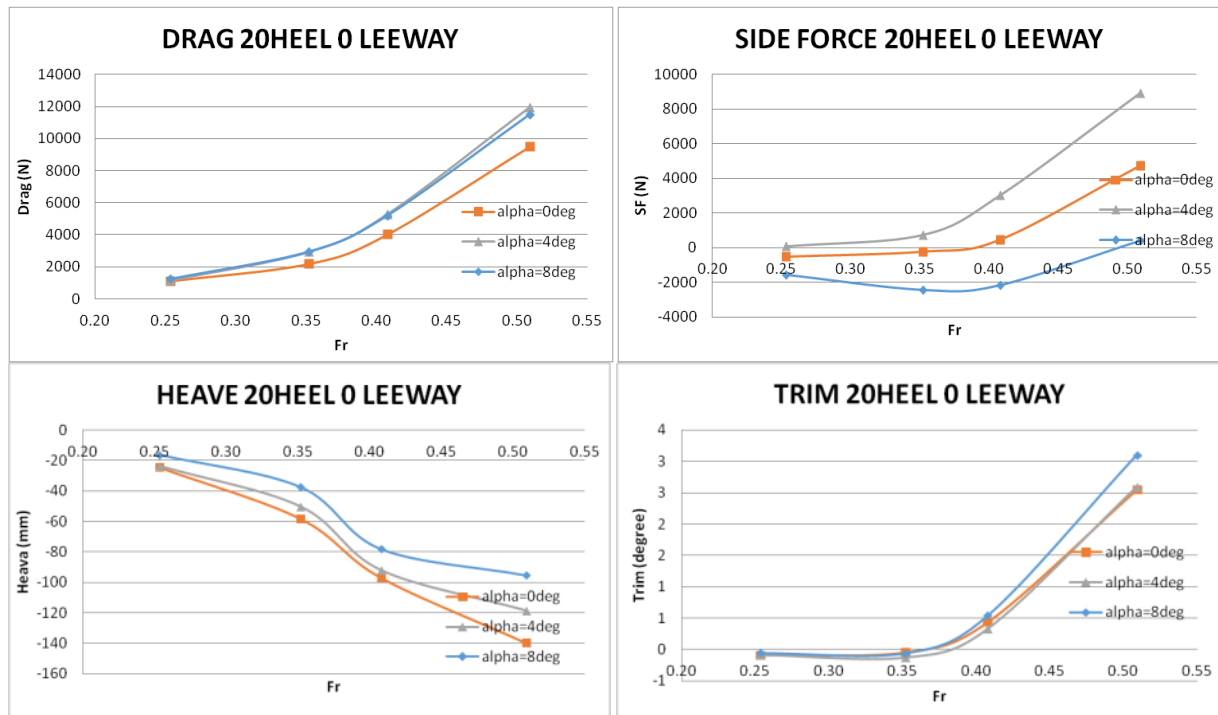


Figure 85: Drag, Side Force, Heave and Trim comparison for different angle of attack with DSS foil. Available from Charles Kitting test results [49].

Looking at the results for Dali foil (Figure 83), there is a decrease in resistance at higher speed for a smaller angle of attack due to the boat raising, as shown by the heave. However, the side force is decreased by a lot and the trim angle is highly increased. So the foils are more efficient in term of side force generation at higher angle of attack as guessed by Aygor Teksen in his last year master thesis [14].

Looking at Figaro foils' results (Figure 84), the main conclusion is that the more the angle of attack, the less the resistance at higher speeds due to the boat raising, as shown by the heave. It is also better in term of side force generation when the angle of attack is higher. Hence, it was a good guess to choose an angle of attack higher than 0 degree when testing Figaro foil.

Figure 85 shows the further tests results carried out by another student in Southampton Solent university [49] with the same model in the towing tank. He went deeper in the analyse on the influence of the angle of attack with the DSS foil. Because the student is designing a longer yacht (LOA=24 m), the range of velocities were not the same, hence, when scaling to model size, the Froude numbers tested are not the same. It gives however a good first overview of the drag, side force, heave and trim behaviour for these Froude numbers. From these graphs, the first remark is that the drag is lower for 0 degree of angle of attack, which is logical.

However, the looking at the heave, the model is sinking the most when no angle of attack, which is not expected looking at the drag. Then, looking at the side force graphs, the tests with no angle of attack is lower than with 4 degree, and when we test with 8 degrees, the side force is even generated on the opposite side, which is a huge drawback. Moreover, the trim angle is higher when tested with 8 degrees. Hence, when testing the DSS foil, it is better not to set the angle not more than 4 degrees.

5.2.4. *Effective Draft Results*

The angle of attack of the foil is fixed for each foil (Table 38). The choice was made in accordance with the quick comparison analysis made for different angle of attack in section 0.

Table 38: Angle of attack chosen for each foil

		DSS	Dali	Figaro
Angle of attack α	degree	0	16	8

As the aim is to be close to the real sailing conditions, few configurations will be selected, complying with the VPP predictions, and the results will be gathered in a table (section 5.2.4.3):

- In upwind condition (TWA from 30 to 80/90 degree and TWS 0 to 25kts):
 - velocity $Fr = 0.35$ at Heel angle 20 degree
 - velocity $Fr = 0.40$ at Heel angle 20 degree
 - velocity $Fr = 0.45$ at Heel angle 20 degree
- In downwind condition (TWA from 80 to 180 degree and TWS 0 to 25kts):
 - velocity $Fr = 0.45$ at Heel angle 10 degree
 - velocity $Fr = 0.50$ at Heel angle 10 degree
 - velocity $Fr = 0.60$ at Heel angle 10 degree
 - velocity $Fr = 0.70$ at Heel angle 10 degree

In order to come to the conclusion of which foil is better in which condition, two different comparisons will be made. First, the best foil in term of the lowest resistance or induced drag will be selected by comparing the total drag (R_T) and side force squared (SF^2) obtained at various leeway angles for a given heel angle and velocity. Then, in order to compare the foils' efficiency in terms of generating lift, the effective draft (T_E) against Froude numbers will be plotted, and the highest value selected as best configuration.

5.2.4.1. Sailing Upwind

The graphs representing the Drag against Side force squared for upwind condition are plotted in Figure 86.

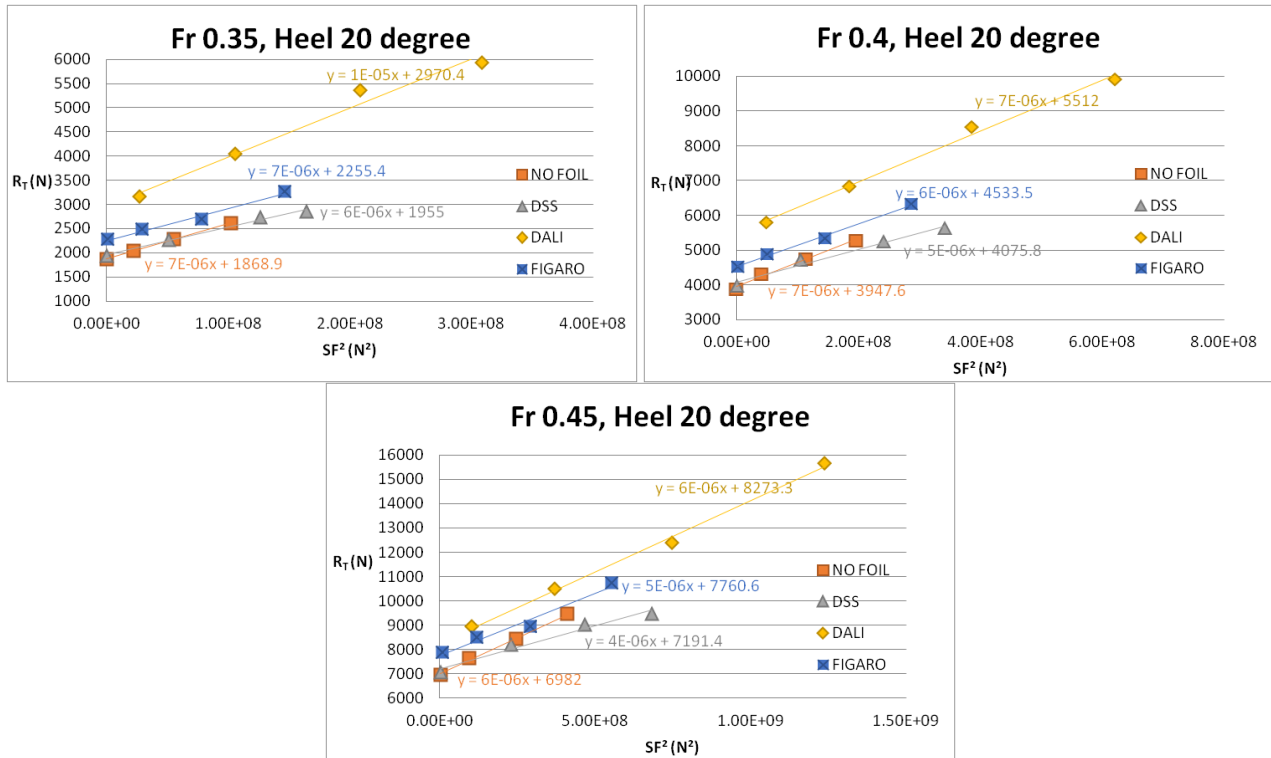


Figure 86: Drag against Side force squared graph for upwind condition (Heel angle 20 degree and Froude number 0.35, 0.40 and 0.45)

It seems that the better configuration is with the DSS foil when considering the Drag/Side force squared ratio at higher leeway angle. The Dali moustache is the worst choice in term of resistance as seen earlier.

At Froude number 0.35, the results without foils are very similar than with the DSS. The more the speed, the better the results with the DSS.

Figure 87 represents the effective draft value against Froude numbers comparison for upwind point of sail (20 degree of heel, Fr 0.35 to 0.5).

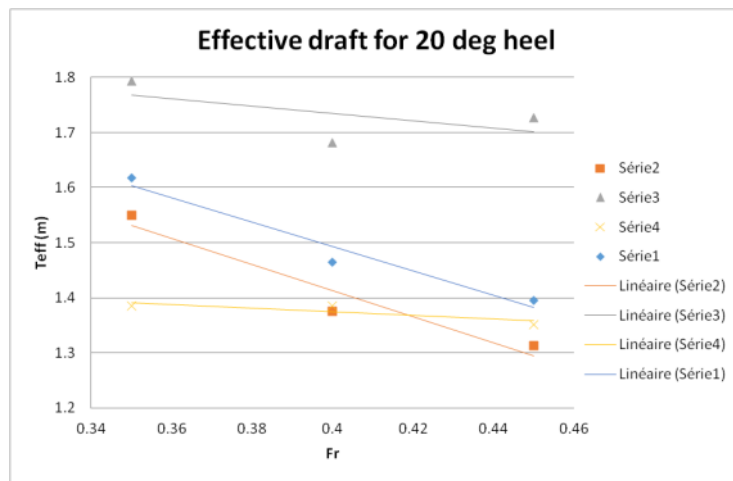


Figure 87: Effective draft graph against Froude number for upwind condition - Heel 20 degree

Looking at Figure 87, the best configuration in term of generating lift for upwind condition is with the DSS foil since it has the most effective draft T_E at low Froude number. The second better configuration is with the Figaro foil. Then, the model with the keel only is the third better option until Froude number 0.45, and after this the model with the Dali moustache is better than without foils.

5.2.4.2. Sailing Downwind

The graphs for downwind condition are plotted below in Figure 88.

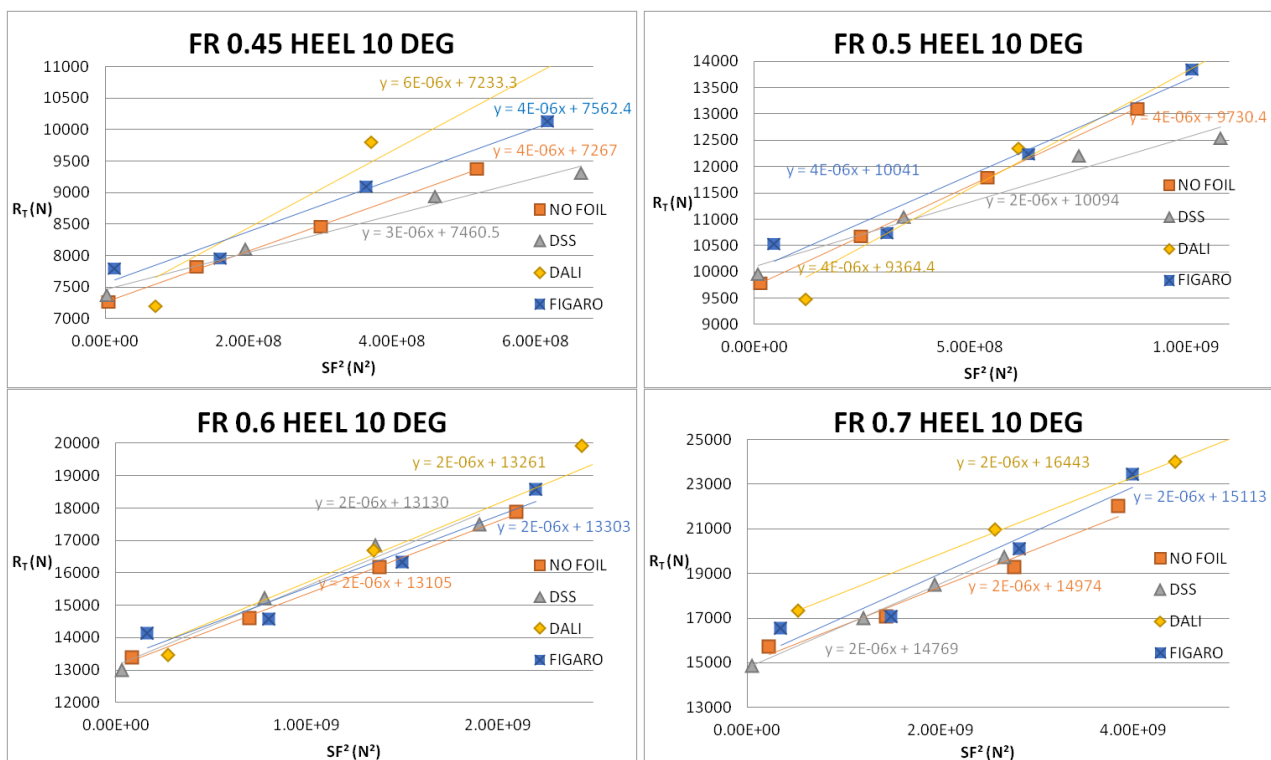


Figure 88: Drag against Side force squared graph for downwind condition (Heel angle 10 degree and Froude number 0.45, 0.50, 0.60 and 0.70). Zoomed for easier comprehension.

Here, it seems that the better configuration there is no significant advantage in having a foil when considering the Drag/Side force squared ratio. The results with foils are very similar or worst to the one without foils for low leeway angles. Comparing only the results with foils, the DSS seems to be the best solution at high speeds ($Fr = 0.7$), and at lower speeds ($Fr = 0.45$ and 0.50), for low leeway angles the Dali moustache actually has a better trend. The results are very close for Froude number 0.60 .

Figure 89 represents the effective draft value against Froude numbers comparison for downwind point of sail (10 degree of heel, Fr 0.45 to 0.7).

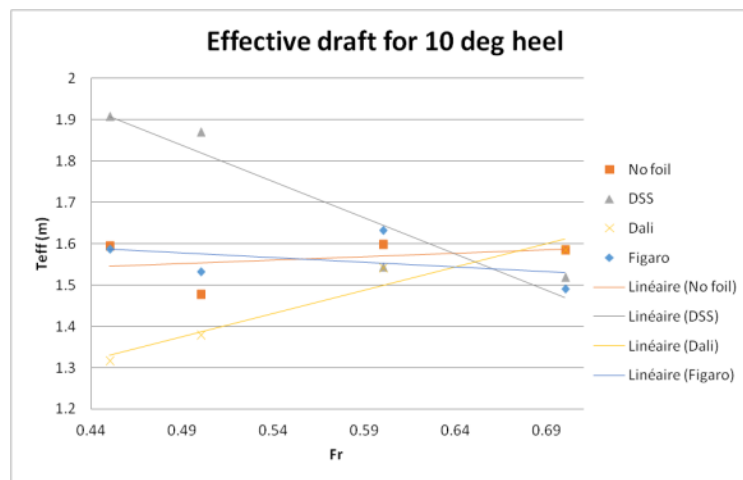


Figure 89: Effective draft against Froude number for downwind condition - Heel 10 degree

According to Figure 89, the best configuration in term of generating lift for downwind condition is with the DSS foil until Froude number 0.65 since it has the most effective draft T_E . Then for the highest speed at $Fr=0.7$, the Dali moustache has the best trend.

The more the speed, the less efficient in lift for the DSS and the more efficient in lift for the Dali. On the other hand, the results of effective draft with only the keel and the Figaro does not change much staying between 1.5 and 1.6 meters when the speed increases.

5.2.4.3. Minimum Drag Configuration

According to the conclusions done for upwind and downwind conditions in sections 5.2.4.1 and 5.2.4.2, tables have been created, summarising the "best configuration" to be selected for each condition, regarding the drag. The results are based on the drag against side force squared ratio at different leeway angles for a particular heel angle and speed, and on the effective draft against speed. Refer to APPENDIX A19: MINIMUM DRAG CONFIGURATION BASED ON THE EFFECTIVE DRAFT.

6. CONCLUSIONS

6.1. Conclusions on the Design

For the design part of the project, the general characteristics of the sailing yacht are quite similar to what was expected in the design brief (Table 1).

The first important remark to outline is that, for some of the design phases, such as sailing equilibrium, or stability, an assumption was made not to take into account the foils while performing the calculations. By not having enough information on the foils' design, it was too risky to rely on them regarding the stability and equilibrium. Indeed, if on the one hand the foil makes the yacht more stable and faster, on the other hand, the yacht should be able to sail without it, in the case a foil breaks while cruising offshore.

The most important conclusions are the following:

- It was found that for applications to cruising yacht, the Dali Moustache foils were not suitable for a yacht of 50 feet due to the lack of volume in the interior layout. It may however be suitable for a longer cruising yacht. Hence, it is still interesting to test the Dali moustache foils in order to compare the three foils efficiency on a hydrodynamic point of view.
- The best configuration between the three foils may be the DSS because the headroom is still enough in the saloon even if the DSS is installed there.
- The Figaro 3 foils can also be a good solution for the yacht, but they require the passengers to bend the head a little bit in the main cabin to access to the bed or the bathroom. This is actually due to the influence of the longitudinal position of the foil along the hull. The DSS is installed aft of the keel, but the Figaro 3 foil is installed in front of the mast, which in the case of the designed GA, is in the main cabin. Therefore, the interior volume is smaller compared to the saloon. Further studies can be carried out to change the longitudinal position of the foils.

In this study, a lot of design topics were not investigated, and could be considered for further works. Firstly, the structure of the foil, the mechanism for retraction of the foil in the hull, and the mounting system of the hydrofoils on the hull were out of topic and could be studied deeper. Furthermore, the shape of the foil was also based on existing design. It could be interesting to see how parameters such as foil profile, span, aspect ratio, and taper ratio affect the performance and the tip vortex energy losses by, for instance, modelling hydrofoils using CFD. Since the lift is proportional to the square of velocity, at lower speeds, the planform area and lift coefficient must be relatively large to ensure enough lift for the hull to rise.

6.2. Conclusions on the Hydrodynamic Analysis

6.2.1. Tank Testing General Observations

The approach by tank testing is a time consuming process since it requires first to build the model hull, keel and foils, and to run the tests in the towing tank. Indeed, CFD validation would take less time nonetheless the method of computation of the software have to be selected carefully. It is also worth comparing the results of towing tank with a CFD approach to complement the conclusions outlined by the towing tank test.

Also, the main problem of a towing tank test method is the numerous uncertainty parameters. However, it was noticed that the uncertainty decreases with velocity increase. For instance, during the Prohaska tests, it was necessary to increase the velocity (or Froude number) to obtain more reliable results.

The software prediction and test results were compared for upright resistance calculation. All predictions are close, but the comparison also highlighted the fact that the calculation method chosen by each software determines if the prediction is overestimating or underestimating the resistance.

One unexpected observation was made at high speeds during the Figaro foil tests. It was noticed that a large bow tube vortex is generated by the bow of the hull, creating a suction on the surface of the foil, and generating sprays around the foil. Hence, there is added resistance, but also less wetted surface area because of the suction. That is where the theory and the experiment diverge since the drag is a function of the wetted surface area, but here the wetted surface area is reduced, and the resistance increased. Therefore, it would be interesting to change the position of the foil to avoid the vortex generated by the hull and see if the tests results comply with the theory again.

Moreover, the full-scale maximum boat speed predicted from the VPP may not be suitable to test at this model size. Reasonable speed would be comprised between $Fr = 0.35$ and 0.5 .

6.2.2. Tank Testing Hydrodynamic Results

The Dali and Figaro V-shape foils have two distinct functions which are lift force vertically and side force horizontally, unlike the flat transverse shape foil DSS, which provides lift force vertically. That is what the predictions based on theory and based on the existing foiling

racing yachts experience was before the tests. After the experiment was performed, and all models compared, three main conclusions were brought to light.

First of all, the hydrodynamic results (drag, side force, heave and trim) were compared between all the foils and the main conclusion is that foils are useless at least from a pure hydrodynamic point of view (refer to APPENDIX A15: DRAG, SIDE FORCE, HEAVE AND TRIM GRAPHS).

Nevertheless, some conclusions can be done comparing the foils only. The DSS provides the more lift and the Dali provides the more side force but also the more drag. Figaro foil also provides more side force than the DSS foil, and does not add too much drag, hence it could be a good compromise in between the three foils from this point of view.

There is virtually no sailing condition where a foil can achieve a lower resistance than the hull with keel only. Therefore, if the benefits are not in the resistance itself, it has to come from stability or in the increased righting moment (RM). The analyse done in section 5.2.2. and APPENDIX A16: RESISTANCE COMPARISON BETWEEN LOW AND HIGH HEEL ANGLE FOR EACH FOIL AT DIFFERENT LEEWAY ANGLE actually proves that the interest of having foils is in the increased RM, enabling to reduce the heel and the resistance. Moreover, it has been shown by a parametric study in section 4.2.2.1 that racing yacht with foils have 10% more sail area than racing yacht without foils. Hence the foils contribute a lot in counteracting the side force generated by the sails.

Then, an important statement is that the results were driven by a chosen angle of attack, which was not the same for all the foils. According to theory, with increasing angle of attack, we can see a higher lift, which allows to reduce resistance by generating more lifts. While a racing boat would adjust the foils by about ± 7 degree, we cannot really have that on a cruising boat. Thus, it is actually important to set the foil at the right angle. Actually, it was decided that the Dali foil should be tested with a greater angle of attack (16 degree), based on a previous master thesis conclusion on a similar topic [14] to provide more side force, and when looking at the quick comparison between 0 and 16 degrees done in section 5.2.3, it was a good choice in term of side force generation, but not in term of resistance reduction. Furthermore, as the Figaro is also a V-shape foil, the angle of attack was chosen higher than 0 degree (8 degree), and again, when looking at the comparison graphs between 0 and 8 degrees in section 5.2.3, it was a good choice since the foils are more efficient in terms of side force generation, but also in reduction of the resistance. For the DSS, it was chosen to keep a 0 degree angle of attack. The comparison in section 5.2.3 actually proved that it was better not

to take an angle greater than 4 degrees. A full analysis into a greater range of the foils' angles of attack will be carried out by another student in Southampton Solent University [49] with the same yacht model and the same three foil models.

Finally, the foils could be ranked for upwind and downwind point of sail, and also quantified by how much one would be better than another based on two types of graphs: the drag against side force squared ratio at different leeway angles for a particular heel angle and speed, and the effective draft against the speed. By this analysis, a designer could see which of the foils would be best, based on the intended speed, leeway and heel. However it should be kept in mind that it does not take into account all the hydrodynamics results such as pure side force or heave and trim angle. The result of this analysis is summarised in APPENDIX A19: MINIMUM DRAG CONFIGURATION BASED ON THE EFFECTIVE DRAFT. APPENDIX A19: The analysis shows that the DSS is the most efficient configuration based on the effective draft graphs. This result is consistent when looking at what is done on the current cruising foiling yachts. Indeed, the main configuration chosen for cruising is the DSS system rather than a V-shape configuration.

6.2.3. Future Works



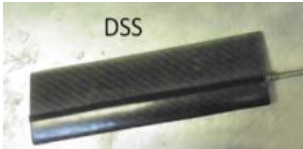
A lot of parallel studies by tank testing can be made based on this master thesis:

- First of all, the longitudinal or vertical position of the foil could be a determinant parameter, as well as a deeper analyse in the influence of the foil's angle of attack.
- The model was tested until 20 degree of heel angle since it was decided to test it for a cruising yacht, and cruising yacht rarely heel more than 20 degree. However, if the aim of the designer is to build a racing yacht, additional test with greater heel angle are required.
- Furthermore, another shape of foil could be tested on the model, for instance the foil from the brand new racing foiling yacht AC75 designed for America's cup.
- Finally, this study was focused on hydrodynamic results, however the stability and the seakeeping are also important advantage of having a foil, especially in the cruising yacht area, where comfort is an important criterion. For the stability, the model could be run free of heel in the towing tank, and the movement of the model could be measured with a pendulum. For the seakeeping, ITTC procedures exist in order to run the model in the towing tank [52].

6.3. Hydrofoils Advantages and Drawbacks

The Table 39 below presents and summarises the advantages and drawbacks of each hydrofoils, based on the two analysis carried out in this study on design and hydrodynamic.

Table 39: Advantages and drawbacks of the three foils based on the design and hydrodynamic analysis

	+	-
	ADVANTAGES	DRAWBACKS
DALI 	<ul style="list-style-type: none"> ❖ Great side force generation ❖ Reduction of the trim angle 	<ul style="list-style-type: none"> ❖ Huge increase in resistance ❖ Needs a great angle of attack to get sufficient side force ❖ Problem of integration in the design: lack of volume in the interior layout
FIGARO 3 	<ul style="list-style-type: none"> ❖ Good compromise in between the three foils in terms of small drag and sufficient side force generation ❖ Minor problems for the integration in the design 	<ul style="list-style-type: none"> ❖ Longitudinal position critical due to the bow vortex interaction ❖ Small increase of the trim angle
DSS 	<ul style="list-style-type: none"> ❖ Easy integration in the design ❖ Generates the more lift ❖ Minimum drag configuration for most of the point of sail 	<ul style="list-style-type: none"> ❖ Almost no contribution in side force ❖ Dependant to a small angle of attack because of the stall angle

7. REFERENCES

- [1] ‘Forlanini hydrofoils’, *USHA United State Hydrofoil Association*. [Online]. Available: <http://www.hydrofoil.org/history.html>. [Accessed: 13-Dec-2017].
- [2] ‘Infiniti 56C - redefining blue water cruising’, *Infiniti Performance Yachts*, 18-Jan-2017. [Online]. Available: <http://www.infinitiperformanceyachts.com/single-post/2017/01/18/Infiniti-56C-redefining-blue-water-cruising>.
- [3] G. S. Barkley, ‘Aero-Hydro Notes’, Southampton Solent University, 2016-2015.
- [4] J.-B. Soupez, ‘Intro to Yacht Equilibrium and Aerodynamics’, Southampton Solent University.
- [5] M. Sheahan, ‘Hydrodynamic resistance with foils’, *Yachting World*, 20-Jul-2015. [Online]. Available: <https://keyassets.timeincuk.net/inspirewp/live/wp-content/uploads/sites/21/2015/07/Foils-graph.jpg>. [Accessed: 13-Dec-2017].
- [6] M. Sheahan, ‘Surface piercing foils’, *Yachting World*, 20-Jul-2015. [Online]. Available: <https://keyassets.timeincuk.net/inspirewp/live/wp-content/uploads/sites/21/2015/07/Foils-1.jpg>. [Accessed: 13-Dec-2017].
- [7] M. Sheahan, ‘Fully submerged foils’, *Yachting World*, 20-Jul-2015. [Online]. Available: <https://keyassets.timeincuk.net/inspirewp/live/wp-content/uploads/sites/21/2015/07/Foils-1a.jpg>. [Accessed: 13-Dec-2017].
- [8] J. Taglang and F. Chevalier, ‘Foils Saga Dernière Partie’, Jul-2015. [Online]. Available: <http://chevaliertaglang.blogspot.com/2015/07/foils-saga-derniere-partie.html>. [Accessed: 13-Dec-2017].
- [9] ‘THE AMERICA’S CUP CLASS AC75 BOAT CONCEPT REVEALED’, *America’s Cup*, 20-Nov-2017. [Online]. Available: https://www.americascup.com/en/news/14_THE-AMERICA-S-CUP-CLASS-AC75-BOAT-CONCEPT-REVEALED.html.
- [10] R. Spilman, ‘Safran IMOCA 60 with the Dali Moustache — Foil User Manual’, *The old Salt Boat*, 19-May-2016. [Online]. Available: <http://www.oldsaltblog.com/2016/05/safran-omoca-60-dali-moustache-foil-user-manual/>. [Accessed: 13-Dec-2017].
- [11] D. Baltateanu, ‘Foiling Week awards 2017 winners and foilers at Giraglia 2018’, *The Foiling Week*, 04-Dec-2017. [Online]. Available: <http://www.sail-world.com/news/199956/Foiling-Week-awards-winners-and-foilers>. [Accessed: 13-Dec-2017].
- [12] ‘Infiniti 56’, *Infiniti Performance Yachts*. [Online]. Available: <http://www.infinitiperformanceyachts.com/infiniti-56>. [Accessed: 13-Dec-2017].
- [13] ‘Designing the IMOCA 60’, *SCUTTLEBUTT Sailing News*, Nov-2016. [Online]. Available: <http://www.sailingscuttlebutt.com/2016/11/08/history-of-the/>.
- [14] T. Aygor, ‘Analyses of Foil Configurations of IMOCA Open 60s with Towing Tank Test Results’, Master Thesis, 2017.
- [15] Press Mare World, ‘FIGARO BÉNÉTEAU 3’, *FOILING WEEK*, 03-Dec-2016. [Online]. Available: <http://www.foilingweek.com/blog/2016/12/figaro-beneteau-3/>. [Accessed: 13-Dec-2017].
- [16] ‘Why Beneteau’s new foil-assisted Figaro 3 is big news for sailing’, *R&R Marine Boat Repair*, 17-Dec-2016. [Online]. Available: <https://rnrmarineservices.wordpress.com/2016/12/17/why-beneteaus-new-foil-assisted-figaro-3-is-big-news-for-sailing/>. [Accessed: 13-Dec-2017].
- [17] F. Chevalier, ‘A history of the Figaro class yacht designs Single-handed racing in France 1966–2017’, 30-Jan-2017. [Online]. Available:

- http://chevaliertaglang.blogspot.co.uk/2017_01_29_archive.html. [Accessed: 13-Dec-2017].
- [18] 'DSS Technology', *Dynamic Stability Systems*. [Online]. Available: <http://www.dynamicstabilitysystems.com/dss-technology/>. [Accessed: 13-Dec-2017].
- [19] 'Infiniti 36 with DSS', *Infiniti Performance Yachts*. [Online]. Available: <http://www.infinitiperformancyachts.com/gallery?lightbox=dataItem-ikia8rxv>. [Accessed: 14-Jan-2018].
- [20] L. Larsson and R. E. Eliasson, *Principles Of Yacht Design*, Second Edition. London: Adlar Coles Nautical, 2000.
- [21] Loyds Register, 'Rules and Regulations for the Classification of Ships'. Jul-2016.
- [22] *AutoCAD*. 2017.
- [23] *Maxsurf Modeler*, Bentley. 2013.
- [24] *Rhinoceros*. Robert McNeel & Associates., 2010.
- [25] J.A. Keuning and U. B. Sonnenberg, 'Approximation of the Hydrodynamic Forces on a Sailing Yacht based on the "Delft Systematic Yacht Hull Series"'. .
- [26] *HullScant / Wolfson Unit MTIA*. .
- [27] *Maxsurf Resistance*, Bentley. 2013.
- [28] *Maxsurf Stability*, Bentley. 2013.
- [29] *WinDesign VPP / Wolfson Unit MTIA*. .
- [30] *Maxsurf VPP*, Bentley. 2013.
- [31] 'BS EN ISO 12215-2-2002'. British Standard, 2002.
- [32] 'BS EN ISO 12215-5-2008+A1-2014'. British Standard, 2008.
- [33] 'BS EN ISO 12215-9-2012'. British Standard, 2012.
- [34] 'BS EN ISO 12217-2-2015'. British Standard, 2015.
- [35] 'ITTC Recommended Procedures and Guidelines_75-01-01-01 - Ship models'. 26th ITTC Resistance Committee, 2011.
- [36] 'ITTC Recommended Procedures and Guidelines_75-02-02-01 - Resistance test'. 26th ITTC Resistance Committee, 2011.
- [37] 'ITTC Recommended Procedures and Guidelines_75-02-02-02 - General Guideline for Uncertainty Analysis in Resistance Tests'. 26th ITTC Resistance Committee, 2014.
- [38] 'ITTC Recommended Procedures and Guidelines_75-02-03-014 - 1978 ITTC Performance Prediction'. 26th ITTC Resistance Committee, 2014.
- [39] I. H. Abbott, A. E. Von Doenhoff, and L. Stivers Jr, 'Summary of airfoil data', 1945.
- [40] I. H. Abbott and A. E. Von Doenhoff, *Theory of wing sections, including a summary of airfoil data*. Courier Corporation, 1959.
- [41] 'The NACA airfoil series'. [Online]. Available: <http://people.clarkson.edu/~pmarzocc/AE429/The%20NACA%20airfoil%20series.pdf>. [Accessed: 26-Dec-2017].
- [42] 'NACA 63-412 AIRFOIL (n63412-il)', *Airfoil Tools*, 2018. [Online]. Available: <http://airfoiltools.com/airfoil/details?airfoil=n63412-il>. [Accessed: 13-Dec-2017].
- [43] 'Vector Freebie - Man Silhouette', *Vecteezy*. [Online]. Available: <https://www.vecteezy.com/people/7321-vector-freebie-man-silhouette>. [Accessed: 13-Dec-2017].
- [44] D. Gerr, *The Nature of Boats*. McGraw Hill Professional, 1995.
- [45] 'ENGINE SELECTION, PROPELLER SIZING FOR A BOAT REPOWER', *Psycho Snail*, 2011. [Online]. Available: http://www.psychosnail.com/sailingarticles_boatrepower.aspx.
- [46] 'Selden mast sections', *Selden Mast*. [Online]. Available: <http://www.seldenmast.com/files/1456483754/excerpts/595-808v7-E-10-11.pdf#toolbar=0&navpanes=0>. [Accessed: 27-Dec-2017].

- [47] ‘Selden Boom sections’, *Selden Mast*. [Online]. Available: <http://www.seldenmast.com/files/1456488856/excerpts/595-808v7-E-54-55.pdf#toolbar=0&navpanes=0>. [Accessed: 27-Dec-2017].
- [48] J. Seo *et al.*, ‘Model tests on resistance and seakeeping performance of wave-piercing high-speed vessel with spray rails’, *Int. J. Nav. Archit. Ocean Eng.*, vol. 8, no. 5, pp. 442–455, Sep. 2016.
- [49] C. Kitting, ‘A luxury 24 meter foil assisted round the world cruiser racer’, Final year project, Southampton Solent University, Southampton, UK, 2018.
- [50] P. Beck, ‘Sailing Yacht - Model testing’, Nantes, May-2017.
- [51] F. S. Hoerner, *Fluid Dynamic Drag, theoretical, experimental and statistical information*. 1965.
- [52] ‘ITTC Recommended Procedures and Guidelines_75-02-07-021 - Seakeeping experiments’. 26th ITTC Resistance Committee, 2014.

8. APPENDICES

<u>APPENDIX A1: GANTT DIAGRAM</u>	115
<u>APPENDIX A2: KEY DESIGN RATIO FROM PARAMETRIC STUDY</u>	116
<u>APPENDIX A3: HULL LINES GEOMETRY - BARE HULL</u>	118
<u>APPENDIX A4: SAIL SIDE FORCE AND KEEL SIDE FORCE CALCULATION</u>	119
<u>APPENDIX A5: GENERAL ARRANGEMENT AND DECK PLAN DRAWINGS</u>	122
<u>APPENDIX A6: MAXSURF HULL RESISTANCE RESULTS</u>	124
<u>APPENDIX A7: ENGINE VOLVO PENTA CHARACTERISTICS</u>	125
<u>APPENDIX A8: HULL AND DECK SCANTLING RESULTS WITH HULLSCANT</u>	127
<u>APPENDIX A9: HULL AND DECK STRUCTURAL ARRANGEMENT</u>	131
<u>APPENDIX A10: MAST AND RIG CALCULATION SPREADSHEET (NBS)</u>	133
<u>APPENDIX A11: TANK LOADING</u>	134
<u>APPENDIX A12: WEIGHT ESTIMATION IN LIGHTSHIP CONDITION</u>	135
<u>APPENDIX A13: VPP TABLES FOR BEST SPEED, HEEL ANGLE, LEEWAY ANGLE AND SAILSET</u>	137
<u>APPENDIX A14: PROHASKA PLOT BARE HULL</u>	140
<u>APPENDIX A15: DRAG, SIDE FORCE, HEAVE AND TRIM GRAPHS</u>	141
<u>APPENDIX A16: RESISTANCE COMPARISON BETWEEN LOW AND HIGH HEEL ANGLE FOR EACH FOIL AT DIFFERENT LEEWAY ANGLE</u>	145
<u>APPENDIX A17: EFFECTIVE DRAFT GRAPHS (DRAG VS SIDE FORCE SQUARED)</u>	
146	
<u>APPENDIX A18: EFFECTIVE DRAFT GRAPHS (T_{EFF} VS FROUDE NUMBER)</u>	149
<u>APPENDIX A19: MINIMUM DRAG CONFIGURATION BASED ON THE EFFECTIVE DRAFT METHOD</u>	150

APPENDIX A1: GANTT DIAGRAM

				Month	July 2017				August 2017				September 2017				October 2017				November 2017				December 2017				January 2018				
				Week	28	29	30	31	32	33	34	35	36	37	38	39	40	41	42	43	44	45	46	47	48	49	50	51	52	1	2	3	4
ACTIVITY	Start	End	Time	Initial date	10-Jul	17-Jul	24-Jul	31-Jul	7-Aug	14-Aug	21-Aug	28-Aug	4-Sep	11-Sep	18-Sep	25-Sep	2-Oct	9-Oct	16-Oct	23-Oct	30-Oct	6-Nov	13-Nov	20-Nov	27-Nov	4-Dec	11-Dec	18-Dec	25-Dec	1-Jan	8-Jan	15-Jan	22-Jan
Internship at Solent University	13-Jul	6-Nov	117																														
Meeting with Solent supervisor	13-Jul	13-Jul	1																														
Parametric study	17-Jul	24-Jul	8																														
Design phase:	17-Jul	4-Sep	50																														
Cruising yacht design	17-Jul	7-Aug	22																														
Hydrofoils design	31-Jul	4-Sep	36																														
Contact with ZUT supervisor	31-Jul	31-Jul	1																														
Manufacturing phase:	21-Aug	25-Sep	36																														
Hull model	21-Aug	15-Sep	26																														
Hydrofoils and keel model	25-Sep	5-Oct	11																														
Experimental phase:	2-Oct	2-Dec	62																														
Towing tank test - ITTC	11-Sep	23-Oct	36																														
Test matrix	11-Sep	29-Sep	19																														
ZUT university	13-Nov	31-Jan	80																														
Meeting with ZUT supervisor	15-Dec	15-Dec	1																														
Meeting with ZUT supervisor	21-Dec	21-Dec	1																														
Writing of the Master thesis	9-Oct	13-Jan	97																														
Master thesis delivery	14-Jan	14-Jan	1																														
Master thesis presentation	31-Jan	31-Jan	1																														

APPENDIX A2: KEY DESIGN RATIO FROM PARAMETRIC STUDY

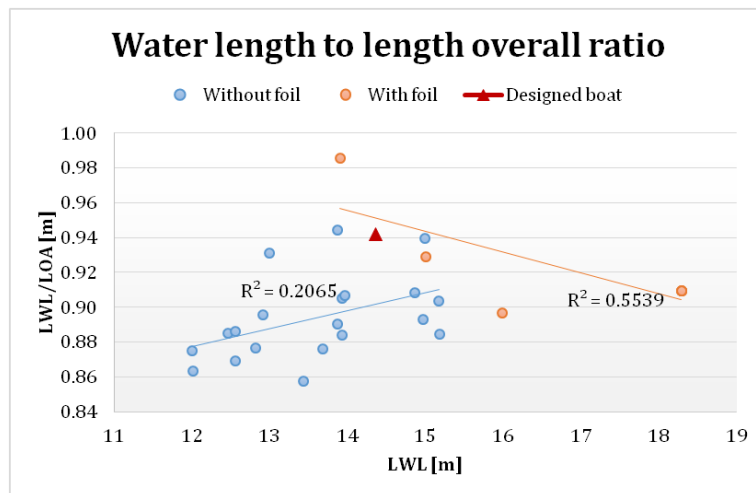


Figure 90: Water length to length overall ratio from parametric study

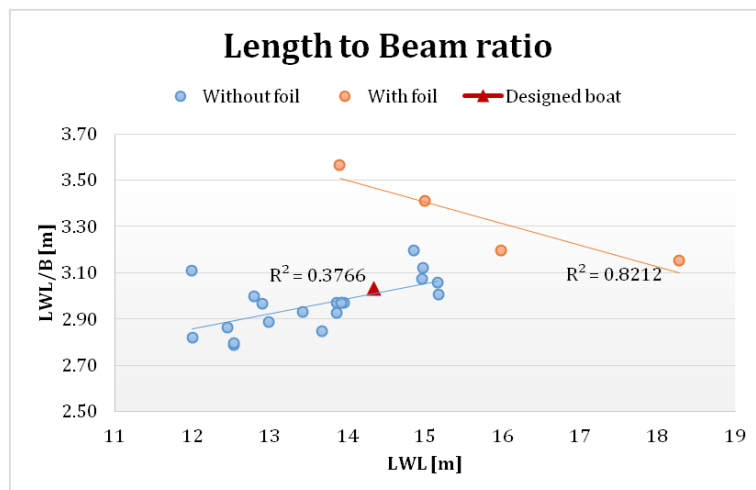


Figure 91: Length to beam ratio from parametric study

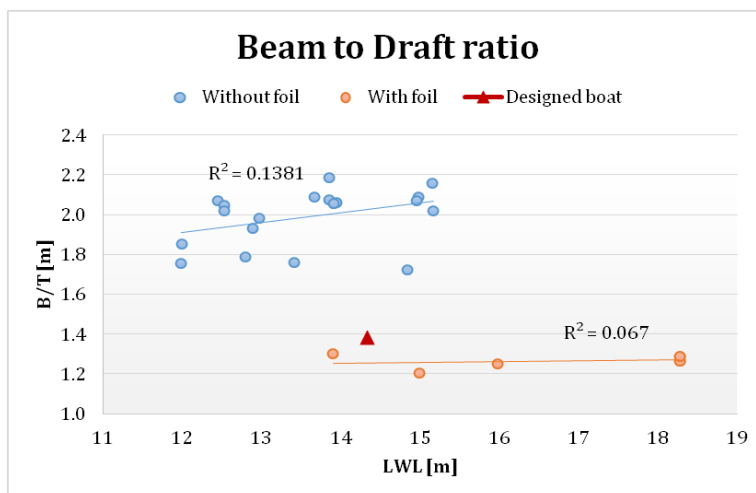


Figure 92: Beam to draft ratio from parametric study

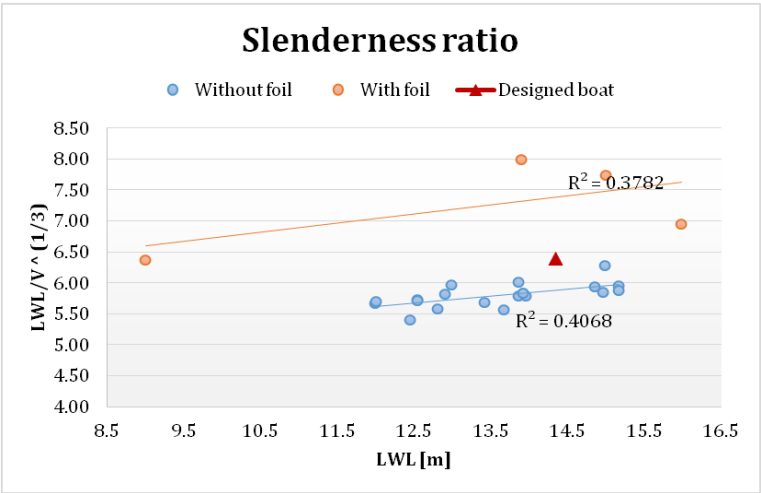


Figure 93: Slenderness ratio from parametric study

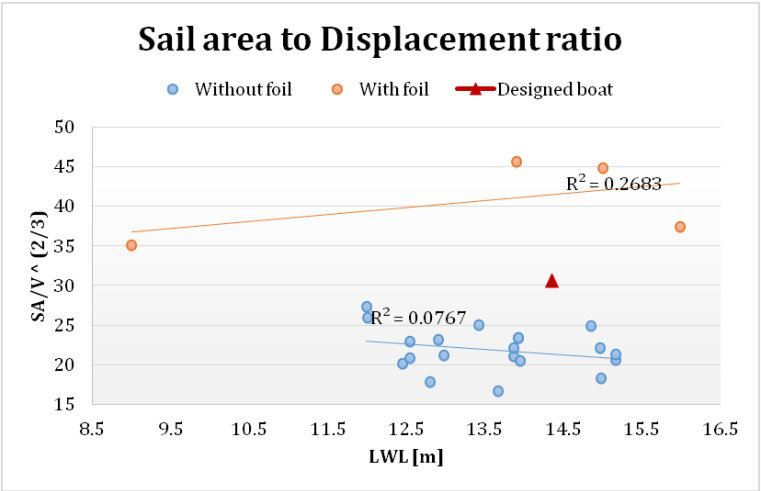


Figure 94: Sail area to displacement ratio from parametric study

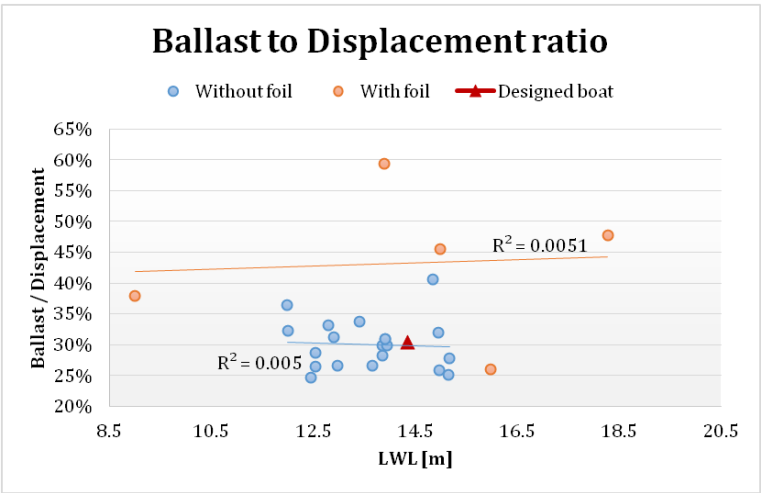
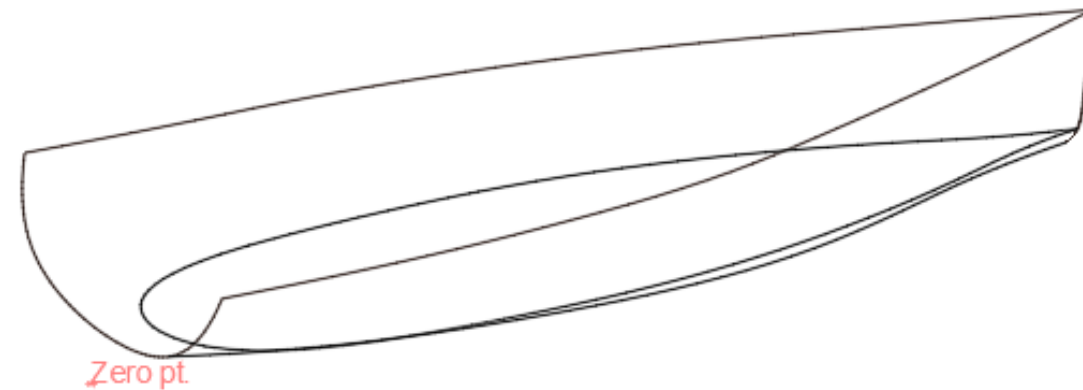
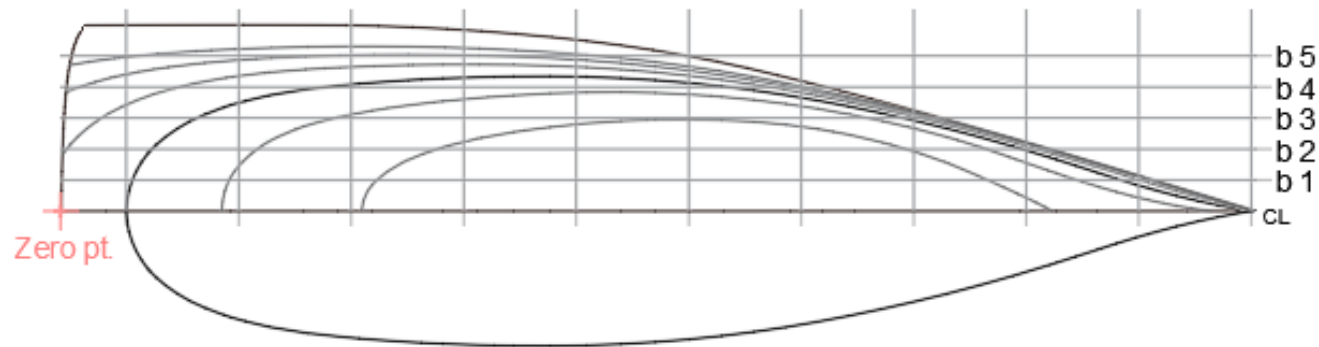
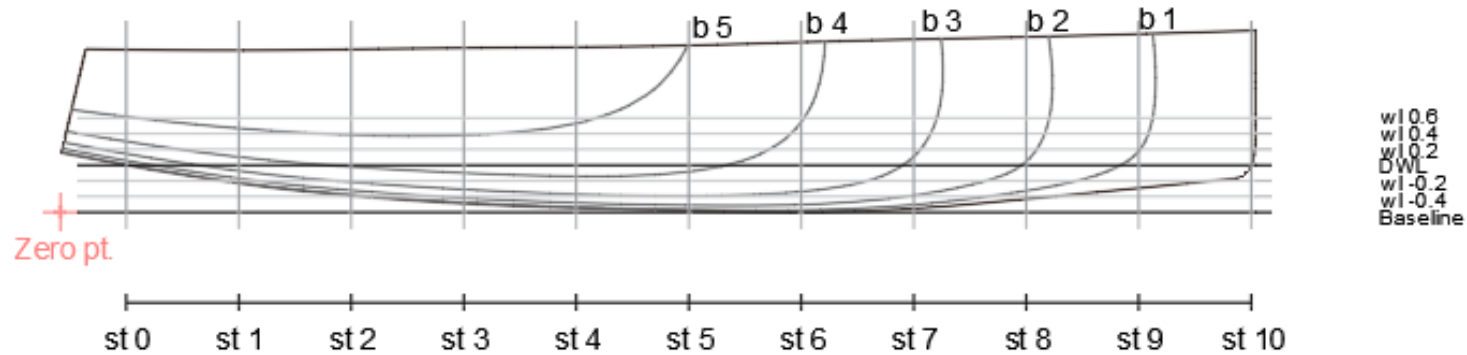
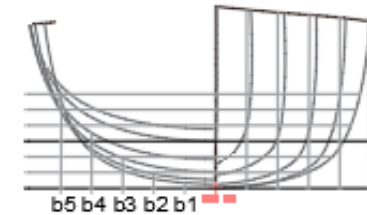


Figure 95: Ballast to displacement ratio from parametric study

APPENDIX A3: HULL LINES GEOMETRY - BARE HULL



wl 0.6
wl 0.4
wl 0.2
DWL
wl -0.2
wl -0.4
Baseline



Hull hydrostatics		
LOA	15.2200	m
LWL	14.3500	m
BOA	4.7200	m
BWL	3.4300	m
TC	0.8000	m
TK	3.8000	m
Displ	11.5000	T
Volume	11.2200	m ³
Cp	0.5400	-
Cb	0.3800	-
WSA	38.8600	m ²
Total Area	92.7700	m ²
LCB	7.4550	from zero pt (+ fwd) m
LCF	8.8890	from zero pt (+ fwd) m

EMSHIP Master thesis	Drawn by: Juliette Dewavrin	
Format: A4	meters	Drawing Title:
Date: 14/01/18	1:100	Hull Linesplan

APPENDIX A4: SAIL SIDE FORCE AND KEEL SIDE FORCE CALCULATION

The method to calculate the SSF and KSF is the following:

- ✓ Establish a realistic sailing condition
- ✓ Calculate the AWA and AWS for that condition
- ✓ Establish lift and drag coefficients
- ✓ Calculate the lift and drag from the sails
- ✓ Solve the sail side force (SSF)
- ✓ For equilibrium, the keel side force (KSF) is equal to 90% of the sail side force (SSF):

A yacht is said to be sailing in force equilibrium when there is no net acceleration on the yacht. Hence, a typical sailing speed is going to be calculated to estimate the sailing forces.

For all the previous equations, AWA and AWS are needed. Without heel angle, knowing the TWS, the TWA and the velocity of the yacht V_B , the AWA and AWS can be calculated (see Figure 96 and Table 40).

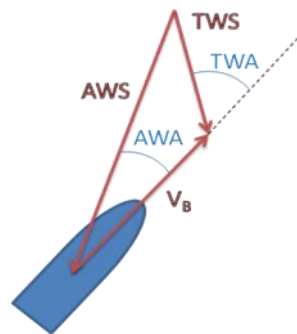
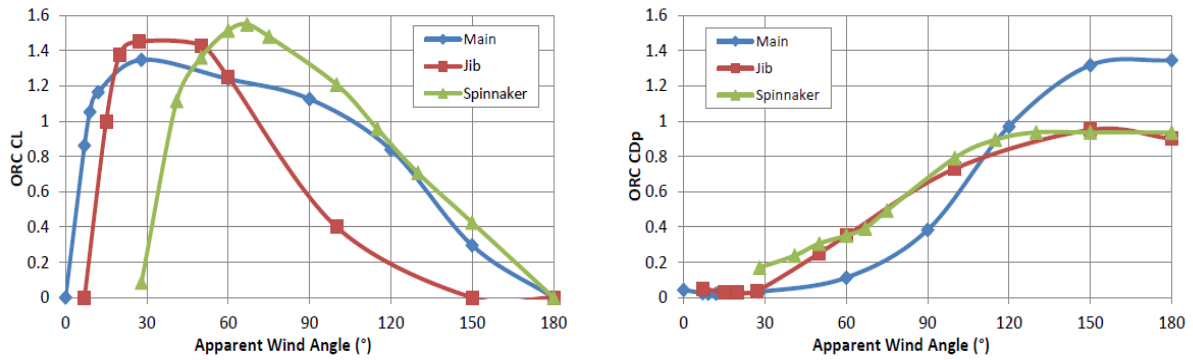


Figure 96: True and Apparent wind representation.

Table 40: Sailing conditions

Parameter	Abbreviation	Value	Unit
True wind speed	TWS	20	knots
True wind angle	TWA	45	degree
Apparent wind angle	AWA	30	degree
Apparent wind speed	AWS	31.5	knots
Boat speed in knots	V_B	16	knots
Boat speed in m/s	V_B	8.23	m/s

Lift and drag coefficient for main sail and jib are taken from the ORC VPP graph below (Figure 97) at 30 degree of apparent wind angle in typical upwind condition:



From: Offshore Racing Congress (2013). *ORC VPP Documentation*.

Figure 97: Lift and drag coefficients versus AWA for sails. Available from [4]

Hull and sail forces are considered to work in the horizontal plane (see Figure 98), irrespective of heel, since this is how they are measured in the towing tank. Sail forces would normally need to be resolved for heel angle, however the heel angle will not be taken into account since the upright resistance is calculated.

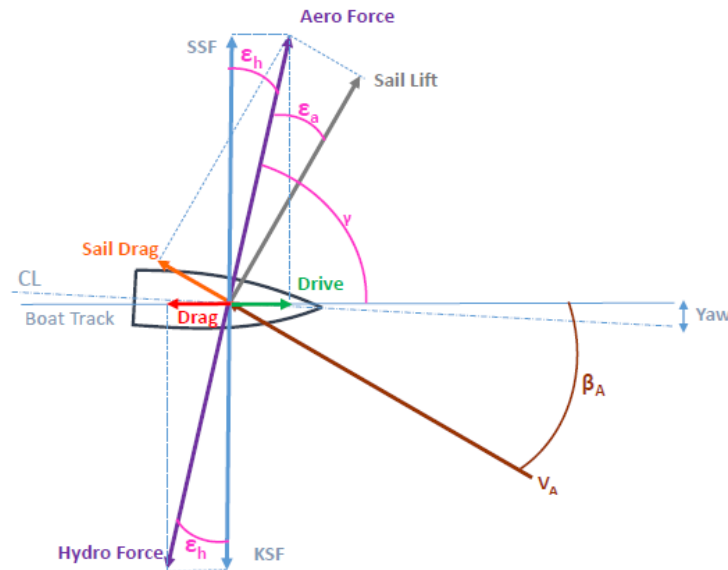


Figure 98: Sailing equilibrium on the horizontal plane. Available from [4]

The Sail Side force is equal to Eq. 59:

$$SSF = L_{sail} \cos(AWA) + D_{sail} \sin(AWA) \quad \text{Eq. 59}$$

with:

- AWA the apparent wind angle in degree,
- L_{sail} , and D_{sail} respectively the lift and drag of the sails in Newton, calculated with Eq. 60 and Eq. 61:

$$L_{sail} = C_{L\,sail} \cdot (1/2 \, \rho_{air} \cdot A \cdot AWS^2) \quad \text{Eq. 60}$$

$$D_{sail} = C_{D\,sail} \cdot (1/2 \, \rho_{air} \cdot A \cdot AWS^2) \quad \text{Eq. 61}$$

with

- AWS the apparent wind speed in m/s,
- A the total area of the sail in m²,
- ρ_{air} , the air density in kg/m³
- $C_{L \text{ sail}}$ and $C_{D \text{ sail}}$, the lift and drag coefficient of the sails, calculated with Eq. 62 and Eq. 63:

$$C_{L \text{ sail}} = (C_{L \text{ main}} \cdot A_{N \text{ main}} + C_{L \text{ jib}} \cdot A_{N \text{ jib}}) / (A_{N \text{ main}} + A_{N \text{ fore}}) \quad \text{Eq. 62}$$

$$C_{D \text{ sail}} = (C_{D \text{ main}} \cdot A_{N \text{ main}} + C_{D \text{ jib}} \cdot A_{N \text{ jib}}) / (A_{N \text{ main}} + A_{N \text{ fore}}) \quad \text{Eq. 63}$$

with

- Lift and drag coefficient for main sail and jib taken from the ORC VPP graph above,
- and nominal area $A_{N \text{ main}}$, $A_{N \text{ jib}}$ and $A_{N \text{ fore}}$ calculated with Eq. 64, Eq. 65 and Eq. 66:

$$A_{N \text{ main}} = 1/2 \cdot P \cdot E \quad \text{Eq. 64}$$

$$A_{N \text{ jib}} = 1/2 \cdot \sqrt{(I^2 + J^2)} \cdot LP \quad \text{Eq. 65}$$

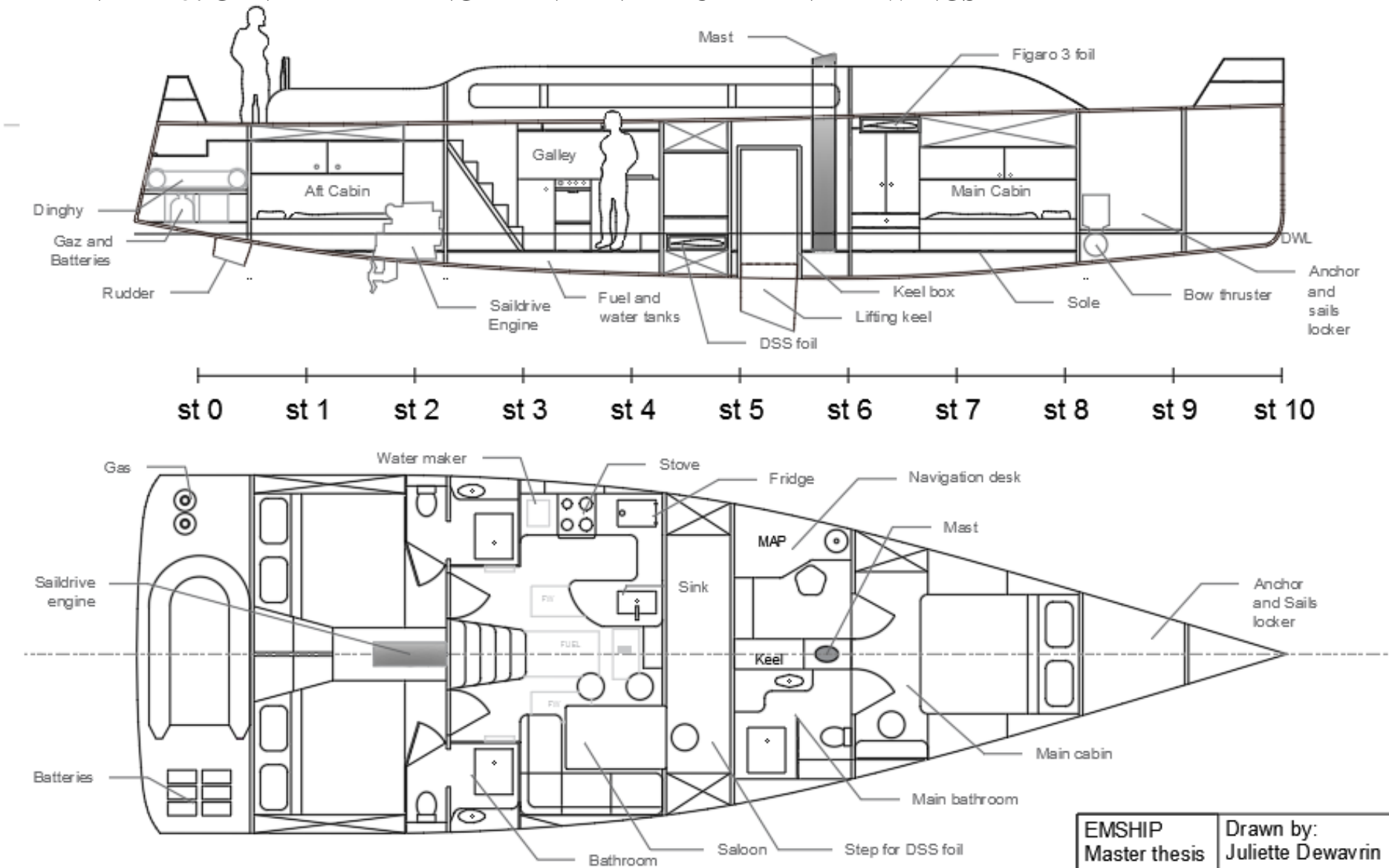
$$A_{N \text{ fore}} = 1/2 \cdot I \cdot J \quad \text{Eq. 66}$$

The Table 41 shows the results of the calculation for the SSF and KSF (the KSF is taken as 90% of the SSF).

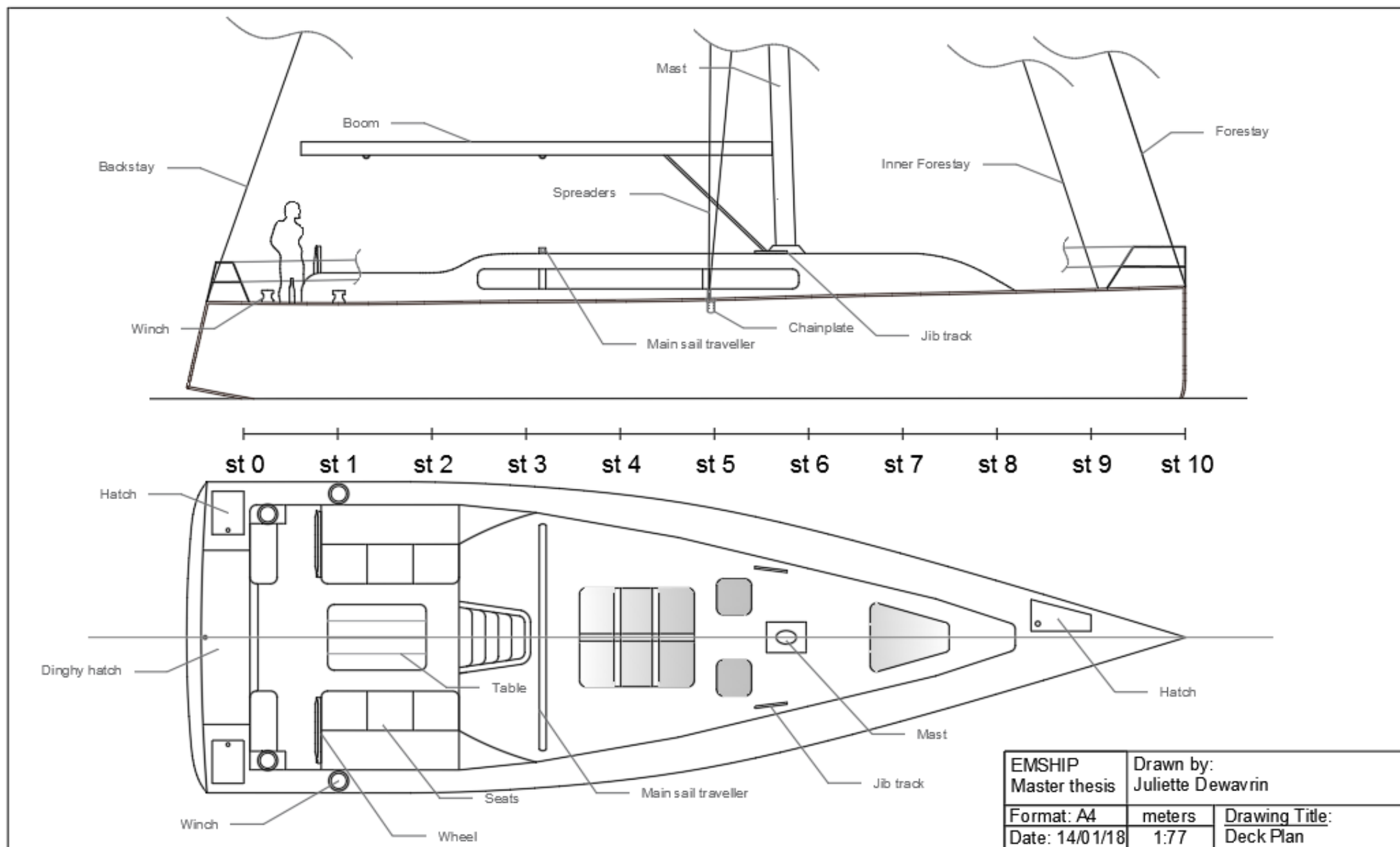
Table 41: Keel and rudder forces calculation

Parameter	Abbreviation	Value	Unit
Main foot	E	7.19	m
Main luff	P	19.88	m
Jib foot	J	5.94	m
Jib leech	I	20.25	m
Jib luff perpendicular	LP	6.18	m
Main sail area theory	$A_{N \text{ main}}$	71.47	m ²
Jib sail area theory	$A_{N \text{ jib}}$	65.21	m ²
Foretriangle area theory	$A_{N \text{ fore}}$	60.14	m ²
Main Lift coefficient-from ORC Coefficients at 30 degree	$C_{L \text{ main}}$	1.35	-
Jib Lift coefficient-from ORC Coefficients at 30 degree	$C_{L \text{ jib}}$	1.45	-
Main Drag coefficient-from ORC Coefficients at 30 degree	$C_{D \text{ main}}$	0.05	-
Jib Drag coefficient-from ORC Coefficients at 30 degree	$C_{D \text{ jib}}$	0.1	-
Sail Lift coefficient	$C_{L \text{ sail}}$	1.43	-
Sail Drag coefficient	$C_{D \text{ sail}}$	0.07	-
Sail Lift	L_{sail}	2578.15	N
Sail Drag	D_{sail}	131.99	N
Sail Side Force	SSF	2112.02	N
Keel Side Force (keel and rudders)	KSF	1900.82	N

APPENDIX A5: GENERAL ARRANGEMENT AND DECK PLAN DRAWINGS



EMSHIP Master thesis	Drawn by: Juliette Dewavrin	
Format: A4	meters	Drawing Title:
Date: 14/01/18	1:77	General Arrangement



APPENDIX A6: MAXSURF HULL RESISTANCE RESULTS

t	Froude Lwl	Froude Vol	Delft I,II Sail Resist	Delft I,II Sail Power	Delft III Sail Resist	Delft III Sail Power	Slender body Resist	Slender body Power
<i>kts</i>	-	-	<i>kN</i>	<i>kW</i>	<i>kN</i>	<i>kW</i>	<i>kN</i>	<i>kW</i>
3	0.13	0.325	0.1	0.365	0.1	0.28	0.2	0.551
3.275	0.142	0.355	0.2	0.6	0.2	0.444	0.3	0.754
3.55	0.154	0.384	0.3	0.809	0.2	0.615	0.3	0.974
3.825	0.165	0.414	0.3	0.886	0.2	0.759	0.4	1.314
4.1	0.177	0.444	0.3	0.978	0.3	0.921	0.5	1.667
4.375	0.189	0.474	0.3	1.111	0.3	1.09	0.6	2.182
4.65	0.201	0.504	0.3	1.261	0.3	1.281	0.7	2.644
4.925	0.213	0.533	0.3	1.448	0.4	1.508	0.8	3.529
5.2	0.225	0.563	0.4	1.655	0.4	1.76	1	4.389
5.475	0.237	0.593	0.4	1.894	0.4	2.094	1	4.839
5.75	0.249	0.623	0.4	2.158	0.5	2.461	1.2	6.096
6.025	0.261	0.653	0.5	2.513	0.5	2.84	1.7	8.539
6.3	0.273	0.682	0.5	2.908	0.6	3.25	2	11.027
6.575	0.284	0.712	0.6	3.357	0.7	3.841	2.2	12.511
6.85	0.296	0.742	0.7	3.848	0.8	4.518	2.2	13.01
7.125	0.308	0.772	0.8	4.943	0.9	5.599	2.2	13.356
7.4	0.32	0.801	1	6.38	1.1	6.92	2.3	14.52
7.675	0.332	0.831	1.3	8.295	1.4	9.03	2.6	17.155
7.95	0.344	0.861	1.6	10.607	1.7	11.775	3.2	21.485
8.225	0.356	0.891	2	13.866	2.1	15.075	3.9	27.4
8.5	0.368	0.921	2.5	18.175	2.6	18.978	4.7	34.587
8.775	0.38	0.95	3.2	23.7	3.2	24.028	5.7	42.667
9.05	0.392	0.98	4	31.074	4	30.831	6.6	51.285
9.325	0.403	1.01	4.8	38.241	4.6	37.164	7.5	60.15
9.6	0.415	1.04	5.4	44.225	5.1	41.697	8.4	69.041
9.875	0.427	1.07	6	50.619	5.5	46.592	9.2	77.805
10.15	0.439	1.099	6.6	57.831	6	52.362	9.9	86.358
10.425	0.451	1.129	6.5	58.38	6.5	58.54	10.6	94.664
10.7	0.463	1.159	7.2	66.075	7.3	66.557	11.2	102.7
10.975	0.475	1.189	7.9	74.101	8	74.923	11.7	110.496
11.25	0.487	1.218	8.4	81.026	8.6	82.837	12.2	118.062
11.525	0.499	1.248	8.9	88.197	9.2	91.052	12.7	125.454
11.8	0.511	1.278	9.5	95.613	9.8	98.767	13.1	132.694
12.075	0.522	1.308	10	103.291	10.3	106.65	13.5	139.826
12.35	0.534	1.338	10.4	110.432	10.8	114.42	13.9	146.884
12.625	0.546	1.367	10.9	117.58	11.3	122.339	14.2	153.912
12.9	0.558	1.397	11.3	124.898	11.7	129.807	14.5	160.919
13.175	0.57	1.427	11.7	132.413	12.1	137.167	14.9	167.953
13.45	0.582	1.457	12.1	140.037	12.6	144.73	15.2	175.032
13.725	0.594	1.486	12.6	147.796	13	152.501	15.5	182.165
14	0.606	1.516	--	--	13.3	159.88	15.8	189.382

APPENDIX A7: ENGINE VOLVO PENTA CHARACTERISTICS

Item	Characteristics	Unit
Model	D2-60/150S	
Brand	Volvo Penta	
Rated rpm	2700-3000	<i>RPM</i>
Efficiency	80	%
Safety factor	15	%
Crankshaft Power, kW	44	<i>KW</i>
Crankshaft Power, hp	60	<i>HP</i>
Number of Cylinders	4	
Displacement	2.2	<i>L</i>
Weight with gearbox	264	kg
Gearbox ratio	2.19:1	
Consumption at 9.2 knots (40 kW)	11.5	L/h
Consumption max	15.5	L/h
Aspiration	Naturally aspirated	
High-pressure fuel injection	Inline injection pump	
Emission compliance	BSO II, EU RCD Stage II, EPA Tier 3	
Use class	R5 (for cruising yachts)	

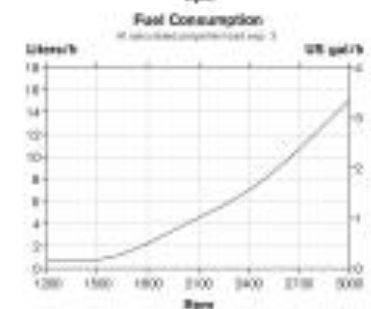
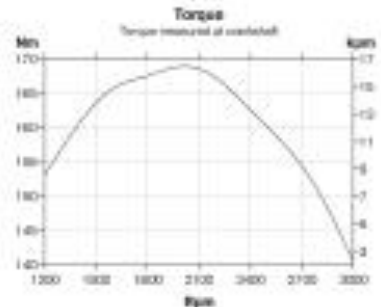
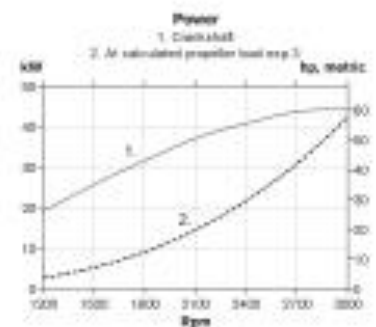
VOLVO PENTA INBOARD DIESEL

D2-60**NEW!****Technical Data**

Engine designation	D2-60
Crankshaft power, kW (hp)	44 (60)
Propeller shaft power, kW (hp)	42 (58)
Engine speed, rpm	2700-3000
Displacement, l (in ³)	2.2 (134.2)
Number of cylinders	4
Bore/stroke, mm (in.)	84/100 (3.31/3.94)
Compression ratio	23.3:1
Dry weight with reverse gear HS25A/MS26, kg (lb)	264/268 (582/590)
Dry weight with solidrive 150S, kg (lb)	264 (582)
Emission compliance	BSD, EU RCD Stage II, US EPA Tier 3
Rating	R5*

Technical data according to ISO 8665. With fuel having an LHV of 42700 kJ/kg and density of 840 g/liter at 15 °C (60 °F). Merchant fuel may differ from this specification which will influence engine power output and fuel consumption.

*RATING 5: For pleasure craft applications, and can be used for high speed planing crafts in commercial applications

**VOLVO
PENTA**

APPENDIX A8: HULL AND DECK SCANTLING RESULTS WITH HULLSCANT

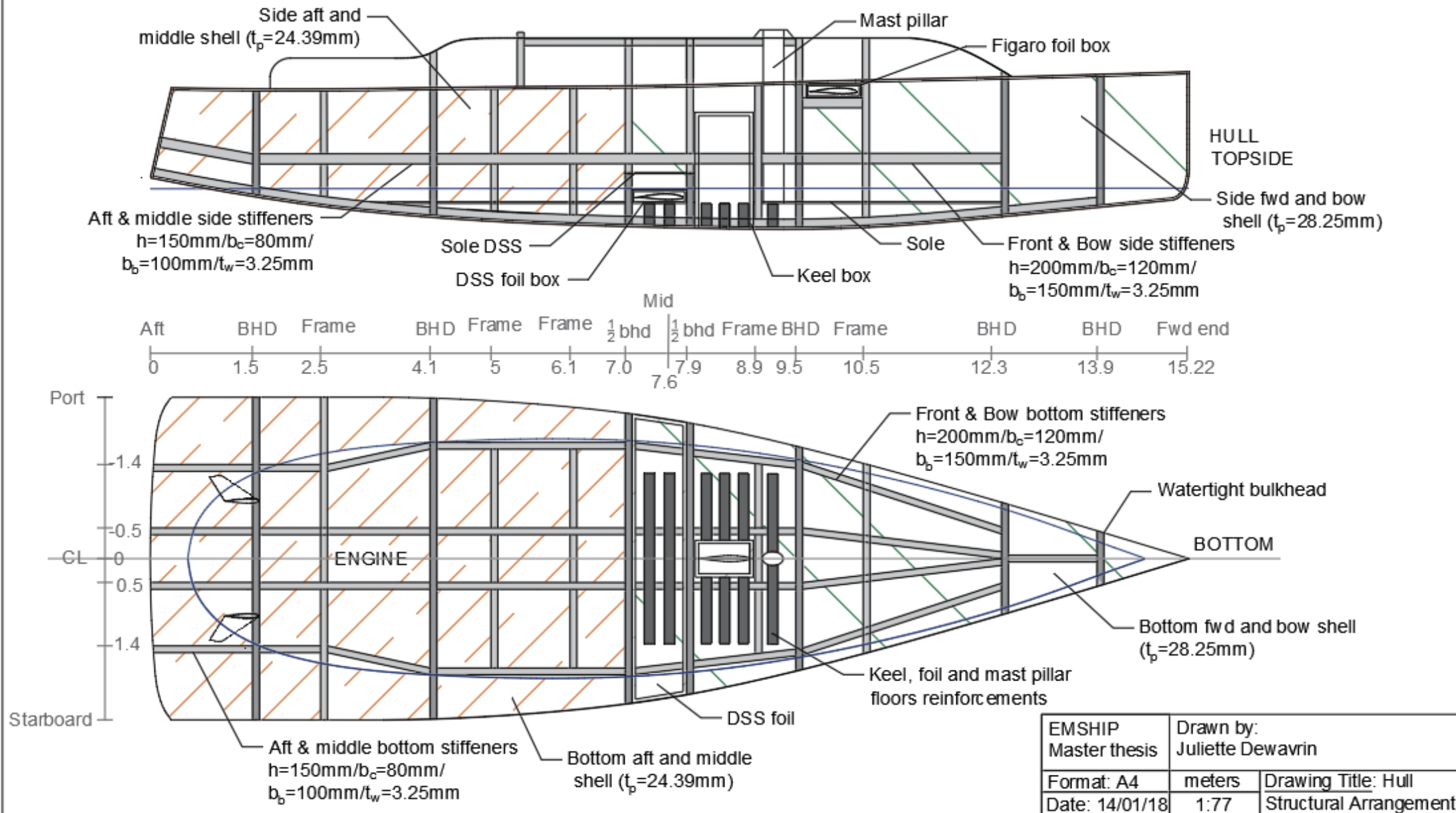
Boat Particulars	
Craft Type	Sailing
Design Category	A, Ocean
Composite Evaluation Level	EL-c, default data with 0.8 factor, ISO fibre content by mass
Displacement, m_{LDC}	8690.0 kg
Length of Hull, L_H	15.240 metres
Waterline Length, L_{WL}	12.360 metres
Waterline Beam, B_{WL}	3.250 metres
Canoe Body Depth, T_C	0.500 metres
General Calculations	
Design Category Factor, k_{DC}	1
Base Bottom Pressure, $P_{BS\ BASE}$	79.430 kN/m ²
Base Deck Pressure, $P_{DS\ BASE}$	21.973 kN/m ²

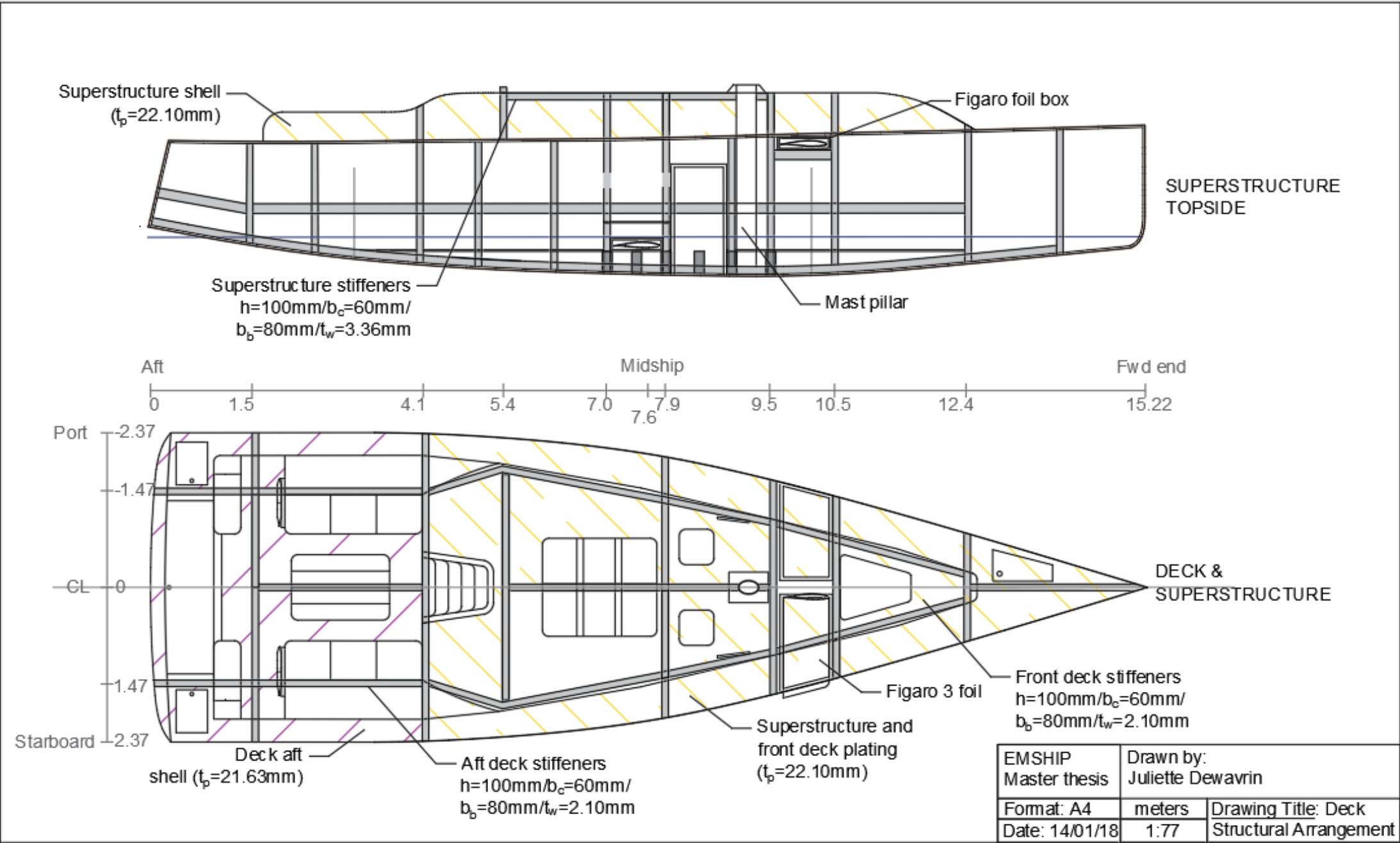
Panel Geometry and Calculations													
Label	Dimensions and Location							Calculations to ISO Standard					
	Length mm	Width mm	Aspect Ratio	Longitudinal Position metres	Location	z metres	Curvature mm	k _L	k _{AR}	k ₂	k ₃	k _z	Design Pressure kN/m ²
Bottom aft shell	1500	1250	1.2	3.34	Bottom	--	60	0.726	0.4	0.384	0.019	--	24.3
Side aft shell	1500	980	1.531	3.34	Side	1.58	80	0.726	0.419	0.5	0.028	0.905	22.5
Bottom center shell	1160	1150	1.009	6.37	Bottom	--	60	0.93	0.458	0.312	0.014	--	33.8
Side center shell	1165	626	1.861	5.8	Side	1.59	80	0.891	0.562	0.491	0.027	0.906	37.1
Bottom front shell	2630	650	4.046	9.9	Bottom	--	400	1	0.5	0.5	0.028	--	39.7
Side front shell	2910	980	2.969	11.06	Side	1.7	100	1	0.5	0.5	0.028	0.912	37.2
Bow side shell	1300	980	1.327	13.1	Side	1.75	100	1	0.5	0.493	0.028	0.886	36.4
Deck aft	2500	1200	2.083	2.15	Deck	--	0	0.646	0.32	0.5	0.028	--	5
Deck front	1300	980	1.327	11	Deck	--	0	1	0.437	0.492	0.027	--	9.6
superstructure	2700	1600	1.688	6	Superstructure. Top, <= 800mm above deck, walking area	--	50	--	0.256	0.5	0.028	--	5

Panel Results																					
Label	Requirements						Offered							Results							
	M_{db}	M_{dl}	EI_b	w_{os}	w_{is}	Shear Force	Label	M_{db}	M_{dl}	EI_b	w_{os}	w_{is}	Shear Force	b Min Ply No. and Stress Ratio	l Min Ply No. and Stress Ratio	EI_b Ratio	w_{os} Ratio	w_{is} Ratio	Shear Force Ratio	Plating Compl y?	Core Compl y?
	N.mm/mm	N.mm/mm	N.m ² /mm	kg/m ²	kg/m ²	N/mm		N.mm/mm	N.mm/mm	N.m ² /mm	kg/m ²	kg/m ²	N/mm								
Bottom aft shell	2148.3	2060	3.677	0.97	0.679	11.1	panel-1	2881.7	2881.7	13.229	2.222	1.611	14.1	3, 1.341	3, 1.399	3.598	2.29	2.372	1.27	yes	yes
Side aft shell	1234.2	667.2	1.65	0.873	0.611	8.6	panel-1	2881.7	933	13.229	1.722	1.111	14.1	3, 2.335	6, 1.398	8.019	1.972	1.818	1.65	yes	yes
Bottom center shell	1991.5	2304.6	2.841	0.97	0.679	12.7	panel-1	2881.7	2881.7	13.229	2.222	1.611	14.1	3, 1.447	3, 1.250	4.656	2.29	2.372	1.109	yes	yes
Side center shell	541.1	777.5	0.374	0.873	0.611	8.7	panel-1	2881.7	2881.7	13.229	2.222	1.611	14.1	3, 5.325	3, 3.706	35.362	2.545	2.636	1.624	yes	yes
Bottom front shell	349.9	390.4	0.187	0.97	0.679	9.1	panel-2	3720.7	933	18.93	1.722	1.111	17	5, 10.635	6, 2.390	101.077	1.775	1.636	1.857	yes	yes
Side front shell	1719.7	856.2	2.11	0.873	0.611	15.7	panel-2	3720.7	933	18.93	1.722	1.111	17	5, 2.164	6, 1.090	8.971	1.972	1.818	1.084	yes	yes
Bow side shell	1662.4	908.3	2.034	0.873	0.611	12.4	panel-2	3720.7	933	18.93	1.722	1.111	17	5, 2.238	6, 1.027	9.306	1.972	1.818	1.364	yes	yes
Deck aft	600	166.7	1.186	0.679	0.475	2.8	panel-3	1659.4	307.4	6.783	0.711	0.711	9.3	5, 2.766	2, 1.844	5.719	1.047	1.496	3.334	yes	yes
Deck front	756.4	246.3	1.215	0.679	0.475	3.8	panel-4	1674.9	483.5	7.329	1.122	0.711	9.4	6, 2.214	6, 1.963	6.03	1.652	1.496	2.512	yes	yes
superstructure	1058	334	2.777	0.679	0.475	3.5	panel-4	1674.9	483.5	7.329	1.122	0.711	9.4	6, 1.583	6, 1.448	2.639	1.652	1.496	2.666	yes	yes

Stiffeners																									
Label	Dimensions and Location						Calculations to ISO Standard					Requirements				Offered					Results				
	Length	Spacing	Longitudi nal Position	Location	z	Curvatu re	k _L	k _{AR}	z	k _z	Design Pressure	Bending Moment	Shear Force	EI	t _w	Label	Bending Moment	Shear Force	EI	t _w	Bending Moment Ratio	Shear Force Ratio	EI Ratio	t _w Ratio	Comply?
	mm	mm	m		m	mm					kN/m²	N.m	N	N.m²	mm		N.m	N	N.m²	m m					
Bottom middle	1160	1300	6.5	Bottom	--	0	0.93 8	0.26 5	- -	--	24.3	3538.8	18311.2	2562.5	4.8	Stiff-1	7859.4	58189 .3	322614.4	6.5	2.221	3.178	125.8 98	1.35	yes
Bottom aft	1500	1000	0.7	Bottom	--	0	0.54 8	0.25	- -	--	24.3	4551.7	18214.1	4262.1	4.8	Stiff-1	7859.4	58189 .3	322614.4	6.5	1.727	3.195	75.69 4	1.354	yes
Bottom front	2630	650	10.2	Bottom	--	0	1	0.25	- -	--	24.3	9095.3	20758	14932.4	5.9	Stiff-2	14498.8	78014 .7	767055.7	6.5	1.594	3.758	51.36 9	1.101	yes
Bow	1300	1220	13	Bottom	--	0	1	0.25 1	- -	--	24.3	4171	19258.3	3384.8	5.7	Stiff-2	14498.8	78014 .7	767055.7	6.5	3.476	4.051	226.6 15	1.143	yes
deck aft	2500	1200	2.15	Deck	--	0	0.64 6	0.25	- -	--	5	3123.8	7500	4875	3.4	Stiff-3	3409.2	31224 .7	106722.3	4.2	1.091	4.163	21.89 2	1.25	yes
deck front	1300	1000	11	Deck	--	0	1	0.26 7	- -	--	5.9	824.8	3808.1	669.3	2.4	Stiff-4	3226.4	31224 .7	103475.9	4.2	3.912	8.199	154.5 98	1.755	yes
superstruc ture/deck	2700	1000	6	Superstructure. Top, <= 800mm above deck, walking area	--	0	--	0.25	- -	--	5	3036.3	6750	5117.6	2.9	Stiff-5	3625.8	25927 .8	87773.6	4.2	1.194	3.841	17.15 1	1.441	yes

APPENDIX A9: HULL AND DECK STRUCTURAL ARRANGEMENT





APPENDIX A10: MAST AND RIG CALCULATION SPREADSHEET (NBS)

Rig Load Evaluation Using Nordic Boat Standard									
No of Spreaders	2		Masthead						
Fore triangle ht l	20.25	m	Deck Stepped						
Fore triangle base J	5.9	m							
Mains'l luff ht P	19.88	m	Backstay Angle		21.0	degrees			
BAD	2.1	m	Forestay Angl		16.3	degrees			
Ht to base of l (free board)	1.48	m	Mast compression PT		83110	N			
Displacement	12000	kg	oring factor		2.7				
GM	2.49	m							
RM @ 30 degrees	12708	12708	kgm						
Panel Number (1 lowest)	Base (spreader) width m	Panel Height m	Shroud angle degrees	vert angle	Proportion of l	mast section cm ⁴			
1	2.25	8.29	15.2	2.4	41%	2082			
2	1.9	7.41	14.4	7.7	37%	1603			
3	0.9	7.0045	7.3		35%	1432			
		22.7045	check panel hts		112%				
Shroud	Shroud Tensions			FoS	Dimensioning Load	Selected wire dia	Selected wire BL	Compliance factor	
	Case 1	Case 2	maximum						
D1 single lower	2006	3111	3111	2.8	8709	11	9450	1.09	
D1 twin lower	2006	3111	3111	2.5	7776	11	9450	1.22	
D2	2116	2097	2116	2.3	4866	9	5870	1.21	
D3	4123	0	4123	3	12369	13	13200	1.07	
V1	2051	2033	2051	3.2	6564	10	7250	1.10	
V2	4127	0	4127	3	12380	13	13200	1.07	
Masthead load F _t	525	kg	Fore Stay		8772	11	9450	1.08	
Head board distance from deck	14.028	m	Inner fore stay		7018	10	7250	1.03	
Mains'l load	1682	kg	Backstay		6890	10	7250	1.05	
Boom load	561	kg							
Head board load	673	kg							
Load Case Calculations									
Panel Number (1 lowest)	hd board abv panel base	Fmain lwr	Fmain upper	Fbu	Fm	Lat load at spreader			
1	0	0	0	142	152	294			
2	5.738	152	521		521	521			
3									

1x19 wire	
BL kg	Dia mm
320	2
500	2.5
720	3
1280	4
2000	5
2400	5.5
2880	6
3550	7
4640	8
5870	9
7250	10
9450	11
10400	12
13200	13
14200	14
18600	16
23200	19
30825	22
41680	26

c Stephen Wallis 2007

c Stephen Wallis 2007

APPENDIX A11: TANK LOADING

		Weight	Number	Mass	LCG	Moment	TCG	Moment	VCG	Moment
Tanks loading		kg/u	u	kg	m	kg.m	m	kg.m	m	kg.m
Light ship										
1	Fuel	0.00	1	0.00	5.6	0.00	0	0.00	0.3	0.00
2	Fresh water	0.00	1	0.00	5.6	0.00	0	0.00	0.3	0.00
3	Grey water	0.00	1	0.00	6.4	0.00	0	0.00	0.25	0.00
Full										
1	Fuel	170.00	1	170.00	5.6	952.00	0	0.00	0.3	51.00
2	Fresh water	176.00	1	176.00	5.6	985.60	0	0.00	0.3	52.80
3	Grey water	61.00	1	61.00	6.4	390.40	0	0.00	0.25	15.25
Start										
1	Fuel	170.00	1	170.00	5.6	952.00	0	0.00	0.3	51.00
2	Fresh water	176.00	1	176.00	5.6	985.60	0	0.00	0.3	52.80
3	Grey water	0.00	1	0.00	6.4	0.00	0	0.00	0.25	0.00
Half										
1	Fuel	85.00	1	85.00	5.6	476.00	0	0.00	0.3	25.50
2	Fresh water	88.00	1	88.00	5.6	492.80	0	0.00	0.3	26.40
3	Grey water	30.50	1	30.50	6.4	195.20	0	0.00	0.25	7.63
End										
1	Fuel	17.00	1	17.00	5.6	95.20	0	0.00	0.3	5.10
2	Fresh water	17.60	1	17.60	5.6	98.56	0	0.00	0.3	5.28
3	Grey water	61.00	1	61.00	6.4	390.40	0	0.00	0.25	15.25
TOTAL										
Light ship										
Full										
Start										
Half										
End										

0.00	-	-	-	-	-	-
407.00	5.72	2328.00	0.00	0.00	0.29	119.05
346.00	5.60	1937.60	0.00	0.00	0.30	103.80
203.50	5.72	1164.00	0.00	0.00	0.29	59.53
95.60	6.11	584.16	0.00	0.00	0.27	25.63

APPENDIX A12: WEIGHT ESTIMATION IN LIGHTSHIP CONDITION

Table 42: Total lightweight with the keel DOWN and Figaro 3 foil

	Mass	LCG	Moment X	TCG	Moment Y	VCG	Moment Z
	<i>kg</i>	<i>m</i>	<i>kg.m</i>	<i>m</i>	<i>kg.m</i>	<i>m</i>	<i>kg.m</i>
Structure	2549.26	5.94	15154.92	0.00	0.00	1.19	3041.14
Painting	110.92	8.01	887.96	0.00	0.00	1.94	214.77
Tankage configuration	0.00	-	-	-	-	-	-
Machinery	861.55	2.87	2471.86	0.74	633.36	0.70	598.95
Deck outfitting	421.30	7.96	3352.14	-0.03	-10.89	2.06	869.66
Rigging	391.92	8.20	3215.24	0.00	0.00	11.00	4312.04
Accommodation	980.00	6.82	6685.80	-0.39	-385.00	1.01	993.95
Crew	660.00	6.30	4158.00	0.00	0.00	1.18	777.60
Appendages with Figaro 3	4614.65	8.35	38524.17	0.00	0.00	-2.06	-9507.29
TOTAL (lifting keel down)	10589.59	7.03	74450.1	0.02	237.5	0.12	1300.8
<i>with Margin 10%</i>	11648.55						

FROM BASELINE

Table 43: Total lightweight with the keel UP and Figaro 3 foil

	Mass	LCG	Moment X	TCG	Moment Y	VCG	Moment Z
	<i>kg</i>	<i>m</i>	<i>kg.m</i>	<i>m</i>	<i>kg.m</i>	<i>m</i>	<i>kg.m</i>
Structure	2549.26	5.94	15154.92	0.00	0.00	1.19	3041.14
Painting	110.92	8.01	887.96	0.00	0.00	1.94	214.77
Tankage conf	0.00	-	-	-	-	-	-
Machinery	861.55	2.87	2471.86	0.74	633.36	0.70	598.95
Deck outfitting	421.30	7.96	3352.14	-0.03	-10.89	2.06	869.66
Rigging	391.92	8.20	3215.24	0.00	0.00	11.00	4312.04
Accommodation	980.00	6.82	6685.80	-0.39	-385.00	1.01	993.95
Crew	660.00	6.30	4158.00	0.00	0.00	1.18	777.60
Appendages Figaro 3	4614.65	8.35	38524.17	0.00	0.00	-0.83	-3807.43
TOTAL (lifting keel up)	10589.59	7.03	74450.08	0.02	237.47	0.66	7000.68
<i>with Margin 10%</i>	11648.55						

FROM BASELINE

Table 44: Total lightweight with the keel DOWN and DSS foil

	Mass	LCG	Moment X	TCG	Moment Y	VCG	Moment Z
	<i>kg</i>	<i>m</i>	<i>kg.m</i>	<i>m</i>	<i>kg.m</i>	<i>m</i>	<i>kg.m</i>
Structure	2549.26	5.94	15154.92	0.00	0.00	1.19	3041.14
Painting	110.92	8.01	887.96	0.00	0.00	1.94	214.77
Tankage conf	0.00	-	-	-	-	-	-
Machinery	861.55	2.87	2471.86	0.74	633.36	0.70	598.95
Deck outfitting	421.30	7.96	3352.14	-0.03	-10.89	2.06	869.66
Rigging	391.92	8.20	3215.24	0.00	0.00	11.00	4312.04
Accommodation	980.00	6.82	6685.80	-0.39	-385.00	1.01	993.95
Crew	660.00	6.30	4158.00	0.00	0.00	1.18	777.60
Appendages DSS	4354.75	8.07	35163.49	0.00	0.00	-2.39	-10428.95
<i>TOTAL (lifting keel down)</i>	10329.69	6.88	71089.4	0.02	237.5	0.04	379.2
<i>with Margin 10%</i>	11362.66						

FROM BASELINE

Table 45: Total lightweight with the keel UP and DSS foil

	Mass	LCG	Moment X	TCG	Moment Y	VCG	Moment Z
	<i>kg</i>	<i>m</i>	<i>kg.m</i>	<i>m</i>	<i>kg.m</i>	<i>m</i>	<i>kg.m</i>
Structure	2549.26	5.94	15154.92	0.00	0.00	1.19	3041.14
Painting	110.92	8.01	887.96	0.00	0.00	1.94	214.77
Tankage conf	0.00	-	-	-	-	-	-
Machinery	861.55	2.87	2471.86	0.74	633.36	0.70	598.95
Deck outfitting	421.30	7.96	3352.14	-0.03	-10.89	2.06	869.66
Rigging	391.92	8.20	3215.24	0.00	0.00	11.00	4312.04
Accommodation	980.00	6.82	6685.80	-0.39	-385.00	1.01	993.95
Crew	660.00	6.30	4158.00	0.00	0.00	1.18	777.60
Appendages DSS	4354.75	8.07	35163.49	0.00	0.00	-1.09	-4729.09
<i>TOTAL (lifting keel up)</i>	10329.69	6.88	71089.40	0.02	237.47	0.59	6079.02
<i>with Margin 10%</i>	11362.66						

FROM BASELINE

APPENDIX A13: VPP TABLES FOR BEST SPEED, HEEL ANGLE, LEEWAY ANGLE AND SAILSET

Table 46: Best boatspeeds (knots)

Best Boatspeeds (kt)

TWA/TWS	4	5	6	7	8	9	10	12	14	16	20
32	3.49	4.4	5.24	6	6.63	7.11	7.48	7.97	8.26	8.45	8.72
36	3.93	4.93	5.83	6.59	7.21	7.65	7.96	8.35	8.6	8.77	9.04
40	4.34	5.4	6.32	7.09	7.68	8.05	8.31	8.65	8.87	9.04	9.31
45	4.79	5.9	6.83	7.6	8.11	8.42	8.64	8.94	9.15	9.33	9.61
52	5.31	6.44	7.4	8.08	8.52	8.79	8.98	9.27	9.49	9.68	9.99
60	5.74	6.89	7.82	8.42	8.83	9.11	9.3	9.58	9.83	10.05	10.43
70	6.08	7.24	8.09	8.65	9.05	9.37	9.61	9.95	10.24	10.49	10.92
80	6.19	7.36	8.17	8.72	9.13	9.48	9.78	10.28	10.6	10.88	11.43
90	6.1	7.26	8.1	8.65	9.07	9.43	9.77	10.41	10.89	11.26	11.97
100	5.83	6.96	7.87	8.67	9.21	9.56	9.78	10.28	10.91	11.54	12.55
110	5.62	6.88	7.97	8.72	9.24	9.63	9.92	10.36	10.73	11.26	12.94
120	5.51	6.74	7.8	8.53	9.05	9.47	9.85	10.5	10.95	11.41	12.39
135	4.75	5.87	6.85	7.7	8.34	8.83	9.26	10.07	10.86	11.72	13.39
150	3.59	4.51	5.4	6.22	6.99	7.68	8.24	9.09	9.83	10.58	12.38
160	2.94	3.71	4.47	5.2	5.91	6.58	7.22	8.28	9.07	9.77	11.25
170	2.6	3.27	3.94	4.6	5.25	5.89	6.49	7.64	8.55	9.28	10.64
180	2.42	3.05	3.67	4.3	4.91	5.51	6.09	7.21	8.17	8.93	10.23
Up.Vs	4.78	5.76	6.54	7.22	7.58	7.8	7.95	8.17	8.32	8.45	8.66
Up.Bt	44.8	43.6	42.1	41.2	39	37.4	36	34	32.7	32.1	31.3
Up.Vmg	3.39	4.18	4.85	5.44	5.89	6.2	6.44	6.78	7	7.16	7.4
Dn.Vs	4.7	5.67	6.43	7.16	7.61	7.97	8.3	8.88	9.43	10.18	12.96
Dn.Bt	135.5	137.1	139.3	140.8	144	146.9	149.3	152.8	155	154.6	146.2
Dn.Vmg	3.35	4.16	4.88	5.55	6.16	6.68	7.14	7.9	8.55	9.2	10.77

Table 47: Best Boatspeeds (Fr)

Best Boatspeeds (Fr)

TWA/TWS	4	5	6	7	8	9	10	12	14	16	20
32	0.15	0.19	0.22	0.25	0.28	0.30	0.32	0.34	0.35	0.36	0.37
36	0.17	0.21	0.25	0.28	0.31	0.32	0.34	0.35	0.36	0.37	0.38
40	0.18	0.23	0.27	0.30	0.33	0.34	0.35	0.37	0.38	0.38	0.39
45	0.20	0.25	0.29	0.32	0.34	0.36	0.37	0.38	0.39	0.40	0.41
52	0.23	0.27	0.31	0.34	0.36	0.37	0.38	0.39	0.40	0.41	0.42
60	0.24	0.29	0.33	0.36	0.37	0.39	0.39	0.41	0.42	0.43	0.44
70	0.26	0.31	0.34	0.37	0.38	0.40	0.41	0.42	0.43	0.44	0.46
80	0.26	0.31	0.35	0.37	0.39	0.40	0.41	0.44	0.45	0.46	0.48
90	0.26	0.31	0.34	0.37	0.38	0.40	0.41	0.44	0.46	0.48	0.51
100	0.25	0.30	0.33	0.37	0.39	0.41	0.41	0.44	0.46	0.49	0.53
110	0.24	0.29	0.34	0.37	0.39	0.41	0.42	0.44	0.46	0.48	0.55
120	0.23	0.29	0.33	0.36	0.38	0.40	0.42	0.45	0.46	0.48	0.53
135	0.20	0.25	0.29	0.33	0.35	0.37	0.39	0.43	0.46	0.50	0.57
150	0.15	0.19	0.23	0.26	0.30	0.33	0.35	0.39	0.42	0.45	0.52
160	0.12	0.16	0.19	0.22	0.25	0.28	0.31	0.35	0.38	0.41	0.48
170	0.11	0.14	0.17	0.20	0.22	0.25	0.28	0.32	0.36	0.39	0.45
180	0.10	0.13	0.16	0.18	0.21	0.23	0.26	0.31	0.35	0.38	0.43
Up.Vs	0.20	0.24	0.28	0.31	0.32	0.33	0.34	0.35	0.35	0.36	0.37
Up.Bt	44.80	43.60	42.10	41.20	39.00	37.40	36.00	34.00	32.70	32.10	31.30
Up.Vmg	0.14	0.18	0.21	0.23	0.25	0.26	0.27	0.29	0.30	0.30	0.31
Dn.Vs	0.20	0.24	0.27	0.30	0.32	0.34	0.35	0.38	0.40	0.43	0.55
Dn.Bt	135.50	137.10	139.30	140.80	144.00	146.90	149.30	152.80	155.00	154.60	146.20
Dn.Vmg	0.14	0.18	0.21	0.24	0.26	0.28	0.30	0.34	0.36	0.39	0.46

Table 48: Best heel angle (degree)

Best Heel Angles (deg)

TWA/TWS	4	5	6	7	8	9	10	12	14	16	20
32	3.67	6.06	7.95	10.14	12.91	15.89	17.53	19.79	21.21	21.56	21.5
36	4.11	6.58	8.63	11.06	14.24	17.2	18.59	20.43	21.48	21.4	21.32
40	5.06	7.02	9.19	11.84	15.28	18.09	19.25	20.8	21.31	21.23	21.16
45	5.4	7.44	9.71	12.53	16.04	18.78	19.73	21.04	21.11	21.04	21
52	5.7	7.79	10.13	12.87	16.15	19.27	20.05	21	20.9	20.85	20.64
60	5.84	7.88	10.08	12.48	15.26	18.53	20.14	20.6	20.58	20.58	20.63
70	5.69	7.57	9.42	11.27	13.33	15.76	18.58	20.57	20.54	20.55	20.6
80	5.24	6.89	8.39	9.77	11.22	12.86	14.8	19.63	20.5	20.51	20.58
90	3.88	5.97	7.19	8.24	9.25	10.33	11.55	14.65	18.56	20.48	20.59
100	2.94	4.24	8.46	11.14	14.72	19.14	20.35	10.79	13.07	16.15	20.65
110	3.8	6.09	8.02	10.23	12.81	15.85	19.23	20.3	20.28	10.87	15.96
120	3.25	5.39	6.97	8.53	10.07	11.7	13.58	18.4	20.36	20.42	20.65
135	1.79	2.76	3.81	5.31	6.12	6.88	7.65	9.38	11.54	14.48	21.26
150	0.51	0.81	1.16	1.55	1.97	2.41	2.84	3.7	5.1	5.99	8.15
160	0.16	0.25	0.36	0.49	0.64	0.82	1.01	1.47	2.07	2.82	5.11
170	0.07	0.11	0.15	0.21	0.27	0.34	0.43	0.63	0.9	1.24	2.09
180	0	0.01	0.01	0.01	0.01	0.02	0.02	0.04	0.05	0.08	0.14
Up	5.39	7.33	9.43	12.03	15.07	17.55	18.58	20.15	21.3	21.56	21.53
Dn	2.42	3.12	3.56	4.02	3.98	3.84	3.71	3.56	3.71	4.6	10.38

Table 49: Best Leeway angle (degree)

Best Leeway (deg)

TWA/TWS	4	5	6	7	8	9	10	12	14	16	20
32	3.16	3.1	3.09	3.13	3.24	3.31	3.2	3.06	2.99	3	3.1
36	2.79	2.75	2.76	2.83	2.94	3	2.92	2.82	2.78	2.82	2.92
40	2.5	2.49	2.52	2.59	2.72	2.79	2.73	2.65	2.64	2.68	2.78
45	2.24	2.24	2.28	2.35	2.51	2.6	2.55	2.48	2.5	2.54	2.62
52	1.96	1.98	2.01	2.11	2.26	2.4	2.36	2.31	2.33	2.36	2.51
60	1.72	1.74	1.78	1.87	2	2.16	2.19	2.23	2.22	2.21	2.22
70	1.48	1.49	1.53	1.6	1.69	1.79	1.91	1.97	1.94	1.92	1.91
80	1.28	1.28	1.3	1.35	1.41	1.48	1.55	1.7	1.71	1.68	1.63
90	1.09	1.09	1.1	1.13	1.17	1.21	1.25	1.33	1.43	1.45	1.36
100	0.92	0.91	1.18	1.29	1.44	1.61	1.65	1.04	1.09	1.12	1.11
110	1.02	1.03	1.07	1.16	1.26	1.36	1.46	1.45	1.41	0.85	0.82
120	0.9	0.91	0.93	0.98	1.03	1.08	1.13	1.22	1.23	1.17	1.05
135	0.67	0.66	0.66	0.66	0.66	0.68	0.7	0.73	0.76	0.76	0.71
150	0.34	0.34	0.33	0.33	0.33	0.33	0.33	0.34	0.36	0.37	0.36
160	0.17	0.16	0.16	0.16	0.16	0.16	0.16	0.17	0.2	0.22	0.26
170	0.09	0.09	0.09	0.08	0.08	0.08	0.08	0.09	0.1	0.11	0.13
180	0.01	0.01	0.01	0.01	0.01	0.01	0.01	0.01	0.01	0.01	0.01
Up	2.25	2.3	2.41	2.53	2.77	2.92	2.93	2.93	2.94	3	3.13
Dn	0.66	0.62	0.57	0.53	0.46	0.39	0.34	0.28	0.26	0.29	0.42

Table 50: Best point of sail (Upwind or Downwind)

Best SailSet TWA/TWS	4	5	6	7	8	9	10	12	14	16	20
32	Up	Up	Up	Up	Up	Up	Up	Up	Up	Up	Up
36	Up	Up	Up	Up	Up	Up	Up	Up	Up	Up	Up
40	Up	Up	Up	Up	Up	Up	Up	Up	Up	Up	Up
45	Up	Up	Up	Up	Up	Up	Up	Up	Up	Up	Up
52	Up	Up	Up	Up	Up	Up	Up	Up	Up	Up	Up
60	Up	Up	Up	Up	Up	Up	Up	Up	Up	Up	Up
70	Up	Up	Up	Up	Up	Up	Up	Up	Up	Up	Up
80	Up	Up	Up	Up	Up	Up	Up	Up	Up	Up	Up
90	Up	Up	Up	Up	Up	Up	Up	Up	Up	Up	Up
100	Up	Up	Dn	Dn	Dn	Dn	Dn	Up	Up	Up	Up
110	Dn	Dn	Dn	Dn	Dn	Dn	Dn	Dn	Dn	Up	Up
120	Dn	Dn	Dn	Dn	Dn	Dn	Dn	Dn	Dn	Dn	Dn
135	Dn	Dn	Dn	Dn	Dn	Dn	Dn	Dn	Dn	Dn	Dn
150	Dn	Dn	Dn	Dn	Dn	Dn	Dn	Dn	Dn	Dn	Dn
160	Dn	Dn	Dn	Dn	Dn	Dn	Dn	Dn	Dn	Dn	Dn
170	Dn	Dn	Dn	Dn	Dn	Dn	Dn	Dn	Dn	Dn	Dn

* *Up*=upwind / *Dn*=downwind

APPENDIX A14: PROHASKA PLOT BARE HULL

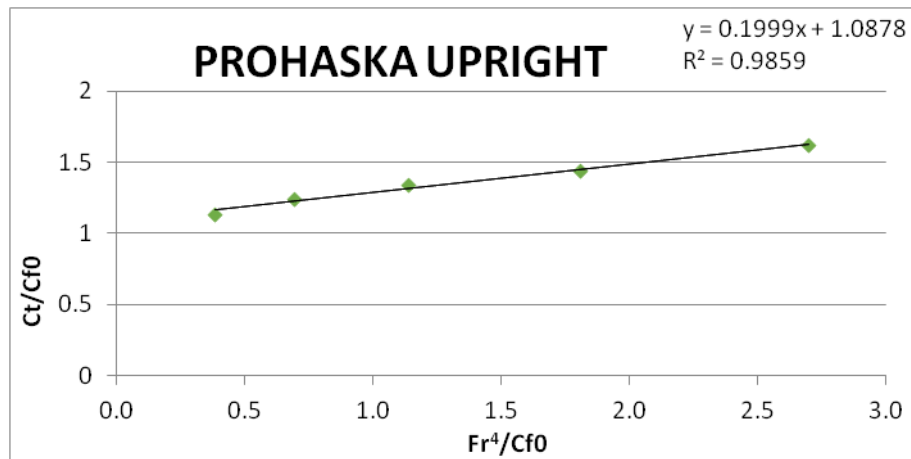


Figure 99: Prohaska plot upright position. Form factor $(1+k) = 1.0878$.

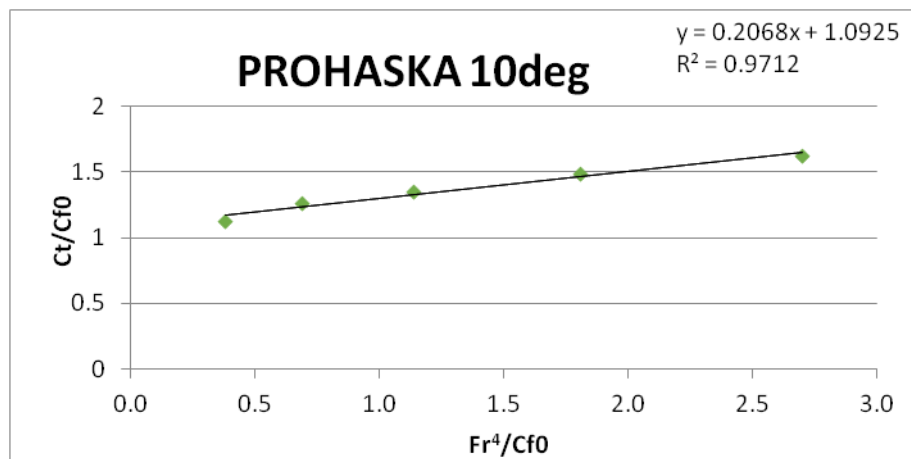


Figure 100: Prohaska plot 10deg heel position. Form factor $(1+k) = 1.0925$.

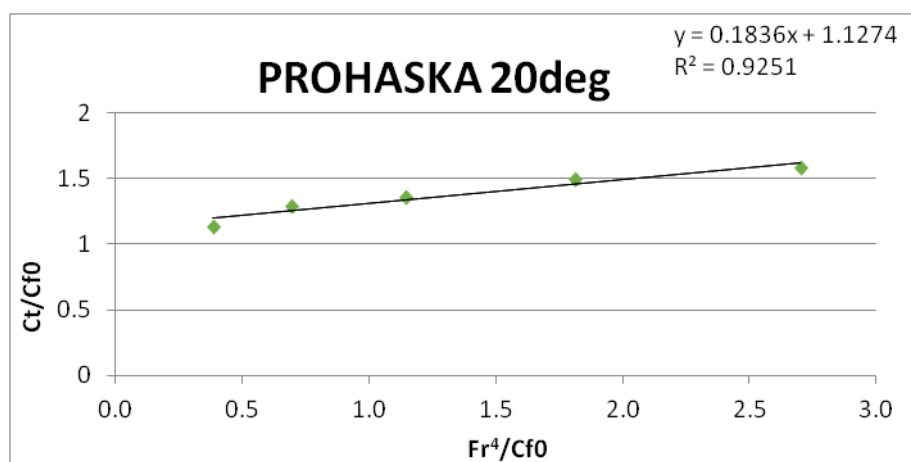


Figure 101: Prohaska plot 20deg heel position. Form factor $(1+k) = 1.1274$.

APPENDIX A15: DRAG, SIDE FORCE, HEAVE AND TRIM GRAPHS

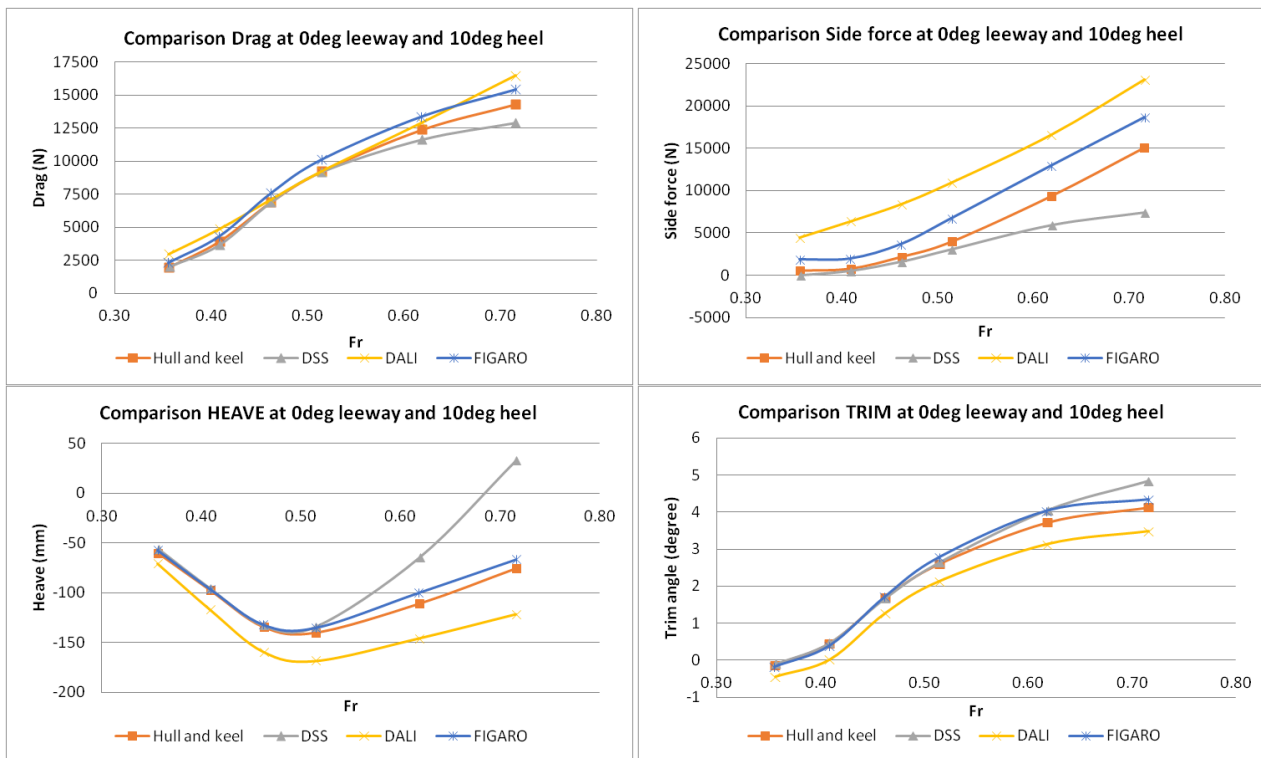


Figure 102: Drag, SF, Heave and Trim comparison for 0deg of leeway and 10deg of heel.

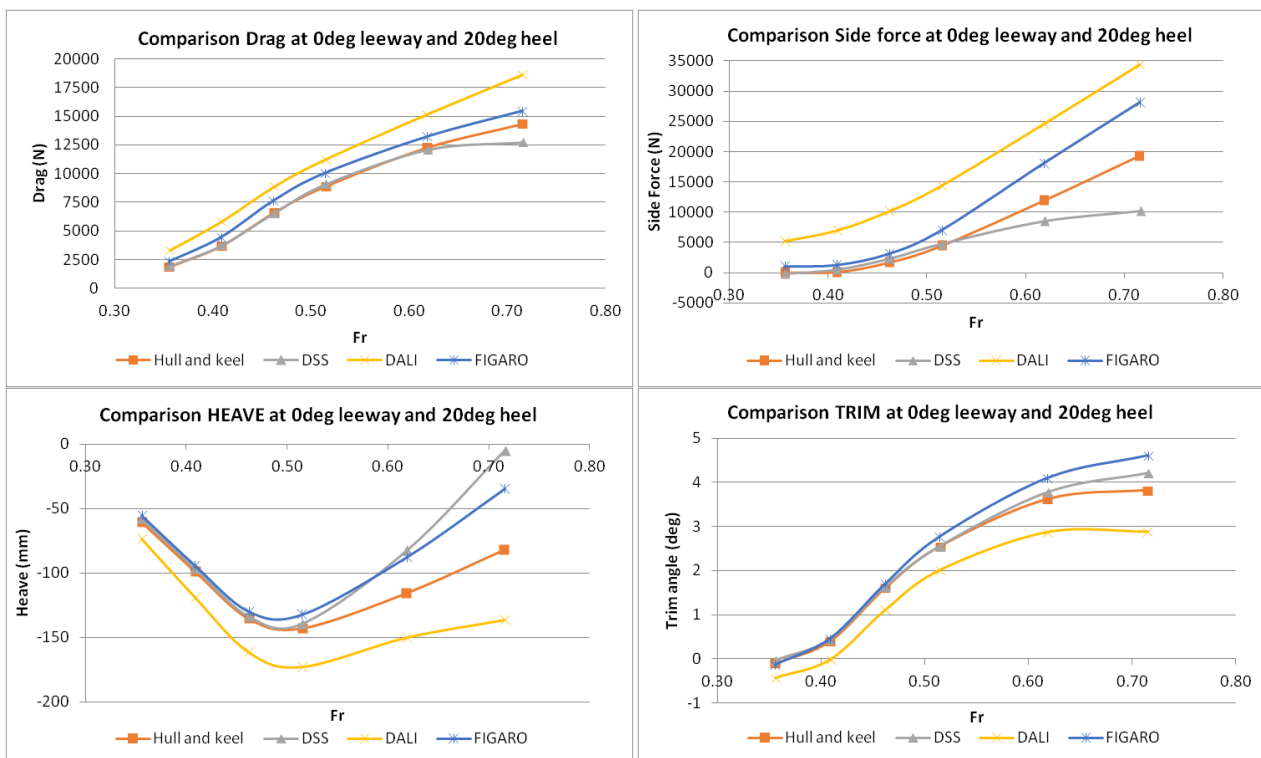


Figure 103: Drag, SF, Heave and Trim comparison for 0deg of leeway and 20deg of heel.

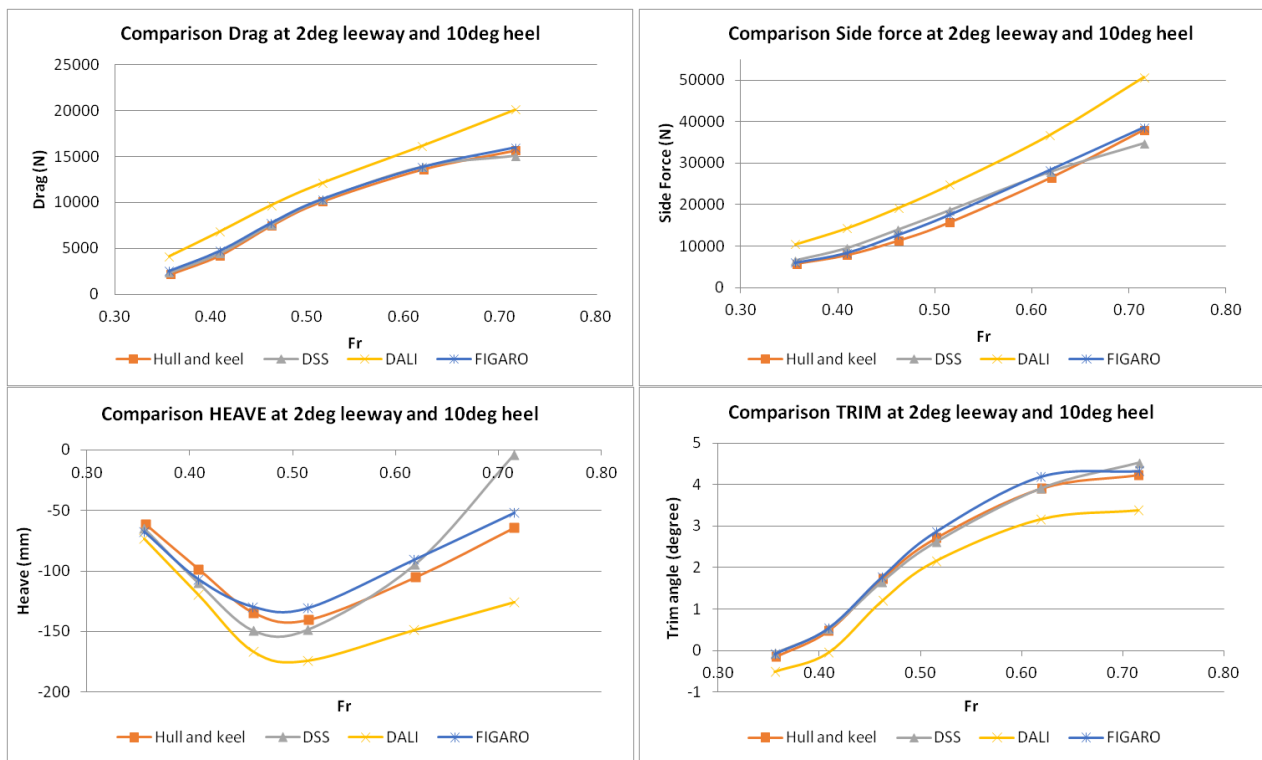


Figure 104: Drag, SF, Heave and Trim comparison for 2deg of leeway and 10deg of heel.

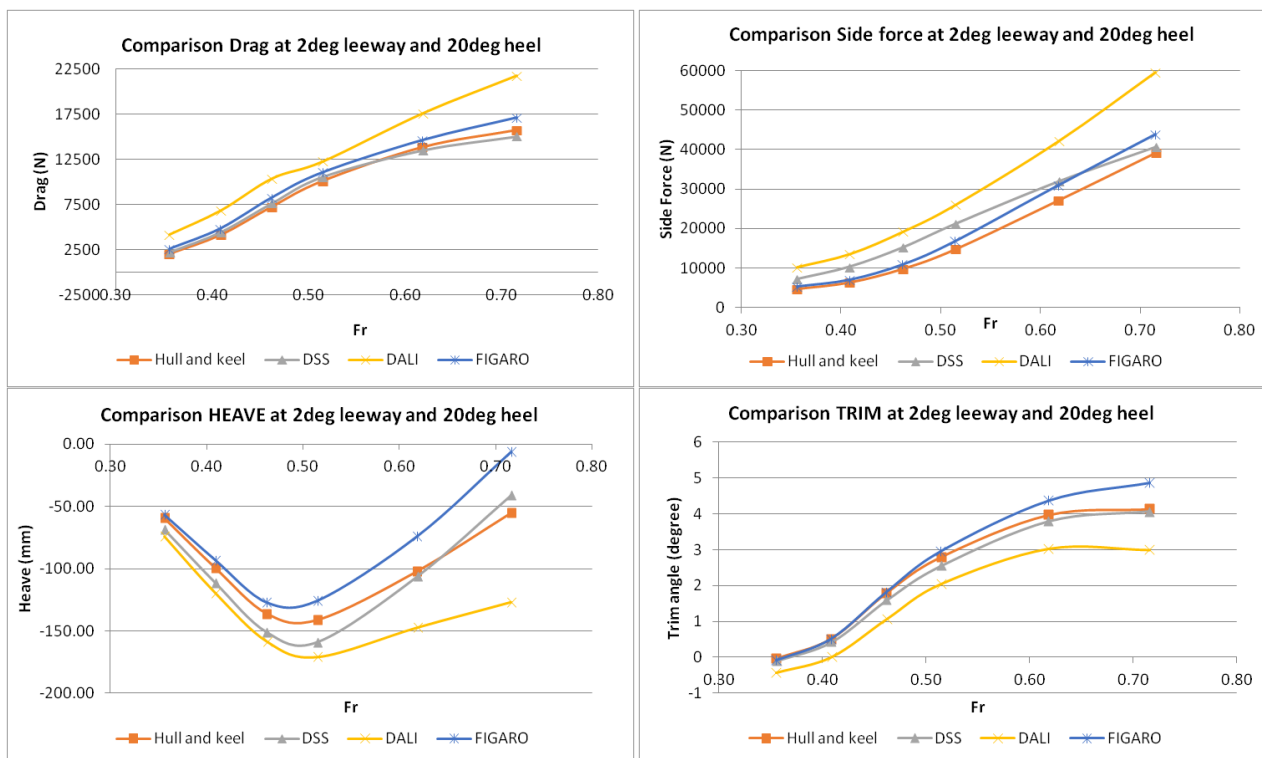


Figure 105: Drag, SF, Heave and Trim comparison for 2deg of leeway and 20deg of heel.

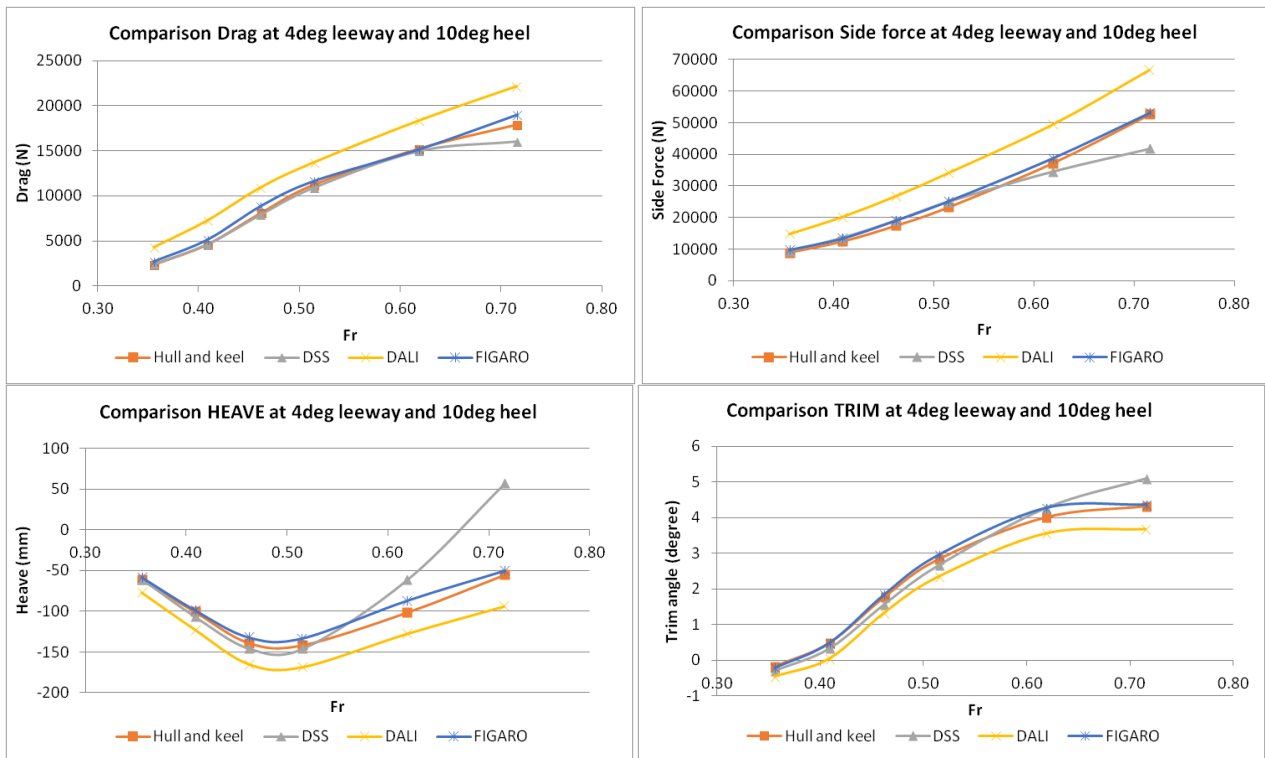


Figure 106: Drag, SF, Heave and Trim comparison for 4deg of leeway and 10deg of heel.

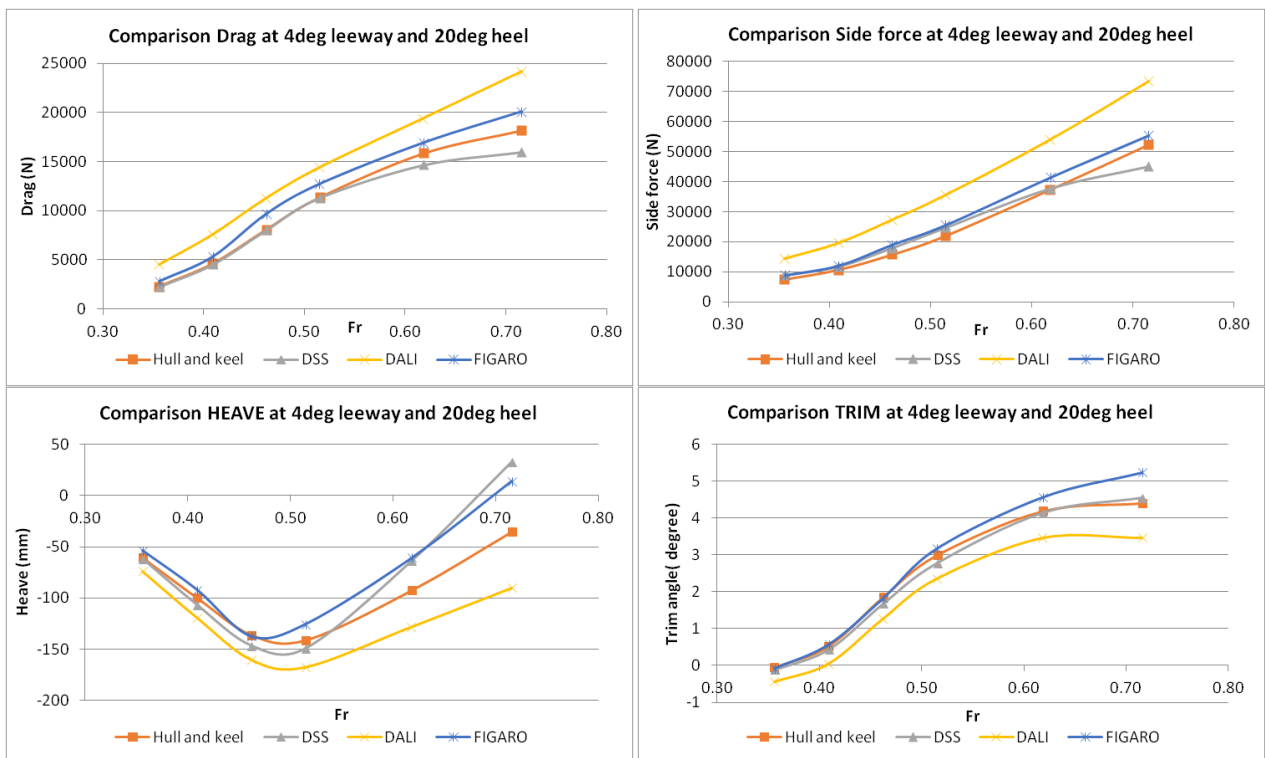


Figure 107: Drag, SF, Heave and Trim comparison for 4deg of leeway and 20deg of heel.

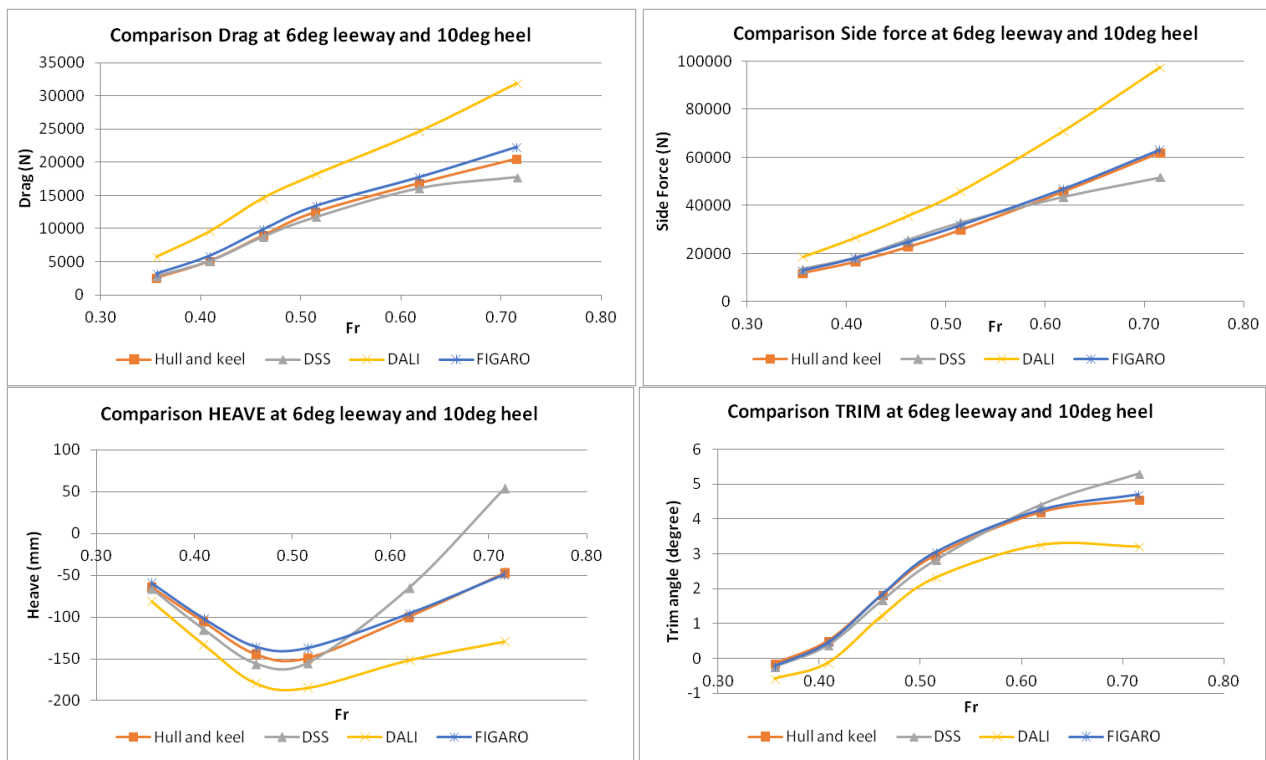


Figure 108: Drag, SF, Heave and Trim comparison for 6deg of leeway and 10deg of heel.

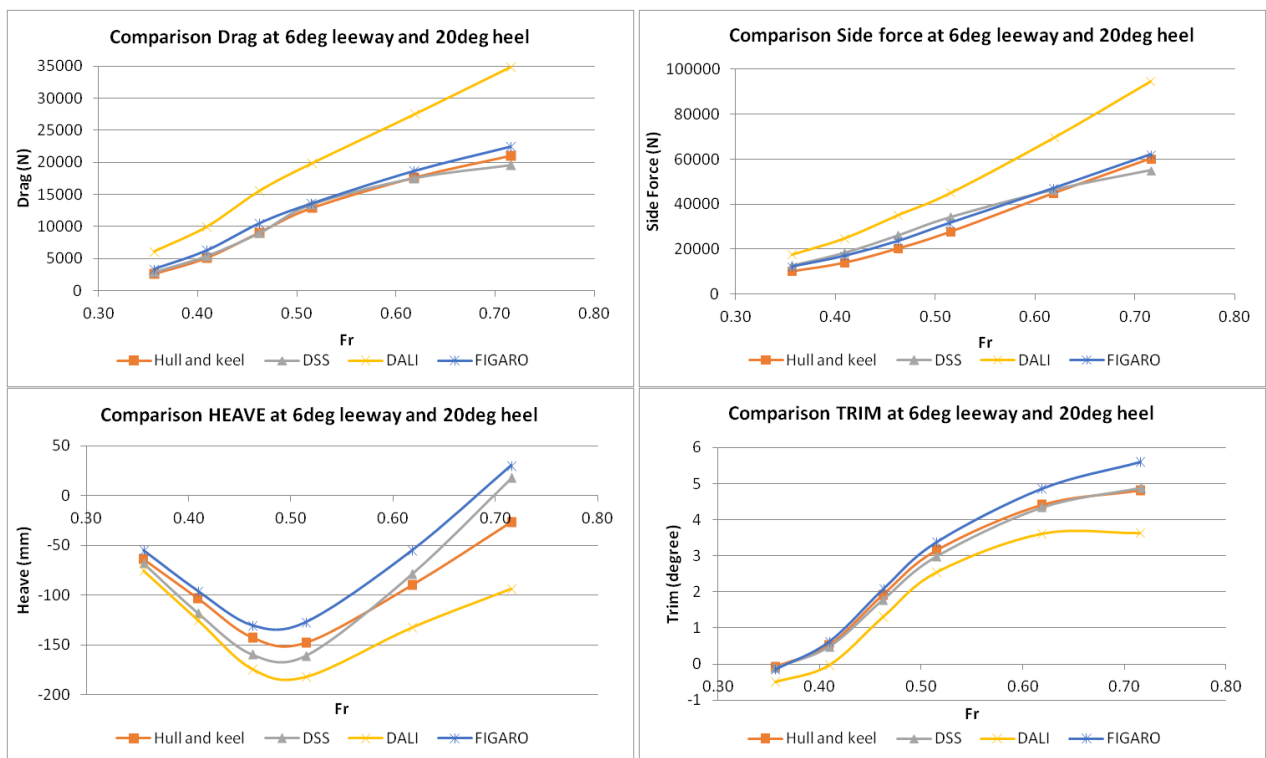
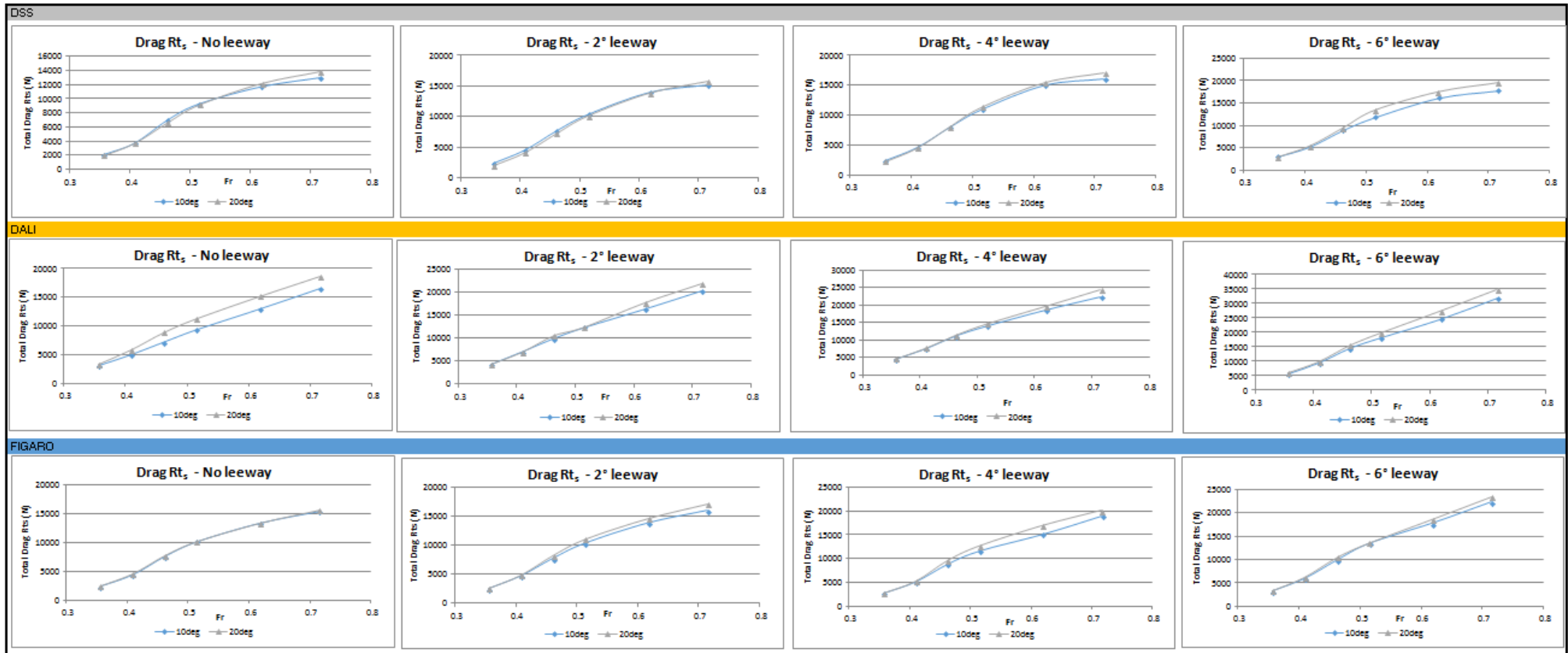
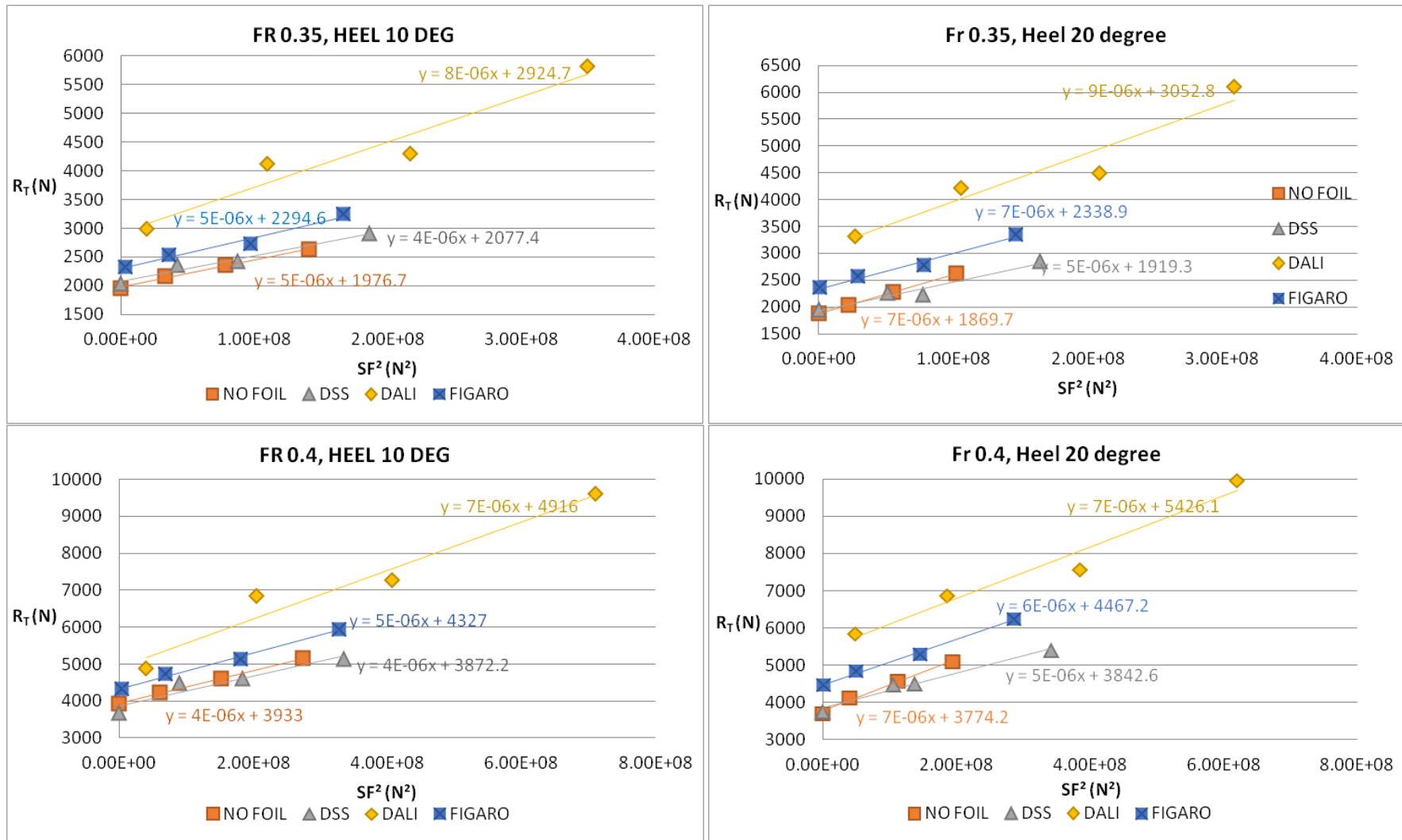


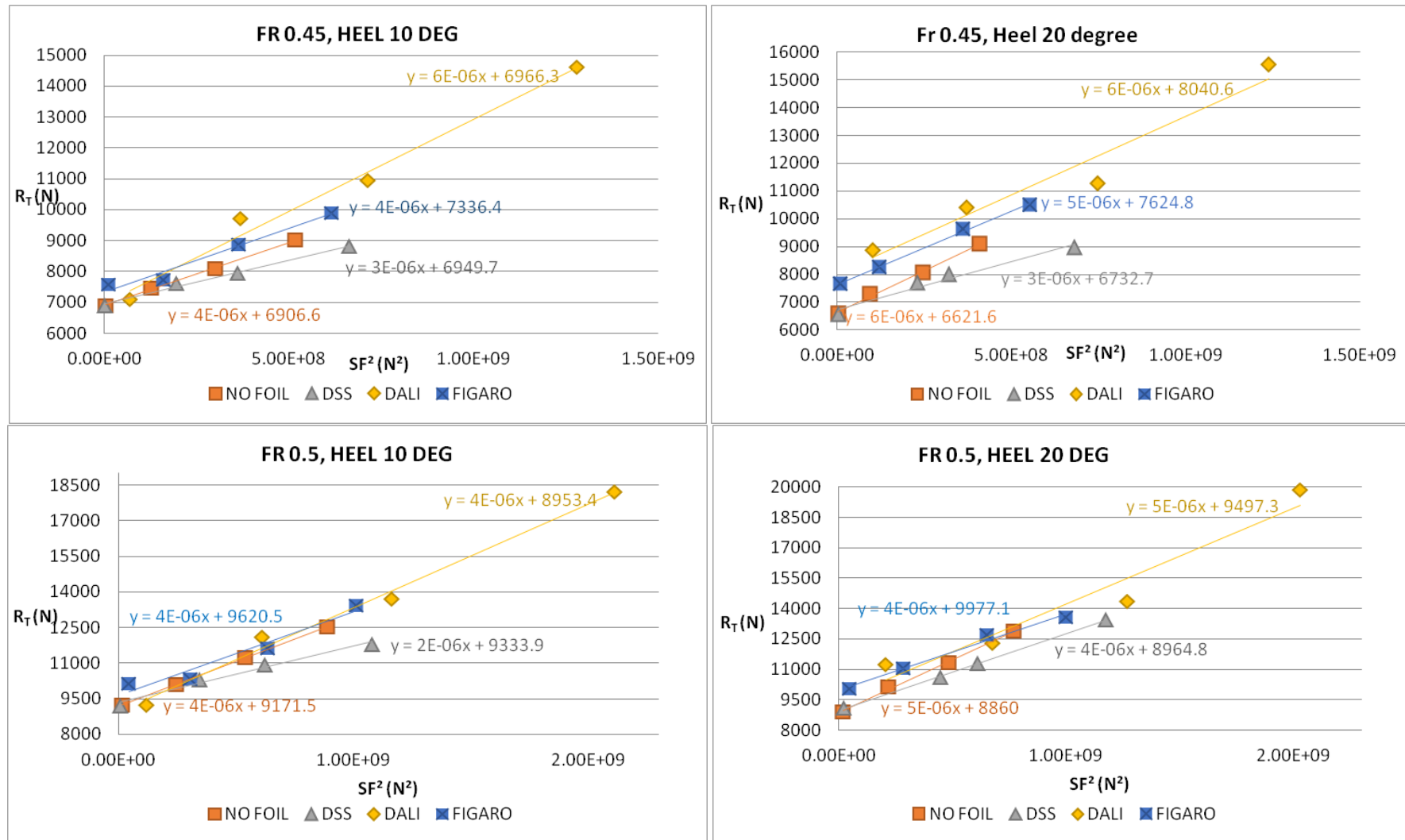
Figure 109: Drag, SF, Heave and Trim comparison for 6deg of leeway and 20deg of heel.

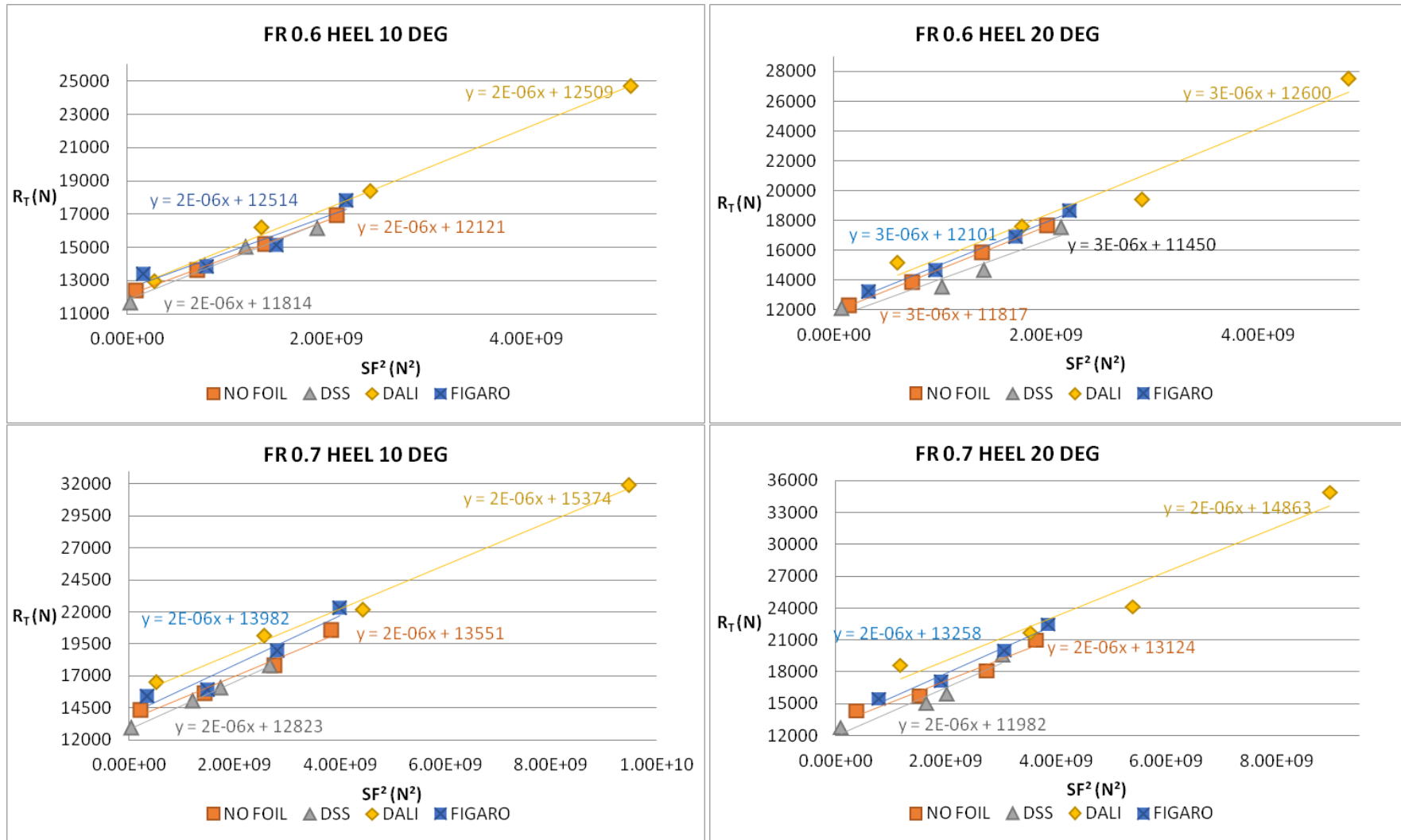
APPENDIX A16: RESISTANCE COMPARISON BETWEEN LOW AND HIGH HEEL ANGLE FOR EACH FOIL AT DIFFERENT LEEWAY ANGLE



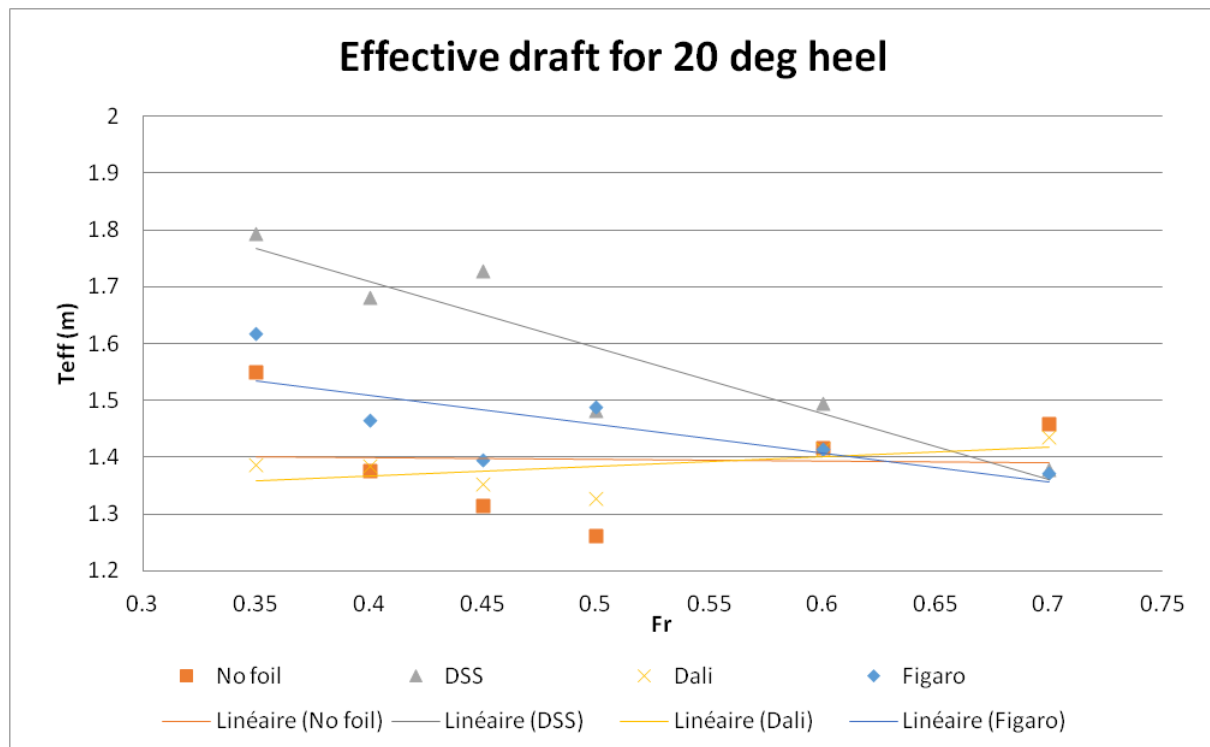
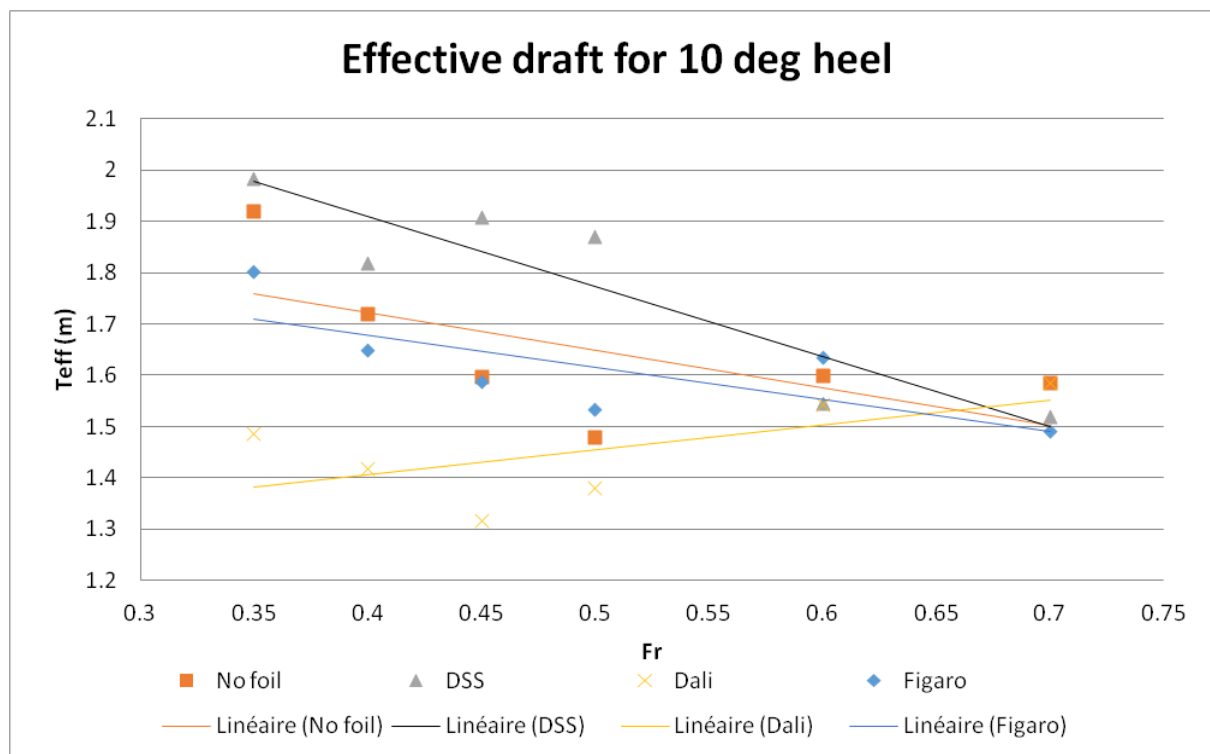
APPENDIX A17: EFFECTIVE DRAFT GRAPHS (DRAG VS SIDE FORCE SQUARED)







APPENDIX A18: EFFECTIVE DRAFT GRAPHS (T_{EFF} VS FROUDE NUMBER)



APPENDIX A19: MINIMUM DRAG CONFIGURATION BASED ON THE EFFECTIVE DRAFT METHOD

Table 51: Best configuration upwind and downwind based on R_T vs SF^2 graphs

		Downwind	Upwind
Heel		10 degree	20 degree
Leeway		0/2°	4/6°
Fr	$V_S (m/s)^*$		
0.35	4.15		DSS
0.4	4.75		DSS
0.45	5.34	Keel	DSS
0.5	5.93	Dali	
0.6	7.12	DSS	
0.7	8.30	DSS	

Table 52: Best configuration upwind and downwind based on T_E vs Fr graphs

		Downwind	Upwind
Heel		10 degree	20 degree
Leeway		0/2	4/6°
Fr	$V_S (m/s)^*$		
0.35	4.15		DSS
0.4	4.75		DSS
0.45	5.34	DSS	DSS
0.5	5.93	DSS	
0.6	7.12	Figaro	
0.7	8.30	Keel or Dali	

**Full scale speed*